# THE POLYPHEMUSIN FAMILY OF ANTIMICROBIAL PEPTIDES: ACTIVITY THROUGH STRUCTURE AND MEMBRANE INTERACTIONS

by

Jon-Paul Steven Powers

B.Sc., Carleton University, 1999

A THESIS SUBMITTED IN PARTIAL FULFILLMENT OF
THE REQUIREMENTS FOR THE DEGREE OF

DOCTOR OF PHILOSOPHY

in

THE FACULTY OF GRADUATE STUDIES

(Microbiology and Immunology)

THE UNIVERSITY OF BRITISH COLUMBIA

February 2006

**Abstract**

Cationic antimicrobial peptides are a class of small, positively charged peptides known for their broad-spectrum antimicrobial activity. These peptides have also been shown to possess anti-viral activity and, most recently, the ability to modulate the innate immune response. Peptides from the horseshoe crab, the polyphemusins and tachyplesins, are some of the most active peptides isolated from nature, possessing high antimicrobial activity against both Gram negative and Gram positive bacteria. Despite their excellent antimicrobial activity, the mechanism of action is not well defined. The goal of this thesis was to investigate structure-activity relationships of two representative polyphemusins, polyphemusin I (PM1) and PV5.

The solution structures of PM1 and PV5 were determined using $^{1}$H-NMR spectroscopy. Both peptides were found to form amphipathic, β-hairpin conformations stabilized by disulfide bond formation. A linear analogue, PM1-S, with all cysteines simultaneously replaced with serine, was found to be dynamic in nature with no favoured conformation. The antimicrobial activity of PM1-S was found to be 4 to 16-fold less than that of PM1 and corresponded with a 4-fold reduction in ability to depolarize bacterial cytoplasmic membranes. Although both PM1-S and PM1 were able to associate with lipid bilayers in a similar fashion,only PM1-S lost its ability to translocate model membranes.. It was concluded that the disulfide constrained, β-sheet structure of PM1 is required for maximum antimicrobial activity.

Model membrane interactions of PM1 and PV5 were investigated using fluorescence spectroscopy and differential scanning calorimetry (DSC). Both peptides were found to have limited affinities for neutral vesicles containing phosphatidylcholine

(PC), and/or cholesterol or phosphatidylethanolamine (PE); however partitioning was increased through the inclusion of anionic phosphatidylglycerol (PG) into PC vesicles. DSC studies supported the partitioning data and demonstrated that neither peptide interacted readily with neutral PC vesicles while both peptides showed affinity for negatively charged membranes incorporating PG, causing significant perturbation of these membranes. The affinity of PV5 was much greater than that of PM1, as the pre-transition peak was absent at low peptide to lipid ratios and the reduction in enthalpy of the main, gel to liquid crystalline transition was greater than that produced by PM1. Both peptides decreased the lamellar to inverted hexagonal phase transition temperature of PE, indicating the induction of negative curvature strain.

Using a biotin-labeled PM1 analogue and fluorescence microscopy, it was demonstrated that the peptide accumulates in the cytoplasm of wild type *E. coli* within 30 min after addition without corresponding membrane damage. Comparison between peptide treated and untreated cells revealed that DNA in peptide treated cells appeared less condensed than untreated cells and was found at the periphery of cells.

Collectively, the results presented here, combined with previous findings that PM1 promotes lipid flip-flop but does not induce significant vesicle leakage, ruled out a membrane disruption mechanism of antimicrobial action for PM1. In addition, the localization of a biotin-labelled PM1 within the cytoplasm of *E. coli* following peptide treatment indicated that the polyphemusins are capable of translocating biological membranes and may act on cytoplasmic components as their target of antimicrobial action.

## Table of Contents

## List of Tables

## List of Figures

## List of Abbreviations

| | |
|---|---|
| ACM | Acetamidomethyl |
| CD | Circular dichroism |
| $D_2O$ | Deuterium oxide |
| DAPI | 4',6-diamidino-2-phenylindole |
| DGSA | Distance geometry simulated annealing |
| DiPoPE | 1,2-Dipalmitoleoyl-*sn*-Glycero-3-Phosphoethanolamine |
| $diSC_35$ | 3,3'-dipropylthiadicarbocyanine iodide |
| DMPC | 1,2-Dimyristoyl-*sn*-Glycero-3-Phosphocholine |
| DMPG | 1,2-Dimyristoyl-*sn*-Glycero-3-[Phospho-*rac*-(1-glycerol)] (Sodium Salt) |
| DMSO | Dimethyl sulfoxide |
| DNS-PE | Dansyl phosphatidylethanolamine |
| DPC | D38-dodecylphosphocholine |
| DQF-COSY | Double quantum filtered correlated spectroscopy |
| DSC | Differential scanning calorimetry |
| EDTA | Ethylenediaminetetraacetic acid |
| Fmoc | N-(9-fluorenyl) methoxycarbonyl |
| FPLC | Fast purification liquid chromatography |
| HEPES | 4-(2-hydroxyethyl)-1-piperazineethanesulfonic acid |
| HPLC | High performance liquid chromatography |
| LB broth | Luria-Bertani broth |
| LPS | Lipopolysaccharide |
| MALDI | Matrix assisted laser-desorption ionization |
| MH broth | Mueller-Hinton broth |
| MHC | Minimum hemolytic concentration |
| MIC | Minimal inhibitory concentration |
| MLV | Multi-lamellar vesicle |
| NMR | Nuclear magnetic resonance |
| NOE | Nuclear Overhauser effect |
| NOESY | Nuclear Overhauser effect spectroscopy |
| NPN | 1-N-phenylnapthylamine |
| PC | Phosphatidylcholine |
| PE | Phosphatidylethanolamine |
| PG | Phosphatidylglycerol |
| PM1 | Polyphemusin I |
| PM1-Biotin | Polyphemusin I with C-terminal biotin |
| PM1-Cys | Polyphemusin I with C-terminal cysteine |
| POPC | 1-Palmitoyl-2-Oleoyl-*sn*-Glycero-3-Phosphocholine |
| POPE | 1-Palmitoyl-2-Oleoyl-*sn*-Glycero-3-Phosphoethanolamine |
| POPG | 1-Palmitoyl-2-Oleoyl-*sn*-Glycero-3-[Phospho-*rac*-(1-glycerol)] (Sodium Salt) |
| PV5 | Polyphemusin I analogue |
| SDS | Sodium dodecyl sulfate |
| SUV | Small unilamellar vesicle |

| | |
|---|---|
| t-BOC | tert-Butyloxycarbonyl |
| TFE | Trifluoroethanol |
| TOCSY | Total correlation spectroscopy |
| Tris | Tris (hydroxymethyl) aminomethane |

**Acknowledgements**

First off, I must thank Bob for letting me come to his lab at a time when I was a lowly public servant and for letting me do pretty much do whatever I wanted when I wanted to do it. The direction was great and so was the independence. Thanks for also realizing I was a little different and always answering the question "so how can we make money from this?"

Thanks to my committee, Pieter, Lawrence and François, for their enthusiastic comments and questions. Thanks for being patient with me. Thanks also to Peter Buist, my undergraduate supervisor, for encouraging me to do my Ph.D. Thanks to NSERC, UBC and Helix BioMedix for the much needed support throughout this degree.

I definitely also need to thank the members of the Hancock Lab, Manjeet, Susan, and Barb for dealing with my "issues" and all the administrative procedures that I could never understand or stop complaining about. Thanks to Mark Okon for help with all things NMR, and David and Morgan for additional science help.

On the personal side of things, I couldn't have done it without Pam, Secko, Joey, Sandeep, and Brett. It wouldn't have been fun at all without you. I also would have quit long ago without the support from Clare and Angie.

I owe Danika a giant thanks for listening to my crazy ideas, scientific and otherwise, and for always letting me go through with them. The emotional and financial support was and is much needed; now let's retire. Finally I'd like to thank my parents. While I'm positive they have no idea of exactly what I do, they understand the most important aspects; it's not pleasant to live on a graduate student salary, with a copy of this thesis, we'll call it even...

## Statement of Authorship

Versions of each chapter have been published or submitted for publication as Powers and Hancock, 2003 (Chapter 1 and 4), Powers *et al*, 2004 (Chapter 2) and Powers *et al*, 2005 (Chapter 3). In all instances where previously published or submitted materials are reproduced in this thesis they represent the original writing of the author. The co-authors A. Rozek (Chapter 2), A. Tan (Chapter 3), and M. Martin and D. Goosney (Chapter 4) are acknowledged as such for their assistance with experimental methods, and in the case of A. Ramamoorthy (Chapter 3) for the kind invitation to visit and work in his laboratory. In addition, R.E.W. Hancock has co-authored all of the publications listed here in the position of thesis supervisor.

## Chapter 1 - Introduction*

### Antimicrobial peptides

Cationic antimicrobial peptides are generally defined as peptides of less than 50 amino acid residues with an overall positive charge, imparted by the presence of multiple lysine and arginine residues, and a substantial portion (50% or more) of hydrophobic residues. These peptides can possess antimicrobial activity against Gram-positive and Gram-negative bacteria, fungi (*1*) and protozoa (*2*) and have demonstrated minimal inhibitory concentrations (MIC) as low as 0.25 to 4 μg/ml (*3*). Certain cationic peptides have been shown to inhibit the replication of enveloped viruses such as influenza A virus (*4*), vesicular stomatitis virus (VSV) and human immunodeficiency virus (HIV-1) (*5, 6*). Cationic peptides may also possess anticancer activity (*7, 8*) or promote wound healing (*9*). Recent studies have also indicated a role for cationic peptides as effectors of innate immune responses. It is these properties that make cationic peptides exciting candidates as new therapeutic agents.

### Structure

Currently, more than 500 cationic antimicrobial peptides have been isolated from a wide range of organisms and can be found in the Antimicrobial Sequences Database (http://www.bbcm.univ.trieste.it/~tossi/antimic.html). Peptides are classified based on their structures of which there are four major classes: β-sheet, α-helical, loop, and extended peptides (*3*), with the first two classes being the most common in nature. For

---

* A version of this chapter has been published as: Powers, J.P.S. and Hancock, R.E.W. The relationship between peptide structure and antibacterial activity. Peptides. 2003, **24**: 1681-91.

clarity, representative structures from each of these classes are indicated in Figure 1.1. In addition to the natural peptides, thousands of synthetic variant peptides have been produced which also fall into these structural classes. A common trait shared amongst the cationic antimicrobial peptides is the ability to fold into amphipathic or amphiphilic conformations, often induced by interaction with membranes or membrane mimics.

**Mechanism of action**

The mechanism of action of cationic antimicrobial peptides is being actively studied and the available information continues to grow. The majority of experiments to date have focused primarily on the interaction of cationic peptides with model membrane systems. Additional studies have also been conducted on whole microbial cells predominantly utilizing membrane potential sensitive dyes and fluorescently labeled peptides. These studies have indicated that all antimicrobial peptides interact with membranes and tend to divide peptides into two mechanistic classes: membrane disruptive and non-membrane disruptive. An alternative perspective is that as a group, cationic antimicrobial peptides have multiple actions on cells ranging from membrane permeabilization to cell wall and division effects to macromolecular synthesis inhibition and that the action responsible for killing bacteria at the minimal effective concentration varies from peptide to peptide and from bacterium to bacterium for a given peptide (*10*). While this review will briefly discuss mechanisms, more detailed reviews can be consulted (*11-16*).

The mechanism of action on Gram negative bacteria will be discussed since this has been best studied. An overview of the interaction of peptide with a Gram negative

bacterial envelope is shown as Figure 1.2. The initial association of peptides with the bacterial membrane occurs through electrostatic interactions between the cationic peptide and anionic LPS in the outer membrane leading to membrane perturbation. It has been shown that cationic peptides have a higher affinity for LPS in the outer leaflet of the outer membrane of Gram negative bacteria than do native divalent cations such as $Mg^{2+}$ and $Ca^{2+}$ (*12*). The cationic peptides displace these cations from the negatively charged LPS leading to a local disturbance in the outer membrane. This facilitates the formation of destabilized areas through which the peptide translocates the outer membrane in a process termed self-promoted uptake (*17*). Access to the cytoplasmic membrane is now possible. The peptides then associate with the outer monolayer of the cytoplasmic membrane. It is at this point that membrane disruptive and non-membrane disruptive mechanisms diverge, depending on whether this reorientation leads to perturbation of the integrity of the cytoplasmic membrane or peptide translocation into the cytoplasm.

**Membrane disruptive peptides**

Membrane disruptive peptides are generally reported to be of the α-helical structural class although, it should be strongly cautioned, that not all α-helical peptides are membrane disruptive. For example, buforin (*18*), CP10A (*19*) and a pleurocidin analogue (*20*) clearly do not have their primary action on membranes. Three mechanistic models, the "barrel stave", "micellar aggregate" and "carpet" models, have been developed to explain membrane disruption. In the barrel-stave model (*21*) the amphipathic peptides reorient perpendicular to the membrane and align (like the staves in a barrel) in a manner in which the hydrophobic side chains face outwards into the lipid

environment while the polar side chains align inward to form transmembrane pores. These pores are proposed to allow leakage of cytoplasmic components and also disrupt the membrane potential. The major argument against this model is the lack of preferred stoichiometries for the "pores" as demonstrated by the wide variability in conductance increases induced by peptides in model membranes (*22*).

The alternative micellar aggregate model (*12, 23*) suggests that the peptides reorient and associate in an informal membrane-spanning micellar or aggregate-like arrangement and further indicates that collapse of these micellar aggregates can explain translocation into the cytoplasm.

In the alternative carpet model (*24*), the peptides do not insert into the membrane but align parallel to the bilayer, remaining in contact with the lipid head groups and effectively coating the surrounding area. This orientation leads to a local disturbance in membrane stability, causing the formation of large cracks, leakage of cytoplasmic components, disruption of the membrane potential and, ultimately, disintegration of the membrane.

Regardless of which model is correct, the net result of membrane disruption would be the rapid depolarization of the bacterial cell leading to rapid cell death, with total killing occurring within five minutes for the most active peptides (*25*). It should be noted that membrane depolarization is not a lethal event per se, and in the absence of evidence of a catastrophic collapse of cytoplasmic membrane integrity, the specific way in which membrane disruption results in cell death is yet to be determined. It should also be noted that each of the above models might be correct depending on the peptide examined, such that certain peptides may function through a barrel-stave mechanism,

while others may function through a micellar aggregate or carpet mechanism. It has been recently shown that sub-inhibitory concentrations of cecropin A, classified as a lytic peptide, induce transcriptional changes within bacteria (*26*). Other studies have indicated that magainin 2 can translocate into the bacterial cytoplasm (*27*). While the significance of these changes is yet to be determined, they may suggest a role for these peptides in a non-membrane disruptive fashion.

**Other peptide mechanisms**

Peptides that do not appear to act on membranes are thought to act on cytoplasmic targets. Translocation across membranes is proposed to occur by a process related to the micellar aggregate mechanism and has been demonstrated for the frog-derived antimicrobial peptide buforin II since, rather than causing large membrane perturbations, the disruption is transient and permeabilization does not occur (*28*). Other peptides demonstrate similar results (*29*). Analogous translocation studies using eukaryotic cells have found that some arginine rich peptides are capable of translocating across both the cellular and nuclear membranes and can serve as delivery agents for conjugated compounds (*30*). Once present in the bacterial cytoplasm, cationic peptides are thought to interact with DNA, RNA and/or cellular proteins and to inhibit synthesis of these compounds. Indeed, DNA and RNA binding has been demonstrated *in vitro* (*18, 31*) and other studies have demonstrated the inhibition of macromolecular synthesis after treatment with sub-lethal peptide concentrations (*20, 32*). In addition, specific enzymatic targets have been identified for certain peptides. The proline-rich insect peptide, pyrrhocoricin, has been shown to bind the heat shock protein DnaK inhibiting chaperone-

assisted protein folding (*33*) while the *Bacillis* lantibiotic, mersacidin has been demonstrated to bind lipid II leading to the inhibition of peptidoglycan biosynthesis (*34*). For these peptides, loss of viability is much slower than with membrane-acting peptides, which exert their antimicrobial effects within minutes (*35, 36*). For pyrrhocoricin, the ability of the peptide to interfere with protein folding in live cells is not observed until 1 hour after exposure (*33*) and observable cell lysis as a result of mersacidin treatment is not seen until 3 hours after treatment (*34*).

**Structure activity relationships**

Rather than attempt to sum up the great number of structure-activity relationship studies that have been conducted to date, a representative peptide from each structural class is chosen for discussion below. For a more detailed review of specific peptides and structural classes there are numerous reviews that may be consulted.

**β-sheet peptides**

This class of peptides is characterized by the presence of an antiparallel β-sheet, generally stabilized by disulfide bonds. Larger peptides within this family may also contain minor helical segments. Perhaps the best characterized β-sheet peptides are the small 17 to 18 residue tachyplesins (Figure 1.1A). Isolated from the hemocytes of the Japanese horseshoe crab, *Tachypleus tridentatus* (*37*), the tachyplesins represent a convenient scaffold for structure-activity studies due to their small size and availability of a high-resolution $^{1}$H-NMR structure. The conformation of tachyplesin I is that of an antiparallel β-sheet (residues 3 to 8 and 11 to 16) connected by a type I β-turn (residues 8

to 11) stabilized by two disulfide bonds (residues 3 and 16 and residues 7 and 12) with an amidated C-terminus (*38*). Tachyplesin I possesses moderate antimicrobial activity (<12.5μg/ml MIC against *E. coli* K12) (*37*) as well as a high affinity for lipopolysaccharides (*39*).

Although the structure and in vitro activity of the tachyplesins are well characterized, the exact mechanism of antimicrobial activity remains poorly understood. While it is known that the tachyplesins have a high affinity for LPS, it is thought that intracellular targets also exist. Indeed, it has been shown that tachyplesin I binds the minor groove of DNA (*31*). Additional studies involving the related β-sheet peptide, polyphemusin I, demonstrate that these peptides are effective at inducing lipid flip-flop and undergoing membrane translocation but do not cause substantial entrapped calcein dye release from within model membrane systems (*29*). This suggests these peptides disrupt lipid organization leading to the translocation of peptide molecules across the bilayer but do not form long-lived pores or channels. Thus, these peptides may function through a micellar-aggregate or related model of translocation.

Several structure-activity relationship (SAR) studies have focused on the requirement of the disulfide bonds for the antimicrobial activity of these compounds. Linearization has been accomplished through adding chemical protecting groups (*40-42*) as well as amino acid substitution (*41, 43*). Studies involving linear tachyplesin chemically protected with Acetamidomethyl groups (T-Acm) demonstrate reduced antimicrobial and antiviral activity of the linear compound (*41*) as well as a reduction in calcein release from model membranes (*40*). Interestingly, although T-Acm was less effective at permeabilization of model membranes, it possessed greater membrane

disrupting ability as assayed by measuring lipid chain orientation (*40*). Additional studies, using liposomes and planar lipid bilayers, demonstrated that the linear analogue completely lacks the ability of the parent peptide to translocate across membranes (*42*). Structural characterization of T-Acm by CD spectroscopy indicated a random coil conformation in $H_2O$ (*41*) while polarized attenuated total reflection spectroscopy suggested an antiparallel β-sheet conformation in lipid environments (*40*).

Tachyplesin analogues linearized through amino acid substitution possessed similar properties to T-Acm. Cysteine residues were simultaneous substituted with aliphatic (A, L, I, V, M), aromatic (F, Y) or acidic (D) residues (*43*). Structural analysis by CD spectroscopy indicated that the analogues primarily adopt unordered and α-helical patterns in aqueous and hydrophobic environments respectively. In acidic liposomes, an isoleucine analogue was the only peptide to display a spectrum characteristic of β-sheet content, but this peptide was found to have reduced antimicrobial activity against *E. coli.*

From these studies it is apparent that, although the stabilizing disulfide bonds of tachyplesin are not absolutely required for antimicrobial activity, they are necessary to permit membrane translocation in model systems. Due to the observed differences in membrane disruption and permeabilization, it may be concluded that the mechanism of antimicrobial activity is different for the parent and linear peptides.

Recently the solution and micelle-bound structures of tachyplesin and a linear analogue were determined by $^1$H-NMR and revealed major differences between the two forms (*44*). Specifically, the association of tachyplesin with micelles (a membrane-like environment) triggers a conformational change leading to the bending of the molecule about the central arginine residues along with an associated exposure of specific

hydrophobic side chains. A linear tachyplesin analogue in which the cysteine residues are substituted with tyrosine was randomly arranged in free solution but, when bound to micelles, adopted a conformation that differs from the hinged structure formed by the native tachyplesin. This indicates that the disulfide bonds impart a stabilizing force to the overall molecule and allow the (hinge-like) bending to occur and that this structural flexibility in what has been traditionally thought of as a rather rigid β-hairpin conformation permits or drives translocation across membranes. These studies thus highlight the need for high-resolution peptide structures, rather than simple conformational analyses by circular dichroism, to provide detailed structure-activity information.

**α-helical peptides**

Peptides of the α-helical class are characterized by their α-helical conformation, and often contain a slight bend in the centre of the molecule. In one study this bending was critical for selectivity by suppressing hemolytic activity (*45*). The α-helical magainins are representative of this structural class (Figure 1.1B). Isolated from the skin of the African clawed frog, *Xenopus laevis*, magainin 1 and 2 are 23 residues in length and possess modest antimicrobial activities (e.g. MIC of 50μg/ml vs. *E. coli*) (*46*). The structure of magainin 2 has been determined by $^{1}$H-NMR in the presence of DPC and SDS micelles. The peptide adopts an amphipathic α-helical conformation with a slight bend centered at residues 12 and 13 (*47*).

The antimicrobial mechanism of magainin has been proposed to involve selective permeabilization of bacterial membranes leading to disruption of the membrane potential

(*48*). This mechanism is further supported by the observation that there are no differences in activity between D and L enantiomeric peptides, ruling out the involvement of a chiral receptor or an enzyme as the target (*49, 50*). A model has been proposed to explain the mechanism of action of magainin 2 (*23*) and follows the micellar-aggregate model of antimicrobial activity. In this model, magainins interacting with negatively charged phospholipids spontaneously form transient, membrane spanning pores, which, upon collapse, permit peptide translocation to the inner leaflet (*23, 27*). Indeed, membrane disruption has been demonstrated in model systems (*51-53*) and magainin induced depolarization has been shown in *E. coli* and model systems (*54, 55*).

Various structure-activity studies have been conducted on the α-helical magainins. N-terminal truncation of magainin 2 indicates that the first 3 residues do not play a major role in antimicrobial activity but the deletion of residue 4 (K) greatly reduces activity and further truncation of residues 5 and 6 (F and L) eliminates activity altogether (*56*). It is thought that truncation of the peptide to fewer than 20 residues (i.e. deletion of residue 4 and above) results in a compound that is unable to span the lipid bilayer and thus, from a mechanistic perspective, explains the corresponding loss of antimicrobial activity (*56*). However, α-helical peptides with as few as 13 residues can possess antimicrobial activity so an ability to span a lipid bilayer is not an obligate requirement for activity of α-helical peptides (*29*).

In both the membrane-disruptive and non-membrane-disruptive mechanisms of peptide antimicrobial activity, the initial step is the interaction of the cationic peptide with the negatively charged cell surface. It thus remains of key interest to determine the forces leading to favourable association, as well as to ascertain if this step is simply

driven by electrostatic attraction. To this end, the contribution of charge toward the activity of magainin 2 has been investigated using analogues with varying cationic charges (*57*). It was determined that charge increase to +5 is accompanied by a corresponding increase in antimicrobial activity. Further increase of charge to +7 did not alter the maximal activity observed at +5, however, hemolytic activity was found to increase. Interestingly, experiments using model membranes composed of the anionic lipid phosphatidylglycerol found that an increase in charge actually led to a decrease in membrane permeabilizing ability. This is likely a result of the corresponding decrease in hydrophobicity that accompanies an increase in charge.

**Extended peptides**

The extended class of peptides lack classical secondary structures, generally due to their high proline and/or glycine contents. Indeed, these peptides form their final structures not through interresidue hydrogen bonds but by hydrogen bond and Van der Waals interactions with membrane lipids. Perhaps the best characterized representative of the extended family of cationic peptides is the tryptophan and proline rich indolicidin (Figure 1.1C). Indolicidin is a 13-residue, C-terminal amidated peptide isolated from the cytoplasmic granules of bovine neutrophils (*58*). Of these 13 residues, 5 are tryptophan thus making indolicidin the peptide with the highest known proportion of tryptophans (*58*). The conformation of indolicidin is dependent on its environment. The structure of indolicidin has been determined by $^{1}$H-NMR in both anionic SDS and zwitterionic dodecylphosphocholine (DPC) micelles (*59*). In both lipid environments the molecule exists in an extended conformation however, in neutral DPC micelles, the molecule takes

on a more bent conformation due to two half-turns about residues 5 and 8. Indolicidin possesses reasonable antimicrobial activity (MIC of 10μg/ml against *E. coli*) but does not have a high affinity for LPS (*60*) when compared to other peptides such as the β-hairpin tachyplesins (*39*).

The antimicrobial mechanism of indolicidin has yet to be unambiguously identified. It was first hypothesized that indolicidin acts by disrupting the cytoplasmic membrane by voltage induced channel formation driven by membrane potential (*60*). This hypothesis is certainly plausible given the size of indolicidin (25 x 32 Å) making it possible to span biological membranes (*59*). However, intact cell experiments demonstrated that, under conditions where greater than 99% of cells were killed, indolicidin was unable to completely depolarize the cytoplasmic membrane of *E. coli* (*22*) and *S. aureus* (*10*) arguing against membrane disruption as a mechanism. In addition to its channel forming ability, indolicidin has also been shown to induce filamentation of *E. coli*, which is thought to be a result of DNA synthesis inhibition (*61*). In order for this mechanism to be effective, membrane translocation must obviously occur. It is interesting to note that, in accordance with the micellar-aggregate model of antimicrobial activity, both hypotheses combine to explain the actions of indolicidin; the formation of informal aggregate channels that, upon collapse, lead to translocation of the peptide into the cytoplasm.

In model membrane studies, indolicidin is not effective at translocating across membranes and we assume that in bacteria the trans-cytoplasmic membrane electrical potential gradient of -140mV is required to drive translocation. To improve upon and understand the structural requirements required for the antimicrobial activity of

indolicidin, various improved analogues have been synthesized. Two particular analogues, CP-11, which possesses an increased cationic charge, and CP10A, in which all proline residues are replaced with alanine, with improved activity versus Gram negative and Gram positive bacteria respectively, are of particular interest. With CP-11, the increase in charge results in a decrease in monolayer insertion, lipid flip-flop and calcein release, and membrane translocation (in the absence of a membrane potential) remained poor (*29*). In the case of CP10A, monolayer insertion, lipid flip-flop and membrane translocation were increased while calcein release was reduced (*29*). Structural analysis by $^{1}$H-NMR revealed that the substitution of proline with alanine enables CP10A to adopt a helical conformation (*19*) rather than the extended structure of the parent indolicidin (*59*). Thus, in the case of the indolicidin family of peptides, it appears to be conformational changes rather than changes in charge or hydrophobicity that account for differences in activity. The change in conformation from extended to helical, led to increased membrane insertion and improved membrane translocation, allowing CP10A better access to the cytoplasm and cytoplasmic targets.

**Loop peptides**

This class of peptides is characterized by their loop structure imparted by the presence of a single bond (disulfide, amide or isopeptide). The only member of the loop family of peptides with an available high-resolution structure is thanatin (Figure 1.1D). Thanatin is a 21-residue, loop peptide isolated from the spined soldier bug, *Podisus maculiventris* (*62*). The solution structure of thanatin has been determined by $^{1}$H-NMR and is that of an anti-parallel β-sheet, formed by residues 8 to 21, stabilized by the single

disulfide bond between residues 11 and 18 (*63*). Thanatin possesses reasonable antimicrobial activity against Gram negative and Gram positive bacteria as well as fungi (*62*) and is comparable in activity to members of the β-sheet family of peptides.

While the exact antimicrobial mechanism of thanatin remains unknown, it is thought to involve targets other than membranes, as treatment with peptide does not induce changes in permeability (*62*). The mechanism of killing is believed to be dependent on the organism and, while both D and L enantiomers are equally active against Gram positive and fungal species, only L-thanatin is active against Gram negative bacteria (*62*). This suggests that a stereospecific target such as a receptor may be involved in Gram negative bacteria while non-specific interactions dominate in both fungi and Gram positive bacteria (*62*). Structure-activity studies have revealed that truncation of the C-terminus or beyond the third N-terminal residue greatly reduces activity and the loop region alone is completely inactive (*62*).

**Lipids and peptide activity**

While great interest in the influence on peptide activity of structure has been evident, very little focus has been directed at other factors directly influencing peptide-membrane interactions. Recently there has been increased attention on membrane lipids and their potential role in peptide activity. While the number of studies investigating the relationship between antimicrobial peptides and membrane lipids remain few and limited in their scope, related compounds, namely cationic lipids, have been investigated. These compounds are similar to antimicrobial peptides in charge, amphipathicity and ability to deliver compounds intracellularly.

Recently, Hafez et al. have proposed a mechanistic model explaining the intracellular delivery of polynucleic acids by cationic lipids (*64*). Briefly, plasmid-cationic lipid complexes are taken up by endocytosis and act to destabilize the endosomal membrane. This is driven by the association of cationic lipid headgroups with the anionic phospholipid headgroups of the inner endosomal membrane resulting in the formation of an ion pair with a supramolecular structure effectively resembling that of a type II lipid. The overall effect is the disruption of the endosomal membrane through hexagonal ($H_{II}$) phase formation. Based upon this mechanism, it is conceivable that cationic peptides act in a similar manner by binding anionic phospholipids that are abundant in bacterial membranes.

**Type II lipids and translocation**

Studies focusing on membrane lipid composition have indicated the importance of specific lipids for normal membrane function. Rietveld et al. demonstrated that *E. coli* mutants deficient in phosphatidylethanolamine synthesis are greatly diminished in their ability to transport proteins across the plasma membrane but this could be increased by the addition of divalent cations or the type II lipid DOPE, both of which induce non-bilayer phase formation (*65*). In a similar study, Bogdanov et al. showed this mutant does not produce a properly folded lactose permease but renaturation of the protein in the presence of PE induces proper folding (*66*).

These studies indicate the importance of non-bilayer-forming lipids to membrane translocation and protein folding. It is therefore conceivable that specific phospholipids

or membrane phases are required for peptide translocation and may play as significant a role as peptide structure in determining translocation efficiency.

**Polyphemusins**

Of particular interest to our laboratory are the β-hairpin polyphemusins. These peptides, closely related to the tachyplesins described above, are isolated from the hemocytes of the American horseshoe crab, *Limulus polyphemus* (*67*). This natural peptide family consists of two members, designated polyphemusin I and II, which differ in a single amino acid (R to K) (Table 1). Based upon sequence similarity to tachyplesin I and its solution structure (*38, 68*), the polyphemusins were assumed to form an amphipathic β-sheet structure, with positively charged termini and β-turn regions that resemble the structure of a hairpin or horseshoe. These peptides possess excellent antimicrobial activity, in the low micromolar range (*67*), but elicit relatively little membrane damage (*29*) and thus, are not believed to function simply through a mechanism involving membrane disruption. In addition, the polyphemusins possess other desirable therapeutic properties such as the ability to bind lipopolysaccharide (*67*) and prevent HIV infection by acting as a CXCR4 antagonist (*69*).

**Objectives**

While the number of antimicrobial peptides that have been chemically characterized continues to grow, the number of those with available high-resolution structures remains relatively small. To date, structure activity analyses of a broad range of peptides reveal two main requirements for antimicrobial activity, 1) a cationic charge

and 2) an induced amphipathic conformation. Indeed, conformational change leading to an active structure seems to be needed as, even the β-hairpin peptide tachyplesin, a peptide once thought to be rigid in conformation, undergoes a major change in a lipid environment. In addition, studies focused on mechanism of action have concentrated primarily upon the chemical and structural properties of the peptides themselves while relatively little interest has been placed upon other factors. Specifically, membrane components may play a significant role in the activity of peptides. Indeed, studies focused upon the translocation of other cationic compounds have revealed major contributions from non-bilayer forming lipids and thus, suggest the importance of these compounds in the mechanism of action of antimicrobial peptides. The diversity of lipids among microorganisms may very well explain the differences in activity of a single peptide between these species and thus, further study of the interactions between antimicrobial peptides and lipids are required to propose an accurate mechanism of activity for each peptide and organism.

This thesis will be focused upon the highly active β-sheet polyphemusins. In an effort to explain the antimicrobial mechanism of action of these peptides it was of interest to begin with a high resolution three dimensional structure (Chapter 2). A brief investigation of structure activity relationships of polyphemusin I, specifically focused on the involvement of the native disulfide bound conformation upon activity was also undertaken (Chapter 2). The interaction of these peptides with whole bacterial cells and model lipid membranes was characterized and used to construct a model of the antimicrobial mechanism of the polyphemusins (Chapter 3). Finally, the localization of polyphemusin I, following incubation with *E. coli* cells, was investigated to provide

further evidence of the membrane translocating ability of these peptides as well as identify potential targets involved in antimicrobial activity (Chapter 4).

**Table 1.1.** Amino acid sequences and chemical properties of the naturally occurring, horseshoe crab, polyphemusin and tachyplesin antimicrobial peptides.

| Peptide | | Residues | Sequence | Charge (pH=7) | Reference |
|---|---|---|---|---|---|
| Polyphemusin | I | 18 | RRWCFRVCYRGFCYRKCR* | 7 | (*67*) |
| | II | 18 | RRWCFRVCYKGFCYRKCR* | 7 | (*67*) |
| Tachyplesin | I | 17 | KWCFRVCYRGICYRRCR* | 6 | (*37*) |
| | II | 17 | RWCFRVCYRGICYRKCR* | 6 | (*67*) |
| | III | 17 | KWCFRVCYRGICYRKCR* | 6 | (*70*) |

* amidated C-terminus

**Figure 1.1.** Structural classes of antimicrobial peptides. A) β-sheet, tachyplesin I (*44*); B) α-helical, magainin 2 (*47*); C) Extended, indolicidin (*59*); D) Loop, thanatin (*63*). Disulfide bonds are indicated in yellow. Figure prepared with MOLMOL (*71*).

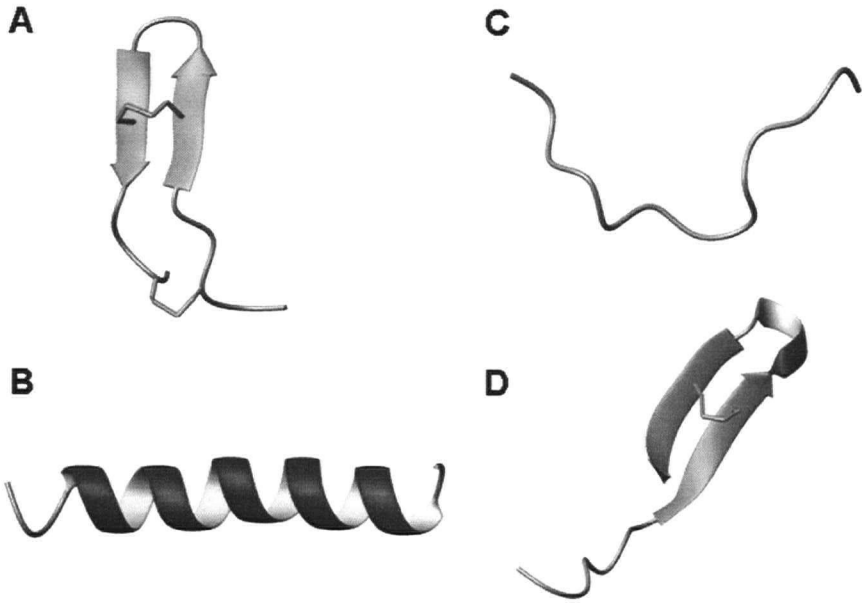

**Figure 1.2.** Proposed mechanism of interaction of cationic antimicrobial peptides with the cell envelope of Gram-negative bacteria. Passage across the outer membrane is proposed to occur by self-promoted uptake. According to this hypothesis, unfolded cationic peptides are proposed to associate with the negatively charged surface of the outer membrane and either neutralize the charge over a patch of the outer membrane, creating cracks through which the peptide can cross the outer membrane (A), or actually bind to the divalent cation binding sites (stars) on LPS and disrupt the membrane (B). Once the peptide has transited the outer membrane, it will bind to the negatively charged surface of the cytoplasmic membrane, created by the headgroups of phosphatidylglycerol and cardiolipin, and the amphipathic peptide will insert into the membrane interface (the region where the phospholipid headgroups meet the fatty acyl chains of the phospholipid membrane) (C). It is not known at which point in this process the peptide actually folds into its amphipathic structure (i.e., during transit across the outer membrane or during insertion into the cytoplasmic membrane). Many peptide molecules will insert into the membrane interface and are proposed to then either aggregate into a micelle-like complex which spans the membrane (D) or flip-flop across the membrane under the influence of the large transmembrane electrical potential gradient (approximately -140 mV) (E). The micelle-like aggregates (D) are proposed to have water associated with them, and this provides channels for the movement of ions across the membrane and possibly leakage of larger water-soluble molecules. These aggregates would be variable in size and lifetime and will dissociate into monomers that may be disposed at either side of the membrane. The net effect of D and E is that some monomers will be translocated into the cytoplasm

and can dissociate from the membrane and bind to cellular polyanions such as DNA and RNA (F). This figure is reproduced from (*12*).

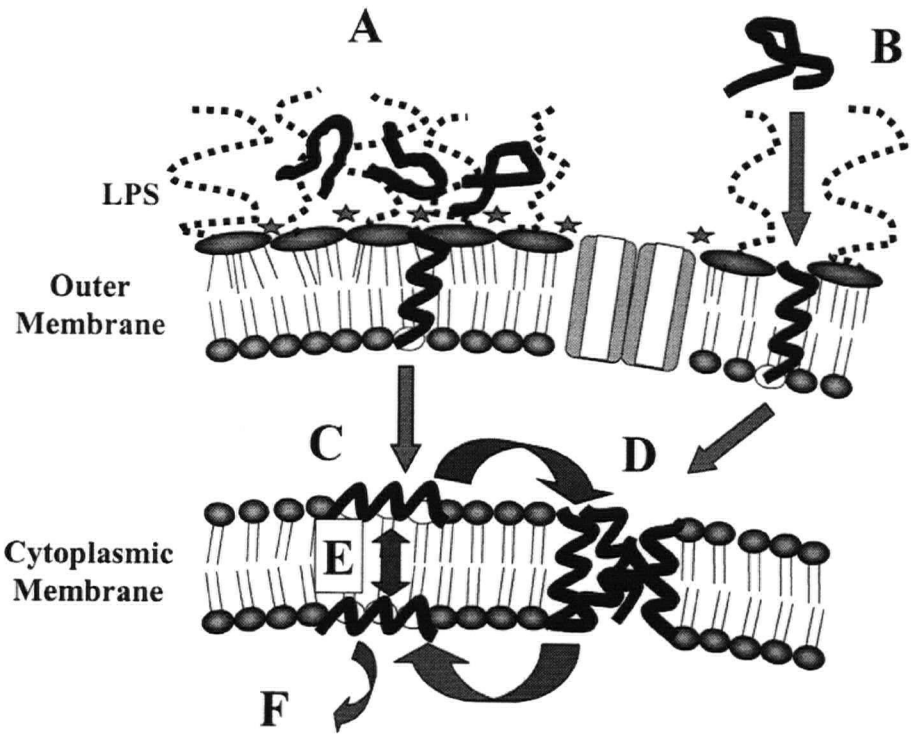

**References**


1. Mohammad, F. V., Noorwala, M., Ahmad, V. U., and Sener, B. (1995) Bidesmosidic triterpenoidal saponins from the roots of Symphytum officinale, *Planta Med 61*, 94.

2. Aley, S. B., Zimmerman, M., Hetsko, M., Selsted, M. E., and Gillin, F. D. (1994) Killing of Giardia lamblia by cryptdins and cationic neutrophil peptides, *Infect Immun 62*, 5397-403.

3. Hancock, R. E. W., and Lehrer, R. (1998) Cationic peptides: a new source of antibiotics, *Trends Biotechnol 16*, 82-8.

4. Murakami, T., Niwa, M., Tokunaga, F., Miyata, T., and Iwanaga, S. (1991) Direct virus inactivation of tachyplesin I and its isopeptides from horseshoe crab hemocytes, *Chemotherapy 37*, 327-34.

5. Morimoto, M., Mori, H., Otake, T., Ueba, N., Kunita, N., Niwa, M., Murakami, T., and Iwanaga, S. (1991) Inhibitory effect of tachyplesin I on the proliferation of human immunodeficiency virus in vitro, *Chemotherapy 37*, 206-11.

6. Masuda, M., Nakashima, H., Ueda, T., Naba, H., Ikoma, R., Otaka, A., Terakawa, Y., Tamamura, H., Ibuka, T., Murakami, T., and et al. (1992) A novel anti-HIV synthetic peptide, T-22 ([Tyr5,12,Lys7]-polyphemusin II), *Biochem Biophys Res Commun 189*, 845-50.

7. Baker, M. A., Maloy, W. L., Zasloff, M., and Jacob, L. S. (1993) Anticancer efficacy of Magainin2 and analogue peptides, *Cancer Res 53*, 3052-7.

8. Johnstone, S. A., Gelmon, K., Mayer, L. D., Hancock, R. E. W., and Bally, M. B. (2000) In vitro characterization of the anticancer activity of membrane-active

cationic peptides. I. Peptide-mediated cytotoxicity and peptide- enhanced cytotoxic activity of doxorubicin against wild-type and p- glycoprotein over-expressing tumor cell lines, *Anticancer Drug Des 15*, 151-60.

9. Gallo, R. L., Ono, M., Povsic, T., Page, C., Eriksson, E., Klagsbrun, M., and Bernfield, M. (1994) Syndecans, cell surface heparin sulfate proteoglycans, are induced by a proline-rich antimicrobial peptide from wounds, *Proc Natl Acad Sci U S A 91*, 11035-9.

10. Friedrich, C. L., Moyles, D., Beveridge, T. J., and Hancock, R. E. W. (2000) Antibacterial action of structurally diverse cationic peptides on gram- positive bacteria, *Antimicrob Agents Chemother 44*, 2086-92.

11. Hwang, P. M., and Vogel, H. J. (1998) Structure-function relationships of antimicrobial peptides, *Biochem Cell Biol 76*, 235-46.

12. Hancock, R. E. W., and Chapple, D. S. (1999) Peptide antibiotics, *Antimicrob Agents Chemother 43*, 1317-23.

13. Epand, R. M., and Vogel, H. J. (1999) Diversity of antimicrobial peptides and their mechanisms of action, *Biochim Biophys Acta 1462*, 11-28.

14. Shai, Y. (1999) Mechanism of the binding, insertion and destabilization of phospholipid bilayer membranes by alpha-helical antimicrobial and cell non-selective membrane-lytic peptides, *Biochim Biophys Acta 1462*, 55-70.

15. Oren, Z., and Shai, Y. (1998) Mode of action of linear amphipathic alpha-helical antimicrobial peptides, *Biopolymers 47*, 451-63.

16. Hancock, R. E. W., and Rozek, A. (2002) Role of membranes in the activities of antimicrobial cationic peptides, *FEMS Microbiol Lett 206*, 143-9.

17. Hancock, R. E. W. (1997) Peptide antibiotics, *Lancet 349*, 418-22.

18. Park, C. B., Kim, H. S., and Kim, S. C. (1998) Mechanism of action of the antimicrobial peptide buforin II: buforin II kills microorganisms by penetrating the cell membrane and inhibiting cellular functions, *Biochem Biophys Res Commun 244*, 253-7.

19. Friedrich, C. L., Rozek, A., Patrzykat, A., and Hancock, R. E. W. (2001) Structure and mechanism of action of an indolicidin peptide derivative with improved activity against gram-positive bacteria, *J Biol Chem 276*, 24015-22.

20. Patrzykat, A., Friedrich, C. L., Zhang, L., Mendoza, V., and Hancock, R. E. W. (2002) Sublethal concentrations of pleurocidin-derived antimicrobial peptides inhibit macromolecular synthesis in Escherichia coli, *Antimicrob Agents Chemother 46*, 605-14.

21. Ehrenstein, G., and Lecar, H. (1977) Electrically gated ionic channels in lipid bilayers, *Q Rev Biophys 10*, 1-34.

22. Wu, M., Maier, E., Benz, R., and Hancock, R. E. W. (1999) Mechanism of interaction of different classes of cationic antimicrobial peptides with planar bilayers and with the cytoplasmic membrane of Escherichia coli, *Biochemistry 38*, 7235-42.

23. Matsuzaki, K., Sugishita, K., Harada, M., Fujii, N., and Miyajima, K. (1997) Interactions of an antimicrobial peptide, magainin 2, with outer and inner membranes of Gram-negative bacteria, *Biochim Biophys Acta 1327*, 119-30.

24. Pouny, Y., Rapaport, D., Mor, A., Nicolas, P., and Shai, Y. (1992) Interaction of antimicrobial dermaseptin and its fluorescently labeled analogues with phospholipid membranes, *Biochemistry 31*, 12416-23.

25. Friedrich, C., Scott, M. G., Karunaratne, N., Yan, H., and Hancock, R. E. W. (1999) Salt-resistant alpha-helical cationic antimicrobial peptides, *Antimicrob Agents Chemother 43*, 1542-8.

26. Hong, R. W., Shchepetov, M., Weiser, J. N., and Axelsen, P. H. (2003) Transcriptional Profile of the Escherichia coli Response to the Antimicrobial Insect Peptide Cecropin A, *Antimicrob Agents Chemother 47*, 1-6.

27. Matsuzaki, K., Murase, O., Fujii, N., and Miyajima, K. (1995) Translocation of a channel-forming antimicrobial peptide, magainin 2, across lipid bilayers by forming a pore, *Biochemistry 34*, 6521-6.

28. Park, C. B., Yi, K. S., Matsuzaki, K., Kim, M. S., and Kim, S. C. (2000) Structure-activity analysis of buforin II, a histone H2A-derived antimicrobial peptide: the proline hinge is responsible for the cell- penetrating ability of buforin II, *Proc Natl Acad Sci U S A 97*, 8245-50.

29. Zhang, L., Rozek, A., and Hancock, R. E. W. (2001) Interaction of cationic antimicrobial peptides with model membranes, *J Biol Chem 276*, 35714-22.

30. Futaki, S., Suzuki, T., Ohashi, W., Yagami, T., Tanaka, S., Ueda, K., and Sugiura, Y. (2001) Arginine-rich peptides. An abundant source of membrane-permeable peptides having potential as carriers for intracellular protein delivery, *J Biol Chem 276*, 5836-40.

31. Yonezawa, A., Kuwahara, J., Fujii, N., and Sugiura, Y. (1992) Binding of tachyplesin I to DNA revealed by footprinting analysis: significant contribution of secondary structure to DNA binding and implication for biological action, *Biochemistry 31*, 2998-3004.

32. Lehrer, R. I., Barton, A., Daher, K. A., Harwig, S. S., Ganz, T., and Selsted, M. E. (1989) Interaction of human defensins with Escherichia coli. Mechanism of bactericidal activity, *J Clin Invest 84*, 553-61.

33. Kragol, G., Lovas, S., Varadi, G., Condie, B. A., Hoffmann, R., and Otvos, L., Jr. (2001) The antibacterial peptide pyrrhocoricin inhibits the ATPase actions of DnaK and prevents chaperone-assisted protein folding, *Biochemistry 40*, 3016-26.

34. Brotz, H., Bierbaum, G., Leopold, K., Reynolds, P. E., and Sahl, H. G. (1998) The lantibiotic mersacidin inhibits peptidoglycan synthesis by targeting lipid II, *Antimicrob Agents Chemother 42*, 154-60.

35. Giacometti, A., Cirioni, O., Greganti, G., Quarta, M., and Scalise, G. (1998) In vitro activities of membrane-active peptides against gram-positive and gram-negative aerobic bacteria, *Antimicrob Agents Chemother 42*, 3320-4.

36. Giacometti, A., Cirioni, O., Barchiesi, F., Del Prete, M. S., and Scalise, G. (1999) Antimicrobial activity of polycationic peptides, *Peptides 20*, 1265-73.

37. Nakamura, T., Furunaka, H., Miyata, T., Tokunaga, F., Muta, T., Iwanaga, S., Niwa, M., Takao, T., and Shimonishi, Y. (1988) Tachyplesin, a class of antimicrobial peptide from the hemocytes of the horseshoe crab (Tachypleus tridentatus). Isolation and chemical structure, *J Biol Chem 263*, 16709-13.

38. Kawano, K., Yoneya, T., Miyata, T., Yoshikawa, K., Tokunaga, F., Terada, Y., and Iwanaga, S. (1990) Antimicrobial peptide, tachyplesin I, isolated from hemocytes of the horseshoe crab (Tachypleus tridentatus). NMR determination of the beta- sheet structure, *J Biol Chem 265*, 15365-7.

39. Hirakura, Y., Kobayashi, S., and Matsuzaki, K. (2002) Specific interactions of the antimicrobial peptide cyclic beta-sheet tachyplesin I with lipopolysaccharides, *Biochim Biophys Acta 1562*, 32-6.

40. Matsuzaki, K., Nakayama, M., Fukui, M., Otaka, A., Funakoshi, S., Fujii, N., Bessho, K., and Miyajima, K. (1993) Role of disulfide linkages in tachyplesin-lipid interactions, *Biochemistry 32*, 11704-10.

41. Tamamura, H., Ikoma, R., Niwa, M., Funakoshi, S., Murakami, T., and Fujii, N. (1993) Antimicrobial activity and conformation of tachyplesin I and its analogs, *Chem Pharm Bull (Tokyo) 41*, 978-80.

42. Matsuzaki, K., Yoneyama, S., Fujii, N., Miyajima, K., Yamada, K., Kirino, Y., and Anzai, K. (1997) Membrane permeabilization mechanisms of a cyclic antimicrobial peptide, tachyplesin I, and its linear analog, *Biochemistry 36*, 9799-806.

43. Rao, A. G. (1999) Conformation and antimicrobial activity of linear derivatives of tachyplesin lacking disulfide bonds, *Arch Biochem Biophys 361*, 127-34.

44. Laederach, A., Andreotti, A. H., and Fulton, D. B. (2002) Solution and micelle-bound structures of tachyplesin I and its active aromatic linear derivatives, *Biochemistry 41*, 12359-68.

45. Zhang, L., Benz, R., and Hancock, R. E. W. (1999) Influence of proline residues on the antibacterial and synergistic activities of alpha-helical peptides, *Biochemistry 38*, 8102-11.

46. Zasloff, M. (1987) Magainins, a class of antimicrobial peptides from Xenopus skin: isolation, characterization of two active forms, and partial cDNA sequence of a precursor, *Proc Natl Acad Sci U S A 84*, 5449-53.

47. Gesell, J., Zasloff, M., and Opella, S. J. (1997) Two-dimensional $^{1}$H NMR experiments show that the 23-residue magainin antibiotic peptide is an alpha-helix in dodecylphosphocholine micelles, sodium dodecylsulfate micelles, and trifluoroethanol/water solution, *J Biomol NMR 9*, 127-35.

48. Matsuzaki, K. (1998) Magainins as paradigm for the mode of action of pore forming polypeptides, *Biochim Biophys Acta 1376*, 391-400.

49. Wade, D., Boman, A., Wahlin, B., Drain, C. M., Andreu, D., Boman, H. G., and Merrifield, R. B. (1990) All-D amino acid-containing channel-forming antibiotic peptides, *Proc Natl Acad Sci U S A 87*, 4761-5.

50. Bessalle, R., Kapitkovsky, A., Gorea, A., Shalit, I., and Fridkin, M. (1990) All-D-magainin: chirality, antimicrobial activity and proteolytic resistance, *FEBS Lett 274*, 151-5.

51. Matsuzaki, K., Harada, M., Handa, T., Funakoshi, S., Fujii, N., Yajima, H., and Miyajima, K. (1989) Magainin 1-induced leakage of entrapped calcein out of negatively-charged lipid vesicles, *Biochim Biophys Acta 981*, 130-4.

52. Matsuzaki, K., Harada, M., Funakoshi, S., Fujii, N., and Miyajima, K. (1991) Physicochemical determinants for the interactions of magainins 1 and 2 with acidic lipid bilayers, *Biochim Biophys Acta 1063*, 162-70.

53. Matsuzaki, K., Murase, O., and Miyajima, K. (1995) Kinetics of pore formation by an antimicrobial peptide, magainin 2, in phospholipid bilayers, *Biochemistry 34*, 12553-9.

54. Juretic, D., Chen, H. C., Brown, J. H., Morell, J. L., Hendler, R. W., and Westerhoff, H. V. (1989) Magainin 2 amide and analogues. Antimicrobial activity, membrane depolarization and susceptibility to proteolysis, *FEBS Lett 249*, 219-23.

55. Juretic, D., Hendler, R. W., Kamp, F., Caughey, W. S., Zasloff, M., and Westerhoff, H. V. (1994) Magainin oligomers reversibly dissipate delta microH+ in cytochrome oxidase liposomes, *Biochemistry 33*, 4562-70.

56. Zasloff, M., Martin, B., and Chen, H. C. (1988) Antimicrobial activity of synthetic magainin peptides and several analogues, *Proc Natl Acad Sci U S A 85*, 910-3.

57. Dathe, M., Nikolenko, H., Meyer, J., Beyermann, M., and Bienert, M. (2001) Optimization of the antimicrobial activity of magainin peptides by modification of charge, *FEBS Lett 501*, 146-50.

58. Selsted, M. E., Novotny, M. J., Morris, W. L., Tang, Y. Q., Smith, W., and Cullor, J. S. (1992) Indolicidin, a novel bactericidal tridecapeptide amide from neutrophils, *J Biol Chem 267*, 4292-5.

59. Rozek, A., Friedrich, C. L., and Hancock, R. E. W. (2000) Structure of the bovine antimicrobial peptide indolicidin bound to dodecylphosphocholine and sodium dodecyl sulfate micelles, *Biochemistry 39*, 15765-74.

60. Falla, T. J., Karunaratne, D. N., and Hancock, R. E. W. (1996) Mode of action of the antimicrobial peptide indolicidin, *J Biol Chem 271*, 19298-303.

61. Subbalakshmi, C., and Sitaram, N. (1998) Mechanism of antimicrobial action of indolicidin, *FEMS Microbiol Lett 160*, 91-6.

62. Fehlbaum, P., Bulet, P., Chernysh, S., Briand, J. P., Roussel, J. P., Letellier, L., Hetru, C., and Hoffmann, J. A. (1996) Structure-activity analysis of thanatin, a 21-residue inducible insect defense peptide with sequence homology to frog skin antimicrobial peptides, *Proc Natl Acad Sci U S A 93*, 1221-5.

63. Mandard, N., Sodano, P., Labbe, H., Bonmatin, J. M., Bulet, P., Hetru, C., Ptak, M., and Vovelle, F. (1998) Solution structure of thanatin, a potent bactericidal and fungicidal insect peptide, determined from proton two-dimensional nuclear magnetic resonance data, *Eur J Biochem 256*, 404-10.

64. Hafez, I. M., Maurer, N., and Cullis, P. R. (2001) On the mechanism whereby cationic lipids promote intracellular delivery of polynucleic acids, *Gene Ther 8*, 1188-96.

65. Rietveld, A. G., Koorengevel, M. C., and de Kruijff, B. (1995) Non-bilayer lipids are required for efficient protein transport across the plasma membrane of Escherichia coli, *Embo J 14*, 5506-13.

66. Bogdanov, M., Sun, J., Kaback, H. R., and Dowhan, W. (1996) A phospholipid acts as a chaperone in assembly of a membrane transport protein, *J Biol Chem 271*, 11615-8.

67. Miyata, T., Tokunaga, F., Yoneya, T., Yoshikawa, K., Iwanaga, S., Niwa, M., Takao, T., and Shimonishi, Y. (1989) Antimicrobial peptides, isolated from horseshoe crab hemocytes, tachyplesin II, and polyphemusins I and II: chemical structures and biological activity, *J Biochem (Tokyo) 106*, 663-8.

68. Tamamura, H., Kuroda, M., Masuda, M., Otaka, A., Funakoshi, S., Nakashima, H., Yamamoto, N., Waki, M., Matsumoto, A., Lancelin, J. M., and et al. (1993) A comparative study of the solution structures of tachyplesin I and a novel anti-HIV synthetic peptide, T22 ([Tyr5,12, Lys7]-polyphemusin II), determined by nuclear magnetic resonance, *Biochim Biophys Acta 1163*, 209-16.

69. Tamamura, H., Arakaki, R., Funakoshi, H., Imai, M., Otaka, A., Ibuka, T., Nakashima, H., Murakami, T., Waki, M., Matsumoto, A., Yamamoto, N., and Fujii, N. (1998) Effective lowly cytotoxic analogs of an HIV-cell fusion inhibitor, T22 ([Tyr5,12, Lys7]-polyphemusin II), *Bioorg Med Chem 6*, 231-8.

70. Muta, T., Fujimoto, T., Nakajima, H., and Iwanaga, S. (1990) Tachyplesins isolated from hemocytes of Southeast Asian horseshoe crabs (Carcinoscorpius rotundicauda and Tachypleus gigas): identification of a new tachyplesin, tachyplesin III, and a processing intermediate of its precursor, *J Biochem (Tokyo) 108*, 261-6.

71. Koradi, R., Billeter, M., and Wuthrich, K. (1996) MOLMOL: a program for display and analysis of macromolecular structures, *J Mol Graph 14*, 51-5, 29-32.

## Chapter 2 - Structure-activity relationships for the β-hairpin cationic antimicrobial peptide polyphemusin I*

### Introduction

The invertebrate hemolymph has been found to contain a variety of substances that act to protect the animal from invading microorganisms (*1*). Included in these substances are cationic antimicrobial peptides. Of interest are two families of β-sheet peptides isolated from horseshoe crabs; the tachyplesins, from the Japanese horseshoe crab *Tachypleus tridentatus*, and the polyphemusins, from the American horseshoe crab *Limulus polyphemus* (*2*). These peptides are 17 to 18 amino acid residues in length, contain two disulfide bonds and have an amidated C-terminal arginine (*1*). Both families of peptides possess antibacterial activity, inhibiting the growth of both Gram positive and Gram negative species, and fungi (*1*), in addition to an ability to prevent the replication of enveloped viruses such as influenza A and HIV (*3*).

The tachyplesins are particularly well characterized. The structure of tachyplesin I has been determined by NMR spectroscopy and was found to consist of an antiparallel β-sheet (residues 3-8 and 11-16), constrained by two disulfide bonds, connected by a β-turn (residues 8-11) (*4*). Due to their high sequence similarity (Tachyplesin I: **K**WCFRVCYRG**I**CYR**R**CR-$NH_2$; Polyphemusin I: **RR**WCFRVCYRG**F**CYR**K**CR-$NH_2$, where the differences are indicated in bold), the structures of the polyphemusins have been assumed to be virtually identical to that of tachyplesin I. Indeed the structure

* A version of this chapter has been published as: Powers, J.P.S., Rozek, A., and Hancock, R.E.W. Structure-activity relationships for the β-hairpin cationic antimicrobial peptide polyphemusin I. Biochimica et Biophysica Acta. 2004, **1698**:239-50.

of a synthetic polyphemusin variant, T22, was determined by NMR spectroscopy and the secondary structure was found to be related to that of tachyplesin I (*3*).

Although the structures of some cationic antimicrobial peptides have been determined, their mechanism of action remains controversial. The earliest proposed mechanism involved the interaction of the peptide with the bacterial membrane, insertion and aggregation to form small pores (*5*). This was believed to lead to membrane depolarization and death of the microorganism. Recent studies have shown that this may not always be the case, as certain antimicrobial peptides (such as bactenecin and indolicidin) do not cause permanent membrane depolarization (*6*). It has been proposed that peptides acting in this manner translocate the cytoplasmic membrane and interact with DNA, RNA or protein synthesis (*7, 8*). Indeed, DNA and RNA binding has been demonstrated *in vitro* (*9, 10*) and other studies have demonstrated the inhibition of macromolecular synthesis after treatment with sub-lethal peptide concentrations (*11, 12*).

The role of disulfide bonds in peptide activity has been previously investigated. Linear forms of human α-defensin HNP-1 are completely inactive (*13*). In contrast the chemotactic activity of human β-defensin 3 requires proper disulfide formation while antimicrobial activity does not, and linear analogues possess similar activity to the parent peptides (*14*). Conversely, the disulfide bond which forms the loop of bovine bactenecin is required for activity against Gram negative organisms and is thought to play a role in outer membrane permeabilization (*15*). Evidence suggests that linear bactenecin can still adopt a secondary structure upon interaction with membranes. Thus, the role of disulfide bonds in antimicrobial activity seems to vary between peptides as opposed to playing a

general role. One possibility is that such a role depends on the ability of linear peptides to form defined amphipathic structures upon membrane contact.

Specific disulfide studies focusing on tachyplesin I have indicated that, in MIC studies with *E. coli*, linear analogues display a reduced activity with the exception of peptides linearized by the substitution with aromatic amino acids (*16*). Structural characterization of these aromatic substituted peptides have revealed that, in the case of tyrosine substituted analogues, aromatic ring stacking serves to stabilize the β-hairpin structure in solution similar to that of a disulfide bond (*17*). These findings suggest that the aromatic substituted "linear" analogues possess similar β-hairpin structure to the parent peptide and thus may account for the similar antimicrobial activity.

In an effort to further explore the role that disulfide bonds and defined, β-hairpin structure play in the antimicrobial activity of these peptides a structure-activity study was undertaken. The peptide polyphemusin I was chosen as a model and an analogue (PM1-S) was synthesized with all four cysteine residues simultaneously substituted with serine. Serine was chosen because in all previous experiments involving linear analogues of tachyplesin, serine analogues were not chosen. In addition, serine is similar in both structure and chemistry to cysteine without the corresponding disulfide bonding ability. To provide a basis for future structure-activity relationship studies of the polyphemusins, the three-dimensional structure of polyphemusin I was determined by $^{1}$H-NMR and the structure and antimicrobial activities of the linear analogue were then compared with those of the parent peptide.

## Materials and methods

### Strains and reagents

The bacterial strains used for the antimicrobial activity assays included *Escherichia coli* (*E. coli*) UB1005 ($F^-$, *nal*A37, *met*B1) and its outer membrane altered mutant DC2 (*18*), a wild type *Salmonella typhimurium* (*S. typhimurium*) and its defensin sensitive mutant (*19*), wild type *Pseudomonas aeruginosa* (*P. aeruginosa*) K799 and its antibiotic sensitive mutant Z61 (*20*), *Enterococcus faecalis* (*E. faecalis*) ATCC29212, methicillin resistant *Staphylococcus aureus* (*S. aureus*) SAP0017, and a clinical isolate of *Staphylococcus epidermidis* (*S. epidermidis*) obtained from Dr. D. Speert (Department of Medicine, University of British Columbia). Antifungal activity was tested using a lab isolate of *Candida albicans* (*C. albicans*) obtained from Dr. B. Dill (Department of Microbiology & Immunology, University of British Columbia). All strains were grown in Mueller Hinton (MH) broth (Difco Laboratories, Detroit, MI) at 37°C unless otherwise noted. All lipids were purchased from Avanti Polar Lipids Inc. (Alabaster, AL). The fluorescent dye, $diSC_35$, was purchased from Molecular Probes (Eugene, OR). The enzyme α-chymotrypsin and trypsin/chymotrypsin inhibitor were purchased from Sigma (St. Louis, MO).

### Peptide synthesis

Both polyphemusin I (PM1, $RRWC^aFRVC^bYRGFC^bYRKC^aR\text{-}NH_2$, where superscript letters define the disulfide connected cysteine residues) and the serine substituted peptide (PM1-S, $RRWSFRVSYRGFSYRKSR\text{-}NH_2$) were synthesized by Fmoc solid-phase peptide synthesis using a model 432A peptide synthesizer (Applied

Biosystems Inc.) at the University of British Columbia Nucleic Acid/Protein service facility. PM1 was then oxidized using a Tris-DMSO-2-propanol solution (100mM Tris-HCl, 25% DMSO, 10% 2-propanol, pH 7.5) for 24 hours at room temperature with constant nutating to promote disulfide bond formation (*21*). The correctly folded PM1 was then purified by reverse-phase chromatography using a model LKB FPLC (Amersham Pharmacia). Correct disulfide bond formation (between cysteine residues 4-17 and 8-13) of the purified peptide was confirmed by MALDI mass spectrometry through an observed 4 mass unit difference between the reduced and oxidized forms of PM1 (data not shown) and further verified through the observation of long range NOEs in the NOESY spectra of PM1. For clarity, the primary structures and disulfide connectivity of the synthesized peptides PM1 and PM1-S are shown in Figure 2.1.

**NMR spectroscopy**

Peptides were dissolved in $H_2O$:$D_2O$ (9:1) at a concentration of 2mM, pH 4.0. All NMR spectra were recorded at 27 °C on a Varian Inova 600 NMR spectrometer operating at a $^1H$ frequency of 599.76 MHz. DQF-COSY (*22*), TOCSY (*23*) and NOESY (*24*) spectra were obtained using standard techniques. Water suppression was achieved using the WATERGATE technique (*25, 26*) or by presaturation. Spectra were collected with 512 data points in F1, 2048 data points in F2. TOCSY spectra were acquired using the Malcolm Levitt (MLEV)-17 pulse sequence (*27*) at a spin-lock time of 20 ms. NOESY spectra were recorded with a mixing time of 150 ms. The NMR data were processed with NMRPIPE (*28*).

**NOE data analysis and structure calculation**

All NMR spectra were analyzed using NMRView version 5.0.3 (*29*). NOE crosspeaks were assigned and integrated. The NOE volumes were converted to distances and calibrated using intraresidue $H^N$-$H^\alpha$ crosspeaks and the mean distance of 2.8 Å determined by Hyberts *et al* (*30*). The distances were then converted into distance restraints by calculating upper and lower distance bounds using the equations of Hyberts *et al* (*30*). Pseudoatom restraints were corrected as previously described (*31*) by adding 1 and 1.5 Å to the upper distance bound of unresolved methylene and methyl protons, respectively, and resolved methylene protons were float-corrected by adding 1.7 Å to the upper distance bound. Structure calculations were performed using Xplor-NIH version 2.9.0 (*32*). One hundred structures were generated by the DGSA protocol and further refined. The refinement consisted of simulated annealing, decreasing the temperature from 310 K to 10 K over 50,000 steps. Forty seven polyphemusin I structures were calculated with no NOE violations > 0.2 Å and the 17 lowest energy conformers with final energies < 25 kcal $mol^{-1}$ were selected for presentation. Structural analysis and visualization were performed using Procheck (*33, 34*) and MOLMOL (*35*).

**Circular dichroism (CD) spectroscopy**

CD spectra were recorded on a model J-810 spectropolarimeter (Jasco) using a quartz cell with a 1 mm path length. Spectra were measured at room temperature between 190 nm and 250 nm at a scan speed of 10 nm/min and a total of 10 scans per sample. Spectra were recorded at a peptide concentration of 100 μg/ml in three environments: 10 mM phosphate buffer, pH 7.3; 50% TFE in water; and in liposomes of

POPC:POPG (7:3 w:w, 2 mM), made as described below under fluorescence spectroscopy. In all cases, the peptide spectra were obtained by subtracting the spectra of the solution components in the absence of peptide.

**Minimal inhibitory/hemolytic concentration**

The peptide MICs, for the microorganisms listed in Strains and Reagents, were determined using the modified broth microdilution method in Muller Hinton (MH) medium (*15*). The MIC was taken as the lowest peptide concentration at which no growth was observed after an overnight incubation at 37°C. The minimal hemolytic concentration (MHC) was determined as previously described (*36*). Briefly, human erythrocytes were collected in the presence of heparin, centrifuged to remove the buffy coat (white blood cells) and washed three times in 0.85% saline. Serial dilutions of peptide in 0.85% saline were prepared and incubated with the erythrocytes for 4 hours at 37°C with constant nutating. The minimal hemolytic concentration was recorded as the concentration of peptide resulting in lysis. Both the MIC and MHC assays were performed three separate times and the mode values recorded.

**Membrane depolarization assay**

The cytoplasmic membrane depolarization activity of the peptides was determined as previously described (*15*) using *E. coli* strain DC2 and the membrane potential sensitive dye, di$SC_3$5. The bacterial cells were collected in mid-log phase, washed in 5 mM HEPES buffer, pH 7.8, and resuspended in this buffer to an $OD_{600}$ of 0.05. A di$SC_3$5 stock solution was added to a final concentration of 0.4 μM and the cell

suspension was nutated at room temperature for 30 minutes. After this time, KCl was added to a final concentration of 100 mM and the suspension was incubated at room temperature for 10 minutes. A 2 ml cell suspension was placed in a 1cm cuvette and a concentration of peptide was added. Changes in fluorescence were recorded with a model LS50B luminescence spectrometer (Perkin Elmer) at an excitation wavelength of 622 nm and an emission wavelength of 670 nm.

**Fluorescence spectroscopy**

Tryptophan fluorescence was recorded using a model LS50B luminescence spectrometer (Perkin Elmer) at an excitation wavelength of 280 nm and an emission range of 300-400 nm. Liposomes were prepared by dissolving POPC and POPG in chloroform at a ratio of 7:3 (w:w). The chloroform was removed under nitrogen and the lipids were dried under vacuum for 2 hours and then suspended in 10 mM phosphate buffer (pH 7.3). Unilamellar vesicles were prepared by freeze-thawing the lipid solution 5 times (liquid $N_2$-air) followed by extrusion through two stacked 0.1mm polycarbonate membranes (AMD Manufacturing Inc.) which was repeated 10 times. Samples were run both in the presence or absence of 0.3 mM liposomes and a peptide concentration of 3 μg/ml. A spectrum of liposomes alone was subtracted to obtain the spectra due to peptide only.

**Peptide translocation**

The ability of peptides to translocate across model membranes was assayed as previously described (*37*). Briefly, lipids (POPC:POPG:DNS-PE, 50:45:5) were

dissolved in chloroform which was removed under a stream of $N_2$ and further dried under vacuum for 2 hours. The lipid mixture was resuspended in a solution of 200 μM α-chymotrypsin in 150 mM NaCl, 20 mM HEPES buffer, pH 7.5. Unilamellar vesicles were prepared as described above under fluorescence spectroscopy. Trypsin/Chymotrypsin inhibitor was then added to inactivate the protease present outside the vesicles. Peptide was added at a concentration of 10 μg/ml and fluorescence transfer from the tryptophan residue in the peptide to the dansyl-group in DNS-PE was monitored for 500 seconds using a model LS50B luminescence spectrometer (Perkin Elmer) at an excitation wavelength of 280 nm and an emission wavelength of 510 nm. This assay was repeated three separate times and a representative trial is shown.

**Results**

**NMR spectroscopy**

Two-dimensional TOCSY, NOESY and DQF-COSY spectra were collected for both PM1 and PM1-S at 27°C and pH 4.0. The PM1 and PM1-S proton resonances were assigned sequentially and the chemical shift assignments for PM1 are recorded in Appendix 1. A region of the TOCSY spectrum is shown as Figure 2.2A indicating the well resolved spin systems in which there was no overlap of residues. The α-amide region of the NOESY spectrum is shown as Figure 2.2B indicating the sequentially assigned backbone proton resonances. Some degree of overlap was observed with the α-proton resonances in the F1 axis however, due to good separation of amide resonances in the F2 axis, this did not pose a problem in the assignment of cross peaks. Strong $d_{\alpha N}(i,i+1)$ contacts were observed throughout the molecule and are typical of β-sheet

structure while strong $d_{NN}(i,i+1)$ contacts observed between residues 10 to 12 are characteristic of a β-turn (*38*). In addition, several long-range contacts, separated by as many as 15 residues, were further evidence of the disulfide-constrained anti-parallel β-hairpin structure that is polyphemusin I. The proton chemical shifts of polyphemusin I have been deposited at the BMRB (http://www.bmrb.wisc.edu/) accession code: BMRB-6020.

**NOE data analysis and structure calculation**

The structure of polyphemusin I was calculated using 143 total NOE restraints (69 intra-residue and 74 inter-residue restraints). Figure 2.3 indicates the distribution of inter-residue restraints, which were spread evenly throughout the molecule rather than originating from a few select residues. With the exception of arginines 6 and 10, the number of inter-residue restraints was greater than or equal to the number of intra-residue restraints for all residues. The set of 17 calculated polyphemusin I structures is presented as Figure 2.4A and have been deposited at the PDB (http://www.rcsb.org/pdb/) accession code: 1RKK. Rather than calculate an average structure, a schematic diagram of the conformer with the lowest average pairwise RMSD to the mean is shown as Figure 2.4B. The structure of polyphemusin I was that of an anti-parallel β-hairpin connected by a type I' β-turn (*39*). The structure was well defined in the β-sheet region (residues 7, 8, 13, 14) with an average pairwise RMSD of 0.22 ± 0.10 Å and 0.86 ± 0.36 Å for backbone and heavy atoms respectively (Table 1). The sheet region was variable throughout the calculated structures but, based upon Procheck analysis (*33, 34*), might extend from residues 4 to 9 and residues 12 to 17 (data not shown). Figures 4C and D show the

contact surface of the molecule painted with the electrostatic potential of the representative PM1 structure. From the hydrophilic face of the molecule shown in panel C, a cationic cleft was observed, running the length of the molecule and wrapping around the surface in a diagonal fashion. A 180 degree rotation of this structure revealed the more hydrophobic face of the molecule and is shown as panel D.

Detailed analysis of the NOESY spectrum of PM1-S yielded 97 unambiguous restraints (58 intra-residue, 39 inter-residue) that were used in structure calculation (data not shown). Of the 39 interresidue restraints the majority was short range (i, i+1) and only two could be classified as medium range (i, i+2 and i, i+3). This led to the generation of a large number of low energy structures with no distinct population displaying a preferred conformation (data not shown).

**Circular dichroism spectroscopy**

The CD spectra of PM1 and PM1-S recorded in phosphate buffer, TFE, and in the presence of liposomes are shown in Figure 2.5. The spectrum of PM1 in buffer displayed two positive bands at 200 nm and 230 nm and one negative band at 210 nm. These bands are indicative of a β structure and a β-turn (*40*) and this spectrum is very similar to that of the related peptide tachyplesin I (*16*). The spectrum of PM1 in TFE displayed a more similar pattern with one of the positive bands shifted slightly to 196 nm and the negative band shifted to 208 nm. These shifts were due to the presence of TFE, which is capable of stabilizing protein conformations that would be unordered in aqueous environments (*16*) thus producing a spectrum that is more similar to that in liposomes than in aqueous buffer. The PM1 spectrum in the anionic liposome environment

displayed a positive band below 197 nm and at 234 nm and a negative band at 204 nm, again indicating the presence of a β-sheet structure and a β-turn. The slight differences in wavelength of the bands are likely to be due to the environment in which the peptide was located and the stabilizing forces imparted by that environment. As the environment decreased in polarity, protein secondary structures, particularly those in small peptides, become stabilized due to decreased interference of hydrogen bonding with surrounding polar molecules (buffer).

The CD spectra of PM1-S indicated that, in all environments, the peptide displayed no observable patterns that could be related to structural features. This indicates PM1-S is a flexible molecule with no favoured conformation.

**Minimal inhibitory concentration**

The MICs of peptides PM1 and PM1-S against a variety of micro-organisms are shown in Table 2. PM1 showed high antimicrobial activity against the Gram negative, Gram positive and fungal specimens tested with MICs ranging from 0.5 to 4 μg/ml. The linear peptide, PM1-S, was not as active as the native peptide, possessing a wide range of MICs from 2 to 64 μg/ml. In addition PM1-S remained active against Gram negative bacteria but displayed poor activity to both Gram positive and fungal micro-organisms. Overall PM1-S was 4 to 16 fold less active than the parent, PM1.

**Membrane depolarization**

To assess bacterial membrane depolarization, the membrane potential sensitive dye di$SC_3$5 was used. This cationic dye concentrates in the cytoplasmic membrane under

the influence of the membrane potential (which is oriented internal negative) resulting in a self-quenching of fluorescence. Upon disruption of the membrane potential, the dye dissociates into the buffer leading to an increase in fluorescence (*8*). Depolarization was monitored over a period of 800 seconds for PM1 and PM1-S (Figure 2.6). The ability of PM1 to depolarize bacterial cells was much greater than that of PM1-S with the lowest concentration of PM1, 1 μg/ml, producing the same fluorescence increase as the maximum utilized concentration of PM1-S, 5 μg/ml. Overall PM1-S displayed a 2 to 4 fold reduction in its ability to depolarize the bacterial cytoplasmic membrane when compared to PM1. In addition, PM1 was fast acting, achieving maximum fluorescence at 400 seconds. In contrast, the lag time of PM1-S was much longer, leading to maximum fluorescence being achieved after 600 seconds.

**Fluorescence spectroscopy**

To determine the local environment of the peptides, the fluorescence emission of the single tryptophan residue was monitored. Tryptophan fluorescence is a widely used method to determine the polarity of the local environment, as it is a natural fluorophore in proteins. In a polar environment, excited fluorophores interact with polar solvent molecules decreasing the energy of the excited state (*41*). This decrease in energy is observed as a reduction of fluorescence intensity and an increase in fluorescence wavelength. As the polarity of the environment decreases, tryptophan fluorescence occurs at a decreased wavelength (a blue shift) with an increase in intensity. The tryptophan fluorescence spectra for PM1 and PM1-S are shown in Figure 2.7. Both PM1 and PM1-S displayed similar blue shifts of -10.1 nm and -8.37 nm respectively when

present in a hydrophobic lipid environment compared to a hydrophilic aqueous environment. The fluorescence intensities of PM1 and PM1-S were also found to increase 6 fold and 5 fold respectively in a liposome solution compared to buffer. These findings indicate that both peptides were able to associate with and insert their tryptophan side chains into the lipid bilayer of the model membrane.

**Peptide translocation**

The ability of the peptides to translocate model membranes was assayed using a system that was previously described in detail (*42*). As the peptides gain access to the internal cavity of the liposome they are digested by protease leading to a reduction in observed fluorescence transfer. The fluorescence spectra of both peptides recorded over a period of 500 seconds are shown in Figure 2.8. The ability of PM1 to translocate the model membrane system was indicated by the steady decrease in fluorescence, beginning almost immediately after addition of the peptide. This finding is in agreement with previously published translocation data for PM1 (*42*). In contrast, no decrease in fluorescence was observed in the spectra of PM1-S throughout the 500 seconds indicating a complete lack of membrane translocation.

**Discussion**

To examine the effects of conformational flexibility and disulfide constrained rigidity upon the antimicrobial peptide polyphemusin I, a cysteine substituted analogue was created. This analogue, PM1-S, was synthesized with all four cysteine residues

simultaneously substituted with serine. Serine was chosen, as its side chain is similar to that of cysteine in structure, polarity and hydrogen bonding ability.

Due to sequence similarity, the structure of polyphemusin I has been assumed to be similar to the NMR structures of the related peptides tachyplesin I, and the polyphemusin variant T22, and indeed only subtle differences were observed here. We determined the three-dimensional solution structure of polyphemusin I by $^{1}$H-NMR and an ensemble of the 17 lowest energy structures is presented here (Figure 2.4). The structure of PM1 is that of an anti-parallel β-hairpin. The amphipathic nature of the molecule is more clearly defined than previously modeled (*43*) and a cationic cleft can be observed running the length of the molecule. The high affinity of polyphemusin I for LPS has been determined previously (*42*) and this cleft may represent the binding site for the negatively charged phosphate groups present on the LPS molecule. The structure of PM1 is well defined throughout the sheet and loop regions but is quite flexible in the tail portion. Structural studies of tachyplesin I have previously reported a central "hinge" region in the molecule which, in a membrane environment, allows the molecule to fold in a manner with an increased hydrophobic surface (*17*). The flexible region of polyphemusin I may flank an analogous hinge and this would be expected to play a role in LPS binding, peptide translocation and antimicrobial activity.

NMR spectroscopy was also used in an attempt to determine the structure of the linear peptide, PM1-S. Analysis of the NOESY spectrum revealed 97 NOEs (58 intra-residue and 39 inter-residue), of which only two could be classified as medium range (one i,i+2, and one i,i+3), and no long range NOEs were observed. From these findings it was concluded that PM1-S is unstructured in solution and further analysis by CD

spectroscopy indicated that the peptide remained unstructured in both 50% TFE and POPC:POPG liposome environments.

Both PM1 and PM1-S displayed antimicrobial properties with the linear peptide being two to sixteen-fold less active. Linearizing the peptide had a marginally lesser effect against Gram-negative than Gram-positive bacteria. We presume this reflects the fact that the linear peptide is better able to access the self promoted uptake pathway, where the initial interacting molecule is lipopolysaccharide. Thus translocation across the outer membrane would be less affected than translocation across the cytoplasmic membrane (which reflects differential translocation as assessed by the liposome translocation assay). Comparing the activity of PM1-S to previously characterized extended and helical peptides (*42, 44*) it should be noted that the linear peptide retains considerable activity when compared to the excellent MICs of polyphemusin I, despite its lack of structure.

In an effort to account for this reduction in activity, a variety of membrane interaction assays were performed. The ability of both peptides to depolarize membranes was assayed using the membrane potential sensitive dye $diSC_35$ and the *E. coli* DC2 strain. The linear peptide PM1-S displayed a four-fold reduction in membrane depolarization, which correlated with the observed reduction in antimicrobial activity. In addition, PM1-S displayed a much longer lag time in reaching maximum fluorescence, suggesting a possible decrease in the rate of membrane association when compared to PM1. A tryptophan fluorescence assay indicated that both peptides were able to associate with model membranes, thus, membrane association per se did not account for differences in activity.

Since polyphemusin I has previously been shown to translocate model membranes and is thought to exert its antimicrobial actions from within the cell (*42*), a translocation assay was performed in an attempt to explain the reduction in PM1-S activity. It was found that, while PM1 is an effective translocator, PM1-S appeared incapable of translocating model membranes. Thus, it appeared that linear peptide acts through a different mechanism of antimicrobial activity than polyphemusin I as the inability of PM1-S to translocate membranes might be expected to lead to a complete loss of activity rather than a four to sixteen-fold reduction. Indeed PM1-S may be acting on membranes in a manner consistent with the aggregate model (*5*) of antimicrobial activity in which structure is not a requirement for function. This is further supported by the ability of PM1-S to bind membranes and depolarize bacterial cells, two outcomes that would be expected from a peptide functioning through such a mechanism.

The data presented here indicate that the disulfide-constrained, β-sheet structure of polyphemusin I is required for maximal antimicrobial activity. Interruption of this β-sheet structure results in a peptide with measurable, albeit reduced, activity and completely abolishes the ability of the peptide to translocate membranes. The lack of preferred conformation and inability to translocate membranes combined with the moderate antimicrobial activity of PM1-S indicates that the linear peptide is acting through a different mechanism than polyphemusin I. In addition, the new availability of the polyphemusin I solution structure makes it possible to conduct future structure-activity studies on this highly active antimicrobial peptide.

**Table 2.1.** Structural statistics of 17 polyphemusin I (PM1) structures determined by Xplor-NIH.

| **NOE Restraints** | | |
|---|---|---|
| Total | 143 | |
| Intra-residue | 69 | |
| Inter-residue | 74 | |
| **Restraint violations (mean number per structure)** | | |
| > 0.1 Å | 0.47 ± 0.62 | |
| **Mean Final Energy (kcal $mol^{-1}$)** | | |
| $E_{Total}$ | 22.8 ± 1.1 | |
| **Mean Pairwise RMSD** | | |
| Alignment | Backbone | Heavy |
| Turn (8-13) | 0.24 ± 0.15 | 1.20 ± 0.35 |
| Sheet (7,8,13,14) | 0.22 ± 0.10 | 0.86 ± 0.36 |

**Table 2.2.** Antimicrobial and hemolytic activity of PM1 and PM1-S.

| Strains | | MIC / MHC (μg/ml) | |
|---|---|---|---|
| | | **PM1** | **PM1-S** |
| Gram$^-$ | *E. coli* UB1005 | 0.5 | 4 |
| | *E. coli* DC2 | 1 | 4 |
| | *S. typhimurium* (defensin sen.) | 0.25 | 2 |
| | *S. typhimurium* | 1 | 8 |
| | *P. aeruginosa* K799 | 2 | 32 |
| | *P. aeruginosa* Z61 | 1 | 16 |
| Gram$^+$ | *S. aureus* SAP0017 | 2 | 32 |
| | *S. epidermidis* | 1 | 16 |
| | *E. faecalis* | 1 | 2 |
| *C. albicans* | | 4 | 64 |
| Human Erythrocytes | | >64 | >256 |

**Figure 2.1.** Primary structures of polyphemusin I (PM1) and its serine substituted, linear derivative PM1-S. Disulfide linkages in PM1 are shown as solid lines.

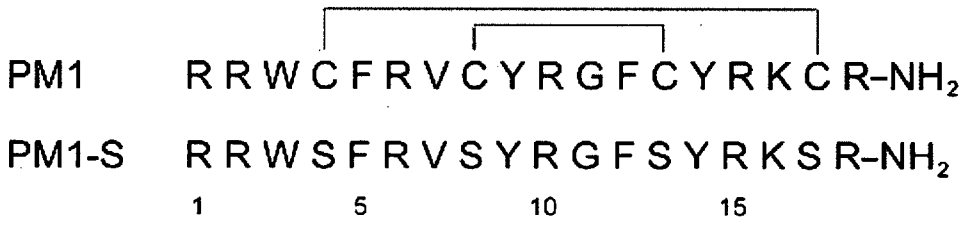

**Figure 2.2.** $^{1}$H-NMR spectra of polyphemusin I (PM1). **A:** Fingerprint region of the TOCSY spectra of PM1 recorded in H2O:D2O (9:1) at 27°C, pH 4.0. The amino acid spin systems are indicated by one letter code and residue number. **B:** NOESY spectra of PM1 recorded in H2O:D2O (9:1) at 27°C, pH 4.0 and a mixing time of 150 ms. The α-amide region is shown and the sequential backbone assignments are connected. For clarity only the intra-residue α-amide crosspeaks are labeled according to residue number.

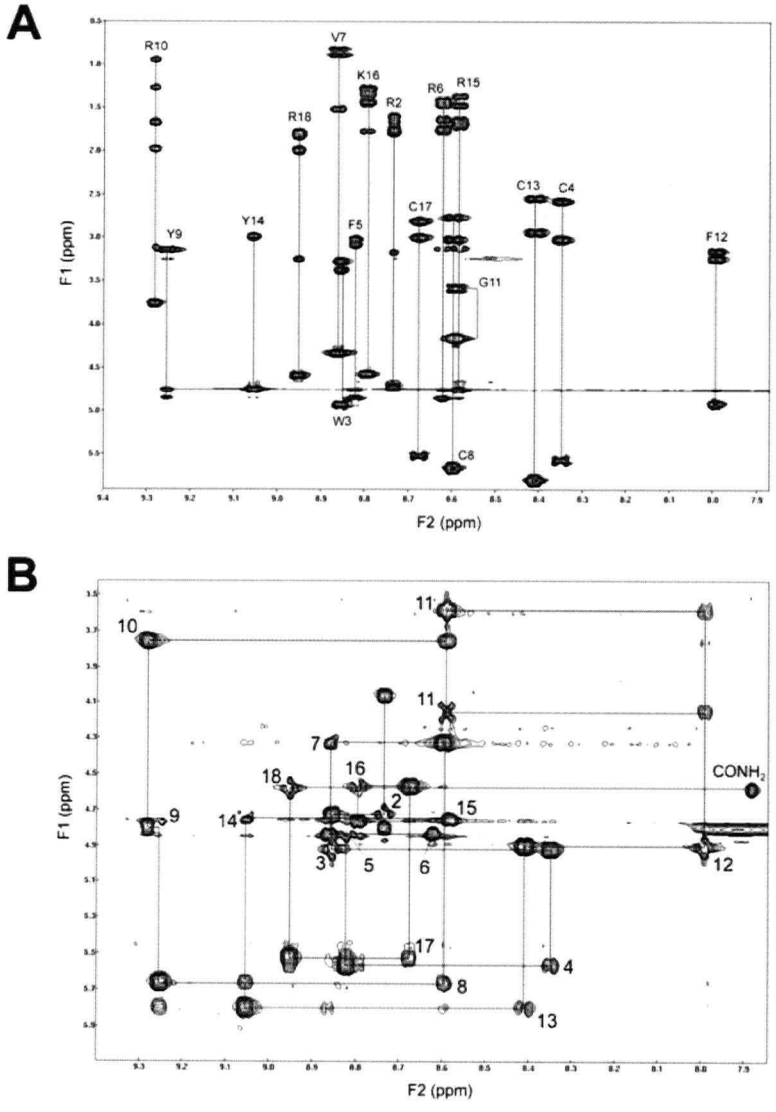

**Figure 2.3.** Number of NOE restraints per residue used during structure calculation of polyphemusin I. Intra-residue and inter-residue restraints are indicated as black and grey bars respectively.

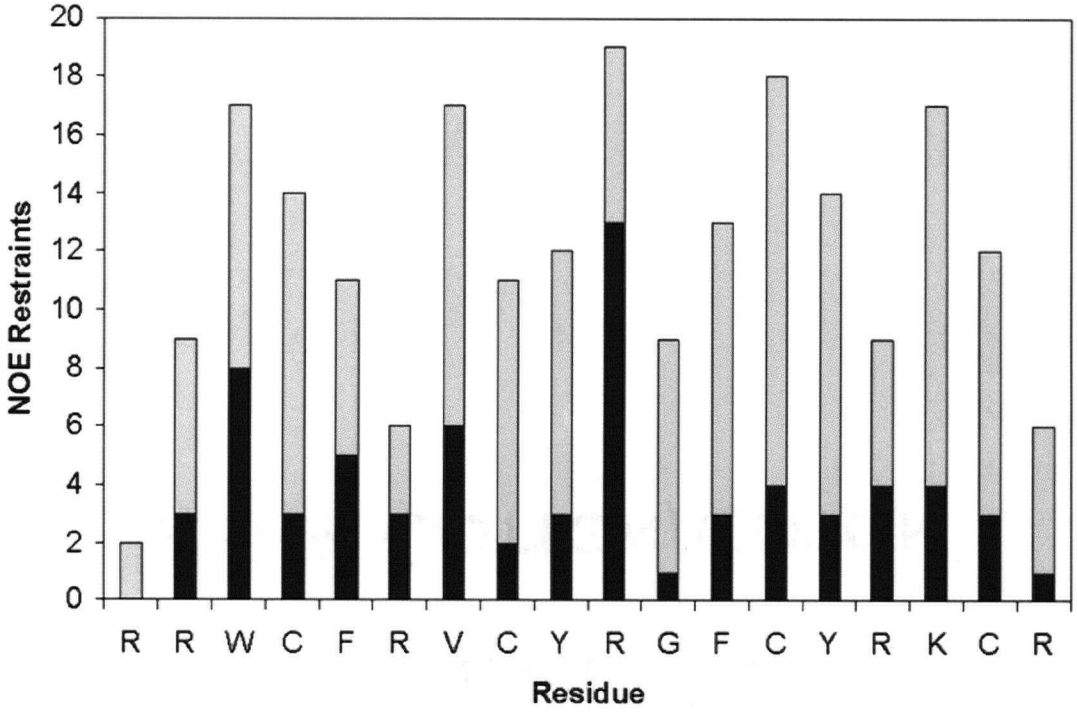

**Figure 2.4.** Three-dimensional solution structure of polyphemusin I (PM1). **A:** the set of 17 structures calculated for PM1. The backbone atoms are coloured black and the cysteine side chains are indicated in yellow. Structures are aligned over the β-sheet residues 7, 8, 13 and 14. **B:** ribbon diagram of a representative PM1 structure. **C:** contact surface painted with the electrostatic potential of a representative PM1 structure. **D:** 180 degree rotation of the structure presented in panel C. In panels B, C and D the structure with the lowest average pairwise RMSD to the mean was selected as the representative. Figures were prepared with MOLMOL (*35*).

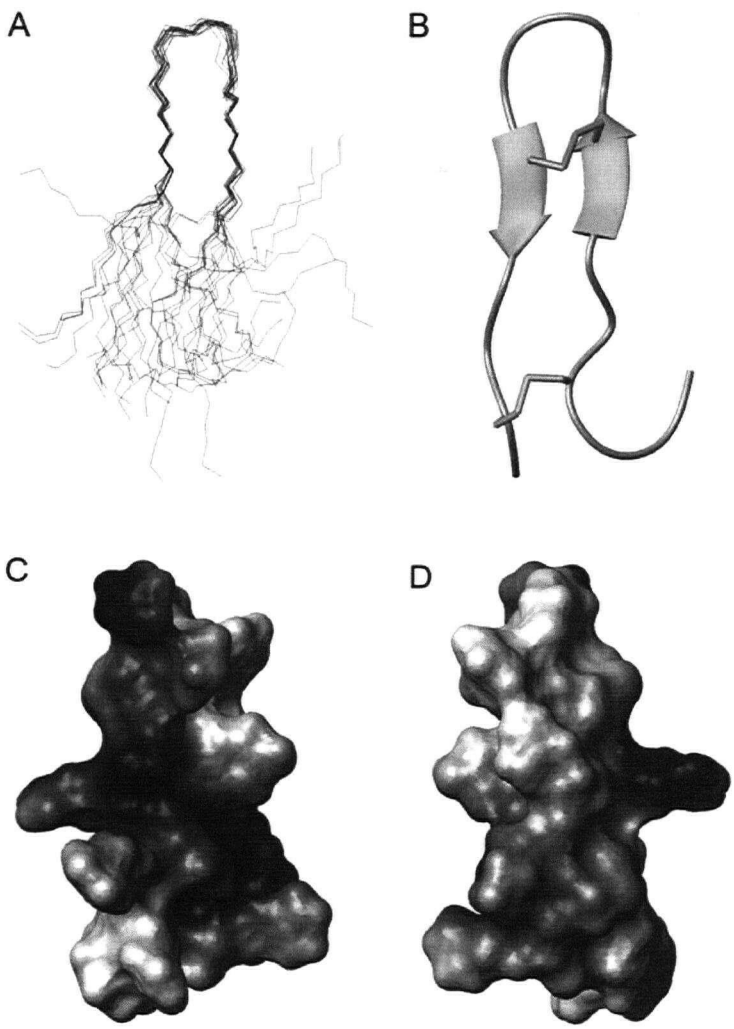

**Figure 2.5.** CD spectra of polyphemusin I (PM1) and PM1-S. Spectra were recorded in 10 mM phosphate buffer, pH 7.3 (circles); 50% TFE in $H_2O$ (squares); and liposomes of POPC:POPG (7:3 w:w, 2 mM) (triangles). Peptide concentration was 100 μg/ml.

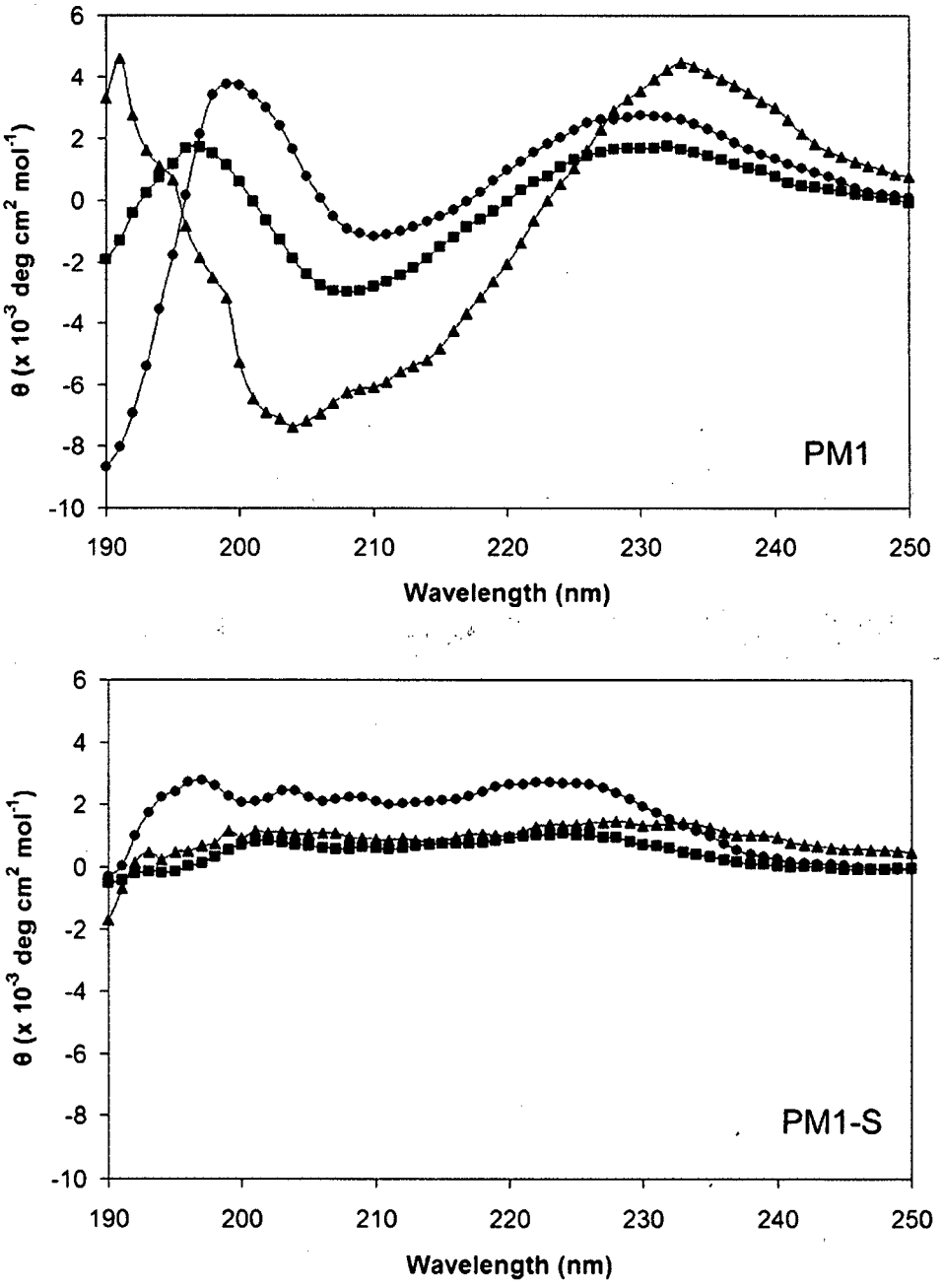

**Figure 2.6.** Cytoplasmic membrane depolarization of *E. coli* DC2 by polyphemusin I (PM1) and PM1-S using the membrane potential sensitive dye, $diSC_35$. Dye release was monitored at an excitation wavelength of 622 nm and an emission wavelength of 670 nm. In each run, peptide was added near the 100 second mark. PM1: A) 5 μg/mL; B) 3 μg/mL; C) 1 μg/mL. PM1-S: D) 5 μg/mL; E) 3 μg/mL; F) 1 μg/mL.

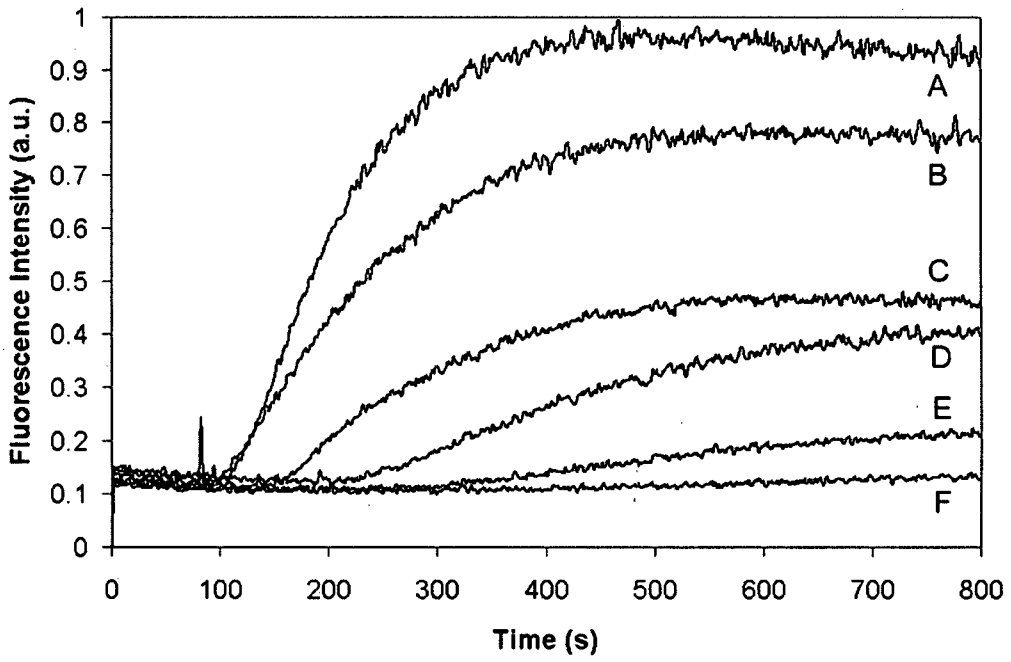

**Figure 2.7.** Fluorescence spectra of polyphemusin I (PM1) and PM1-S in aqueous solution and in the presence of liposomes. Samples contained 3 μg/mL peptide in 10 mM phosphate buffer, pH 7.3, and 0.3mM POPC:POPG (7:3 w:w) liposomes. Excitation wavelength was 280 nm. Solid and dotted lines indicate PM1 and PM1-S respectively.

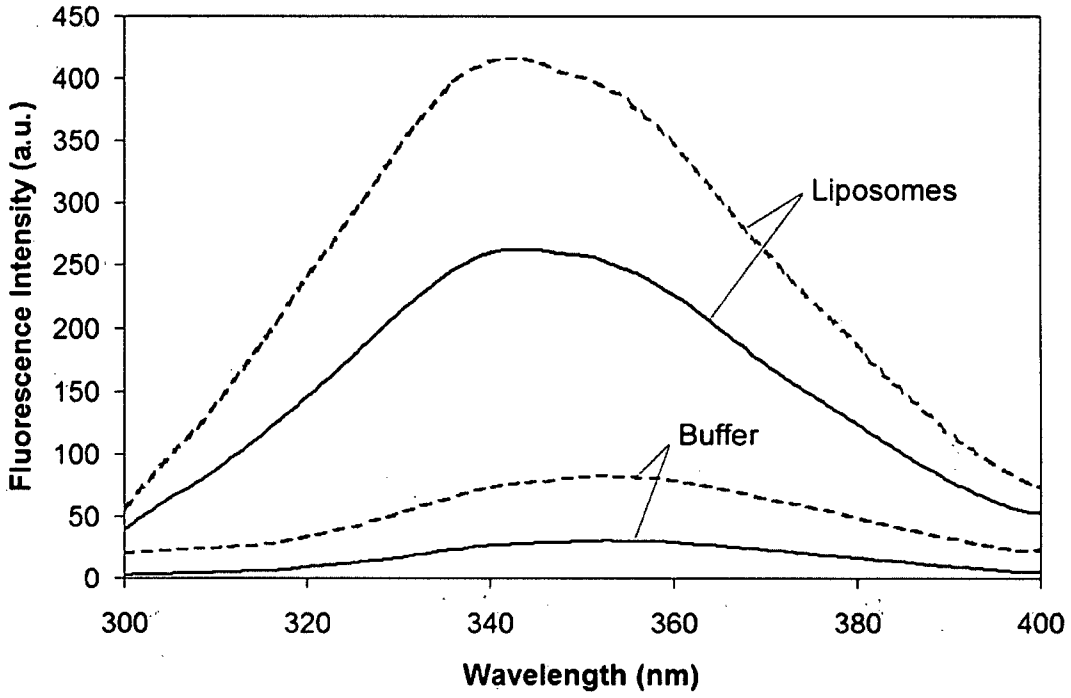

**Figure 2.8.** Membrane translocation of polyphemusin I (PM1) and PM1-S as measured by fluorescence transfer from tryptophan to DNS-PE. A decrease in fluorescence transfer, due to proteolytic degradation of the peptide by internalized α-chymotrypsin, is used as measure of membrane translocation. The lipid concentration was 200 μM and the peptide concentration was 10 μg/mL. Fluorescence transfer was monitored at an excitation wavelength of 280 nm and an emission wavelength of 510 nm.

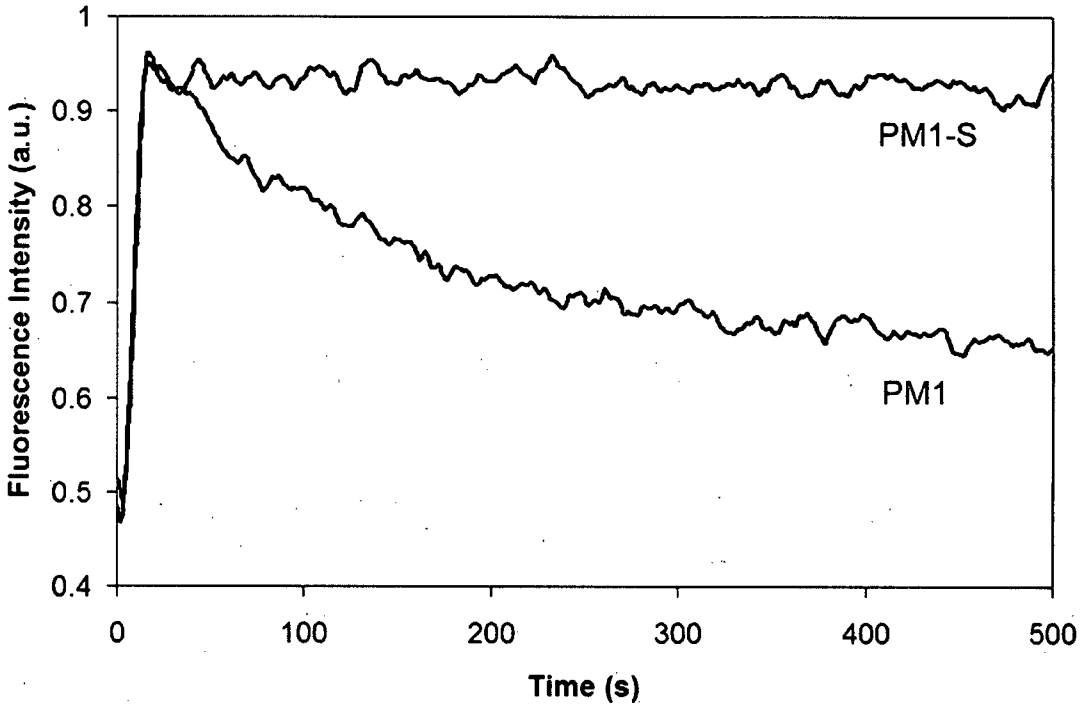

**References**


1. Miyata, T., Tokunaga, F., Yoneya, T., Yoshikawa, K., Iwanaga, S., Niwa, M., Takao, T., and Shimonishi, Y. (1989) Antimicrobial peptides, isolated from horseshoe crab hemocytes, tachyplesin II, and polyphemusins I and II: chemical structures and biological activity, *J Biochem (Tokyo) 106*, 663-8.
2. Nakamura, T., Furunaka, H., Miyata, T., Tokunaga, F., Muta, T., Iwanaga, S., Niwa, M., Takao, T., and Shimonishi, Y. (1988) Tachyplesin, a class of antimicrobial peptide from the hemocytes of the horseshoe crab (Tachypleus tridentatus). Isolation and chemical structure, *J Biol Chem 263*, 16709-13.
3. Tamamura, H., Kuroda, M., Masuda, M., Otaka, A., Funakoshi, S., Nakashima, H., Yamamoto, N., Waki, M., Matsumoto, A., Lancelin, J. M., and et al. (1993) A comparative study of the solution structures of tachyplesin I and a novel anti-HIV synthetic peptide, T22 ([Tyr5,12, Lys7]-polyphemusin II), determined by nuclear magnetic resonance, *Biochim Biophys Acta 1163*, 209-16.
4. Kawano, K., Yoneya, T., Miyata, T., Yoshikawa, K., Tokunaga, F., Terada, Y., and Iwanaga, S. (1990) Antimicrobial peptide, tachyplesin I, isolated from hemocytes of the horseshoe crab (Tachypleus tridentatus). NMR determination of the beta- sheet structure, *J Biol Chem 265*, 15365-7.
5. Andreu, D., and Rivas, L. (1998) Animal antimicrobial peptides: an overview, *Biopolymers 47*, 415-33.
6. Hancock, R. E. W., and Rozek, A. (2002) Role of membranes in the activities of antimicrobial cationic peptides, *FEMS Microbiol Lett 206*, 143-9.

7. Boman, H. G., Agerberth, B., and Boman, A. (1993) Mechanisms of action on Escherichia coli of cecropin P1 and PR-39, two antibacterial peptides from pig intestine, *Infect Immun 61*, 2978-84.

8. Wu, M., Maier, E., Benz, R., and Hancock, R. E. W. (1999) Mechanism of interaction of different classes of cationic antimicrobial peptides with planar bilayers and with the cytoplasmic membrane of Escherichia coli, *Biochemistry 38*, 7235-42.

9. Park, C. B., Kim, H. S., and Kim, S. C. (1998) Mechanism of action of the antimicrobial peptide buforin II: buforin II kills microorganisms by penetrating the cell membrane and inhibiting cellular functions, *Biochem Biophys Res Commun 244*, 253-7.

10. Yonezawa, A., Kuwahara, J., Fujii, N., and Sugiura, Y. (1992) Binding of tachyplesin I to DNA revealed by footprinting analysis: significant contribution of secondary structure to DNA binding and implication for biological action, *Biochemistry 31*, 2998-3004.

11. Lehrer, R. I., Barton, A., Daher, K. A., Harwig, S. S., Ganz, T., and Selsted, M. E. (1989) Interaction of human defensins with Escherichia coli. Mechanism of bactericidal activity, *J Clin Invest 84*, 553-61.

12. Patrzykat, A., Friedrich, C. L., Zhang, L., Mendoza, V., and Hancock, R. E. W. (2002) Sublethal concentrations of pleurocidin-derived antimicrobial peptides inhibit macromolecular synthesis in Escherichia coli, *Antimicrob Agents Chemother 46*, 605-14.

13. Mandal, M., and Nagaraj, R. (2002) Antibacterial activities and conformations of synthetic alpha-defensin HNP-1 and analogs with one, two and three disulfide bridges, *J Pept Res 59*, 95-104.

14. Wu, Z., Hoover, D. M., Yang, D., Boulegue, C., Santamaria, F., Oppenheim, J. J., Lubkowski, J., and Lu, W. (2003) Engineering disulfide bridges to dissect antimicrobial and chemotactic activities of human beta-defensin 3, *Proc Natl Acad Sci U S A 100*, 8880-5.

15. Wu, M., and Hancock, R. E. W. (1999) Interaction of the cyclic antimicrobial cationic peptide bactenecin with the outer and cytoplasmic membrane, *J Biol Chem 274*, 29-35.

16. Rao, A. G. (1999) Conformation and antimicrobial activity of linear derivatives of tachyplesin lacking disulfide bonds, *Arch Biochem Biophys 361*, 127-34.

17. Laederach, A., Andreotti, A. H., and Fulton, D. B. (2002) Solution and micelle-bound structures of tachyplesin I and its active aromatic linear derivatives, *Biochemistry 41*, 12359-68.

18. Clark, D. (1984) Novel antibiotic hypersensitive mutants of Escherichia coli genetic mapping and chemical characterization, *FEMS Microbiol Lett 21*, 189-95.

19. Fields, P. I., Groisman, E. A., and Heffron, F. (1989) A Salmonella locus that controls resistance to microbicidal proteins from phagocytic cells, *Science 243*, 1059-62.

20. Angus, B. L., Carey, A. M., Caron, D. A., Kropinski, A. M., and Hancock, R. E. W. (1982) Outer membrane permeability in Pseudomonas aeruginosa: comparison

of a wild-type with an antibiotic-supersusceptible mutant, *Antimicrob Agents Chemother 21*, 299-309.

21. Tam, J., Wu, C., Liu, W., and Zhang, J. (1991) Disulfide bond formation in peptides by dimethyl sulfoxide. Scope and applications, *J Am Chem Soc 113*, 6657-62.

22. Rance, M., Sorensen, O. W., Bodenhausen, G., Wagner, G., Ernst, R. R., and Wuthrich, K. (1983) Improved spectral resolution in cosy $^{1}H$ NMR spectra of proteins via double quantum filtering, *Biochem Biophys Res Commun 117*, 479-85.

23. Braunschweiler, L., and Ernst, R. R. (1983) Coherence transfer by isotropic mixing: application to proton correlation spectroscopy, *J Magn Res 53*, 521-8.

24. Jeener, J., Meier, B. H., Bachmann, P., and Ernst, R. R. (1979) Investigation of exchange processes by two-dimensional NMR spectroscopy, *J Chem Phys 71*, 4546-53.

25. Piotto, M., Saudek, V., and Sklenar, V. (1992) Gradient-tailored excitation for single-quantum NMR spectroscopy of aqueous solutions, *J Biomol NMR 2*, 661-5.

26. Sklenar, V., Piotto, M., Leppik, R., and Saudek, V. (1993) Gradient-Tailored Water Suppression for $^{1}H$-$^{15}N$ HSQC Experiments Optimized to Retain Full Sensitivity, *J Magn Res A 102*, 241-5.

27. Bax, A., and Davis, D. G. (1985) MLEV-17 based two-dimensional homonuclear magnetization transfer spectroscopy, *J Magn Res 65*, 355-60.

28. Delaglio, F., Grzesiek, S., Vuister, G. W., Zhu, G., Pfeifer, J., and Bax, A. (1995) NMRPipe: a multidimensional spectral processing system based on UNIX pipes, *J Biomol NMR 6*, 277-93.

29. Johnson, B. A., and Blevins, R. A. (1994) NMRView: A computer program for the visualization and analysis of NMR data, *J Biomol NMR 4*, 603-14.

30. Hyberts, S. G., Goldberg, M. S., Havel, T. F., and Wagner, G. (1992) The solution structure of eglin c based on measurements of many NOEs and coupling constants and its comparison with X-ray structures, *Protein Sci 1*, 736-51.

31. Friedrich, C. L., Rozek, A., Patrzykat, A., and Hancock, R. E. W. (2001) Structure and mechanism of action of an indolicidin peptide derivative with improved activity against gram-positive bacteria, *J Biol Chem 276*, 24015-22.

32. Schwieters, C. D., Kuszewski, J. J., Tjandra, N., and Clore, G. M. (2003) The Xplor-NIH NMR Molecular Structure Determination Package, *J Magn Res 160*, 66-74.

33. Morris, A. L., MacArthur, M. W., Hutchinson, E. G., and Thornton, J. M. (1992) Stereochemical quality of protein structure coordinates., *Proteins 12*, 345-64.

34. Laskowski, R. A., MacArthur, M. W., Moss, D. S., and Thornton, J. M. (1993) PROCHECK: a program to check the stereochemical quality of protein structures., *J Appl Cryst 26*, 283-91.

35. Koradi, R., Billeter, M., and Wuthrich, K. (1996) MOLMOL: a program for display and analysis of macromolecular structures, *J Mol Graph 14*, 51-5, 29-32.

36. Zhang, L., Benz, R., and Hancock, R. E. W. (1999) Influence of proline residues on the antibacterial and synergistic activities of alpha-helical peptides, *Biochemistry 38*, 8102-11.

37. Kobayashi, S., Takeshima, K., Park, C. B., Kim, S. C., and Matsuzaki, K. (2000) Interactions of the novel antimicrobial peptide buforin 2 with lipid bilayers: proline as a translocation promoting factor, *Biochemistry 39*, 8648-54.

38. Wuthrich, K. (1986) *NMR of Proteins and Nucleic Acids*, John Wiley & Sons, Toronto.

39. Richardson, J. S. (1981) The anatomy and taxonomy of protein structure, *Adv Protein Chem 34*, 167-339.

40. Fasman, G. D. (1996) *Circular dishroism and the conformational analysis of biomolecules*, Plenum Press, New York.

41. Campbell, I. D., and Dwek, R. A. (1984) *Biological spectroscopy*, The Benjamin/Cummings Publishing Company Inc., Menlo Park.

42. Zhang, L., Rozek, A., and Hancock, R. E. W. (2001) Interaction of cationic antimicrobial peptides with model membranes, *J Biol Chem 276*, 35714-22.

43. Zhang, L., Scott, M. G., Yan, H., Mayer, L. D., and Hancock, R. E. W. (2000) Interaction of polyphemusin I and structural analogs with bacterial membranes, lipopolysaccharide, and lipid monolayers, *Biochemistry 39*, 14504-14.

44. Falla, T. J., Karunaratne, D. N., and Hancock, R. E. W. (1996) Mode of action of the antimicrobial peptide indolicidin, *J Biol Chem 271*, 19298-303.

## Chapter 3 – Solution structure and interaction of the antimicrobial polyphemusins with lipid membranes*

### Introduction

The polyphemusins are a group of cationic peptides isolated from the American horseshoe crab, *Limulus polyphemus* (*1*) and share a great similarity to the tachyplesins, from the Japanese horseshoe crab, *Tachypleus tridentatus* (*2*). These peptides are 17 to 18 amino acid residues in length and contain two disulfide bonds which act to constrain the peptide backbone into an antiparallel β-hairpin connected by a β-turn. To date, the solution and micelle bound structures of tachyplesin I (*3*) and the solution structure of polyphemusin I (*4*) as well as the structures of various analogues have been determined by nuclear magnetic resonance. These structures have served as templates for peptide design as well as tools for investigating structure-activity relationships as an approach to determine the mechanism of action of this family of peptides.

The mechanism of action of the polyphemusins and tachyplesins, while not clear, is believed to involve membrane translocation (*4-6*). Previous studies utilizing model membranes have shown that, at low peptide:lipid ratios, polyphemusin I readily induces lipid flip-flop between membrane leaflets but produces a low degree of entrapped calcein release (*5*). In addition, a translocation assay has demonstrated that polyphemusin I becomes digested by liposome entrapped protease (*5*). Combined, these findings indicate that polyphemusin I is capable of accessing the interior of liposomes and does so without greatly disrupting or permeabilizing the lipid bilayer.

---

* A version of this chapter has been published as: Powers, J.P.S., Tan, A., Ramamoorthy, A. and Hancock, R.E.W. Solution structure and interaction of the antimicrobial polyphemusins with lipid membranes. Biochemistry. 2005, **44**: 15504-13.

In an effort to improve the high intrinsic antimicrobial activity of the polyphemusins, a series of analogues were designed with increased charge and amphipathic character as indicated by computer modeling (*7*). Characterization of these analogues revealed a two to four fold decrease in antimicrobial activity however, one analogue in particular, PV5, with an additional arginine inserted into the turn region, displayed a two-fold reduction in hemolytic activity and substantially improved protection in mouse models of endotoxemia (*7*). Specifically, PV5 produced a 50% survival rate in galactosamine sensitized mice challenged with *E. coli* LPS compared to 10% survival produced by polyphemusin I and no survival without peptide treatment. Recently, the related peptide tachyplesin has been demonstrated to function as a secondary secretagogue of LPS-induced hemocyte exocytosis presumably through a G protein mediated pathway (*8*). While these studies were conducted using horseshoe crab hemocytes, it is conceivable that interaction of these β-hairpin peptides with mammalian hemocytes could elicit the same response resulting in amplification of the innate immune system. This may explain the ability of the polyphemusins to protect mice challenged with LPS but does not account for the differences observed between polyphemusin I and PV5.

To continue to investigate the mechanism of action of the polyphemusins, we have determined here the three dimensional solution structure of PV5 in the presence and absence of DPC micelles using two-dimensional proton NMR and compared it to the previously determined structure of polyphemusin I (*4*). The interactions of both polyphemusin I and PV5 with model membranes, representing eukaryotic and prokaryotic compositions, were investigated using fluorescence spectroscopy and

differential scanning calorimetry. A mechanism of membrane translocation for the polyphemusins is proposed based on the results presented here as well as previous findings.

## Materials and methods

### Peptide synthesis

Polyphemusin I (RRWCFRVCYRGFCYRKCR-$NH_2$) and PV5 (RRWCFRVCYRGRFCYRKCR-$NH_2$) were synthesized by Fmoc solid-phase peptide synthesis using a model 432A peptide synthesizer (Applied Biosystems Inc.) at the University of British Columbia. Both peptides were oxidized using a Tris-DMSO solution (100mM Tris-HCl, 20% DMSO, pH 8) for 24 hours at room temperature to promote disulfide bond formation (*9*). The correctly folded peptides were then purified by reversed-phase chromatography using a Pharmacia model LKB FPLC. Correct disulfide bond formation (between cysteine residues 4-17 and 8-13 of polyphemusin I and 4-18 and 8-14 of PV5) of the purified peptides was confirmed by MALDI mass spectrometry through an observed 4 mass unit difference between the reduced and oxidized forms of the peptides (data not shown) and further verified through the observation of long range NOEs in the NOESY spectra of PV5 and previously for polyphemusin I (*4*). For clarity, the primary structures and disulfide connectivity of the synthesized peptides are shown in Figure 3.1.

**NMR spectroscopy**

PV5 was dissolved in $H_2O$:$D_2O$ (9:1) at a concentration of 2mM, with or without 300mM DPC. The pH of the final samples were 3.80 and 3.95 in the absence and presence of DPC. NMR spectra of PV5 without DPC were recorded at 25°C on a Varian Unity 500 NMR spectrometer operating at a $^1H$ frequency of 499.94 MHz. NMR spectra of PV5 containing 300mM DPC were recorded at 40°C on a Varian Inova 600 NMR spectrometer operating at a $^1H$ frequency of 599.84 MHz. DQF-COSY (*10*), TOCSY (*11*) and NOESY (*12*) spectra were obtained using standard techniques. Water suppression was achieved using the WATERGATE technique (*13, 14*) or by presaturation. Spectra were collected with 512 data points in F1, 2048 data points in F2. TOCSY spectra were acquired using the Malcolm Levitt (MLEV)-17 pulse sequence (*15*) at a spin-lock time of 60 ms. NOESY spectra were recorded with a mixing time of 150 ms. The NMR data were processed with NMRPIPE (*16*).

**NOE data analysis and structure calculation**

All NMR spectra were analyzed using NMRView version 5.0.3 (*17*). NOE crosspeaks were assigned and integrated. The NOE volumes were converted to distances and calibrated using intraresidue $H^N$-$H^\alpha$ crosspeaks and the mean distance of 2.8 Å determined by Hyberts *et al* (*18*). The distances were then converted into distance restraints by calculating upper and lower distance bounds using the equations of Hyberts *et al* (*18*). Pseudoatom restraints were corrected as previously described (*19*) by adding 1 and 1.5 Å to the upper distance bound of unresolved methylene and methyl protons, respectively, and resolved methylene protons were float-corrected by adding 1.7 Å to the

upper distance bound. Structure calculations were performed using Xplor-NIH version 2.9.0 (*20*). One hundred structures were generated by the DGSA protocol and further refined. The refinement consisted of simulated annealing, decreasing the temperature from 310 K to 10 K over 50,000 steps. In the sample without DPC, 49 PV5 structures were calculated with no NOE violations > 0.3 Å and the 16 lowest energy conformers with final energies < 28 kcal $mol^{-1}$ were selected for presentation. In the sample containing DPC, 26 PV5 structures were calculated with no NOE violations > 0.2 Å and the 17 lowest energy conformers with final energies < 36 kcal $mol^{-1}$ were selected for presentation. Structural analysis and visualization were performed using Procheck (*21, 22*) and MOLMOL (*23*).

**Membrane partitioning**

The ability of polyphemusin I and PV5 to associate with and partition into lipid membranes was investigated using fluorescence spectroscopy as previously described (*24*). Liposomes were made by dissolving lipids at the indicated molar ratios in a chloroform:methanol (2:1) solution. Liquid was removed under a stream of nitrogen and the lipid film was further dried under vacuum for a minimum of 2 hours. The lipid film was suspended in 10mM HEPES, 150mM NaCl, pH 7.4 with vortexing and liposomes were formed by sonicating to clarity. A 1μM peptide solution in 10mM HEPES, 150mM NaCl, pH 7.4 was added to a cuvette and the tryptophan fluorescence was measured on a PerkinElmer model LS50B luminescence spectrometer (Boston, MA) at an excitation wavelength of 280nm and emission range of 300-400nm giving the 100% unbound peptide spectra. Aliquots of the desired SUV composition at a stock concentration of

13.2mM lipid in 10mM HEPES, 150mM NaCl, pH 7.4 were added and the fluorescence spectra were recorded as above. In all cases, binding experiments were performed three times.

To determine the binding of peptide to liposomes, binding isotherms were analyzed as partition equilibrium as previously described (*24-26*) using the formula $X_b = K_p C_f$, where $X_b$ was the molar ratio of bound peptide per total lipid, $K_p$ was the partition coefficient, and $C_f$ was the equilibrium concentration of free peptide in solution. To determine $X_b$, the fluorescence signal arising from all peptide in the lipid bound form, $F_\infty$, had to be determined. This value was estimated from the fluorescence plateau reached during titration (in the case of POPC:POPG SUVs, Figure 3.4C) or extrapolated from the Y-intercept of a double reciprocal plot of total peptide fluorescence (F) *vs.* the total concentration of lipid ($C_L$), as previously described by Schwarz *et al* (*25*) (data not shown). Thus, knowing the fluorescence intensities of the free ($F_o$, no lipid added) and bound ($F_\infty$) peptide forms, the fraction of membrane bound peptide, $f_b$, was determined by the formula $f_b = (F - F_o)/(F_\infty - F_o)$; where F was the peptide fluorescence after each addition of vesicles. An additional assumption was made that the peptides interact solely with the lipids in the outer leaflet of the vesicles (60% of total lipid) (*26*) and thus $X_b$ values were corrected according to the formula $X_b^* = Xb/0.6$.

**Differential scanning calorimetry**

The interaction of polyphemusin I and PV5 with phospholipid membranes was investigated using differential scanning calorimetry. In all cases, synthetic lipids were purchased from Avanti Polar Lipids, Inc. (Alabaster, AL) and used without further

purification and all buffers and samples were degassed under vacuum for 15 minutes prior to loading into the calorimeter. For experiments involving DMPC (1,2-Dimyristoyl-*sn*-glycero-3-phosphocholine) and DMPG (1,2-Dimyristoyl-*sn*-glycero-3-[phospho-*rac*-(1-glycerol)], sodium salt) lipid species, lipids were dissolved in chloroform:methanol (2:1) at the indicated molar ratios, dried under a stream of $N_2$ and held under vacuum overnight. The lipid film was then suspended in 10mM Tris, 150mM NaCl pH 7.4 to yield multi-lamellar vesicles (MLVs) at a working concentration of 1mg/ml. DSC scans were recorded on a CSC Nano II differential scanning calorimeter (Lindon, UT). Scans were performed from 5 to 40°C with a temperature increase of 1°C/min and a 10min equilibration period before each scan. Between scans, peptide was added from a concentrated stock solution to give the indicated peptide:lipid mole ratios. In all cases, the thermogram of buffer alone was subtracted prior to plotting and analysis. The raw data were converted to molar heat capacity using the CPCalc program using the corresponding lipid concentrations and molecular weights and the partial specific volume of 0.988mL/g (*27*).

For experiments involving DiPoPE (1,2-Dipalmitoleoyl-*sn*-glycero-3-phospho-ethanolamine), lipid and peptide were co-dissolved in chloroform:methanol (2:1) at the indicated mole ratios, dried under a stream of $N_2$ and held under vacuum overnight. The peptide-lipid film was suspended in 10mM Tris, 100mM NaCl, 2mM EDTA pH 7.4 to yield multi-lamellar vesicles (MLVs) at a working lipid concentration of 7.5mg/ml. The fluid lamellar ($L_\alpha$) to inverted hexagonal ($H_{II}$) phase transition temperature of the lipids was measured with a MicroCal VP-DSC differential scanning calorimeter (Northampton, MA). A minimum of three scans were performed from 10 to 60°C with a temperature

increase of 1°C/min and a 15min equilibration period before each scan. In all cases, the thermogram of buffer alone was subtracted prior to plotting and analysis using MicroCal Origin 7.0.

## Results

### NMR spectroscopy

DQF-COSY, TOCSY and NOESY spectra were collected for PV5 at 25°C, pH 3.8, and at 40°C, pH 3.95 in the absence and presence of 300mM DPC respectively. Proton resonances were assigned sequentially and the chemical shift assignments are recorded in Appendix 2 and deposited at the BMRB. The TOCSY spectra indicated good separation of spin systems, with minor overlap occurring between residues Arg-6 and Arg-16 (data not shown). It was possible to assign the complete or partial spin systems of all residues with the exception of the N-terminal arginine for which the amide resonance was not observed. The NOESY spectra indicated strong dαN(i,i+1) contacts throughout the molecule and are characteristic of a β-sheet structure (*28*). In addition, several long-range connectivities, separated by as many as 13 residues, were further confirmation of the disulfide-constrained anti-parallel β-hairpin structure of PV5.

### NOE analysis and structure generation

The solution structure of PV5 was calculated using 129 total NOE restraints of which 67 were intra-residue and 62 were inter-residue restraints (Table 1). The structure of PV5 in the presence of DPC micelles was calculated using 137 total NOE restraints of which 68 were intra-residue and 69 were inter-residue restraints (Table 1). In both the

solution and micelle associated samples, NOE restraints were distributed evenly throughout the molecule and complete lists of NOE derived distance restraints have been deposited in the PDB. The ensemble of the 16 lowest energy calculated PV5 structures is shown in Figure 3.2A. The 16 structures aligned well over the β-sheet region (residues 7, 8, 14 and 15) with an average pairwise RMSD of 0.21 ± 0.05 Å and 0.79 ± 0.09 Å for backbone and heavy atoms respectively. The 17 lowest energy structures of PV5 in the presence of 300mM DPC (Figure 3.2C) micelles showed modest differences to the structures determined in the absence of DPC. These 17 structures also aligned well over the β-sheet region with average pairwise RMSDs of 0.18 ± 0.09 Å and 1.18 ± 0.18 Å for backbone and heavy atoms respectively.

For clarity, the structure with the lowest average pairwise RMSD to the mean has been chosen as a representative structure for both the aqueous and DPC-associated samples (Figure 3.2B and D respectively). The structure of PV5 was found to be an anti-parallel β-sheet connected by a turn region. In both DPC and non-DPC samples, the sheet region was relatively flat with the turn and tail regions projecting out of this plane although the degree of projection appeared less in the DPC environment. Figure 3.3A shows the contact surface of the representative structure of PV5 painted according to the electrostatic potential of the molecule. PV5 did not appear to be a highly amphipathic molecule in solution but rather was more amphiphilic, with its cationic loop and termini regions separated by a hydrophobic midsection. However, due to the dynamic termini, as evidenced by the poor overlay of these regions (Figure 3.2A), it appeared to demonstrate substantial conformational flexibility. This appeared to be reduced in the micelle-bound structure in which the variation in lowest energy structures was substantially reduced,

possibly reflecting a requirement for the PV5 molecule to adopt a more amphipathic conformation upon interaction with a hydrophobic environment. Indeed, the structure of PV5 determined in the presence of DPC micelles indicated an amphipathic conformation as indicated in Figure 3.3B. Reorganization of the side chains of the molecule result in a hydrophobic face and an area of cationic charge due to the clustering of the arginine residues. The amphipathic conformation of PV5 in lipid environments was in fact similar to the inherent amphipathic character of the parent peptide, polyphemusin I, in solution alone (Figure 3.3C).

A backbone overlay of the representative structures of PV5, in both the absence and presence of DPC micelles, and polyphemusin I (*4*) revealed only minor differences between the peptides (Figure 3.3C). The head and tail regions of solution PV5 projected further out of the plane formed by the backbone compared to those of polyphemusin I, due to the insertion of an arginine residue at position 12 of PV5. This insertion disrupted the classical four member β-turn region of polyphemusin and was the only sequence difference. Addition of DPC micelles reduced the non-planar nature of the PV5 backbone and resulted in a structure similar to that of polyphemusin I.

**Membrane partitioning**

The ability of polyphemusin I and PV5 to associate with and partition into lipid bilayers was determined using fluorescent spectroscopy, with the single tryptophan residue in each peptide serving as an intrinsic fluorophore. Tryptophan fluorescence is common and useful method to determine the influence of the polarity of the local environment. In a polar environment, excited tryptophan residues interact with polar

solvent molecules, suppressing their mobility and thus decreasing the energy of the excited state (*29*). This decrease in energy can be observed by the minimal fluorescence intensity. As the polarity of the environment decreases, the tryptophan fluorescence shifts to a lower wavelength (a blue shift) with a corresponding increase in intensity. As liposomes were titrated into a cuvette containing either polyphemusin I or PV5, the fluorescence signal, monitored at 335nm, was observed to increase. Representative fluorescence spectra are included in Figures 3.4A, C, E, and G.

Peptide partition coefficients ($K_p$) were determined from the slope of the initial, linear portion of the binding isotherms of bound peptide per total lipid ($X_b$*) *vs.* the equilibrium concentration of free lipid ($C_f$) (see Figures 3.4B, D, F, and H for representative binding isotherms). Both peptides had low affinity for neutral POPC vesicles with partition coefficients (means ± standard deviations of 3 separate experiments) of 2.7 ± 0.5 x $10^3$ $M^{-1}$ and 1.3 ± 0.2 x $10^3$ $M^{-1}$ for polyphemusin I and PV5 respectively (Table 2). Incorporation of 25 mole percent of the negative lipid, POPG which served as a simple model of an anionic prokaryotic membrane, increased the affinity of both peptides, but had a greater effect on PV5 (53 ± 2 x $10^3$ $M^{-1}$) which had a partition coefficient almost double that of polyphemusin I (31 ± 9 x $10^3$ $M^{-1}$). Incorporation of 25 mole percent cholesterol, which served as a model of a eukaryotic membrane, showed little effect on the affinity of both peptides compared to that of POPC alone with partition coefficients of 1.4 ± 0.2 x $10^3$ $M^{-1}$ for polyphemusin I and 1.0 ± 0.1 x $10^3$ $M^{-1}$ for PV5. Incorporation of 25 mole percent zwitterionic POPE, resulted in similar partition coefficients for both polyphemusin I and PV5 of 2.2 ± 0.3 x $10^3$ $M^{-1}$ and 2.0 ± 0.4 x $10^3$ $M^{-1}$ respectively.

**Differential scanning calorimetry**

In this study, the effects of polyphemusin I and PV5 on the thermotrophic phase behaviour of zwitterionic DMPC and anionic DMPC:DMPG multi-lamellar vesicles were observed by DSC. DSC is a useful tool for characterizing the interaction of compounds with lipid bilayers. Since the phase transition temperatures and transition enthalpies of phospholipid bilayers, particularly those incorporating phosphatidylcholine and phosphatidylglycerol (*30*), have been extensively studied and are well understood, the effects of exogenously added compounds can be determined by monitoring the changes in these values. Indeed DSC has been used in a variety of peptide-lipid studies (*31-34*). The effect of added peptide on the pre-transition and main gel to liquid crystalline transition serves as an indicator of the ability of the peptide to associate with lipid headgroups and disrupt the lipid acyl chain packing respectively. In addition the effect of peptide on the lamellar ($L_\alpha$) to inverted hexagonal ($H_{II}$) phase transition temperature ($T_H$) serves as an indicator of induced curvature strain and is often used to provide insights into the mechanism of action of a particular peptide (*35, 36*) . Together, this data provides an insight to the overall mechanism of the interaction of the peptide with the lipid bilayer studied.

DSC thermograms indicating the pre-transition (lamellar gel, $L_\beta'$, to rippled gel, $P_\beta'$) and main gel to liquid crystalline transition ($L_\alpha$) are shown in Figure 3.5 for DMPC and Figure 3.6 for DMPC:DMPG vesicles. The DSC thermograms of pure DMPC MLVs (Figure 3.5, for a peptide to lipid ratio of 0:800) indicated a small, broad pre-transition peak at 15.1°C, and a tall, narrow $L_\alpha$ peak centered at 24.2°C. Addition of increasing concentrations of either polyphemusin I or PV5 had only minor effects indicating that

neither peptide readily associated with or disrupted the acyl chain packing of net-neutral (zwitterionic) DMPC bilayers. For example, at low to moderate peptide concentrations (peptide: lipid ratios < 1:200) the $L_\alpha$ transition peak at 24.2°C was only slightly reduced in amplitude compared to the untreated DMPC control. The pre-transition peak at 15.1°C was still observed, even at high peptide concentrations (peptide: lipid ratios > 1:100), indicating that the interaction of the peptide with the lipid headgroups was minimal. At all peptide concentrations, the enthalpy of both the pre-transition and main transition peaks, as revealed by the peak heights and areas, was somewhat less in the presence of polyphemusin I than in the presence of PV5, indicating that polyphemusin I interacted more strongly with zwitterionic DMPC vesicles than did PV5.

While eukaryotic membranes contain predominantly zwitterionic lipids, bacterial membranes contain substantial (up to 30 mole percent) amounts of negatively charged lipids like phosphatidylglycerol (PG) and cardiolipin. The DSC thermograms of anionic DMPC:DMPG (3:1 molar ratio) multi-lamellar vesicles (Figure 3.6, peptide to lipid ratios of 0:800) appeared similar to those of pure DMPC, with a small, broad pre-transition peak at 15.2°C, and a tall, narrow Lα peak centered at 24.6°C. The addition of increasing concentrations of polyphemusin I or PV5 caused much more prominent changes than in the case of zwitterionic DMPC vesicles, indicating that both peptides readily associated with and disrupted the acyl chain packing of the negatively charged vesicles. At low peptide concentrations (peptide: lipid ratios < 1:400), the main transition peak at 24.6°C was considerably reduced in magnitude compared to untreated control DMPC:DMPG vesicles. At moderate concentrations (peptide: lipid ratios of 1:100), this peak was almost entirely abolished indicating the near absence of a phase transition. The pre-transition

peak at 15.2°C was greatly reduced at low peptide concentrations (peptide: lipid ratios < 1:800) and abolished almost entirely at a PV5:lipid ratio of 1:400 and a polyphemusin I:lipid concentration of 1:200 indicating there were very significant interactions of both peptides with the lipid headgroups. At all peptide concentrations, the enthalpies of both the pre-transition and $L_\alpha$ transitions were less in the presence of PV5 than in the presence of polyphemusin I, indicating that, opposite to the results for zwitterionic DMPC vesicles, PV5 interacted more strongly with negative DMPC:DMPG vesicles than polyphemusin I.

DSC was also used to determine the effects of polyphemusin I and PV5 on membrane curvature by monitoring the temperature ($T_H$) of the phase transition of DiPoPE vesicles from the liquid crystalline ($L_\alpha$) to inverted hexagonal ($H_{II}$) phase. The DSC thermogram of pure DiPoPE indicated a $T_H$ of 43.8°C as indicated by the vertical line (Figure 3.7). At very low concentrations of PV5 (peptide to lipid ratio of 1:1000) the $T_H$ was reduced indicating that PV5 induced negative curvature. An increase in peptide concentration (peptide to lipid ratio of 1:500) further reduced the $T_H$ and led to a slight broadening of the transition peak. Very low concentrations of polyphemusin I (peptide to lipid ratio of 1:1000) also caused a reduction in $T_H$ compared to untreated DiPoPE vesicles, indicating negative curvature strain, and similarly resulted in a broadening in peak width. This peak was also asymmetric in shape indicating a reduction in lipid cooperativity of the transition most likely due to the presence in the membrane of peptide-rich regions. Further increasing the polyphemusin I concentration (peptide to lipid ratio of 1:500) actually increased the $T_H$ slightly above that observed at the lower polyphemusin I. While this suggests polyphemusin I stabilizes the lamellar form, it

should be noted that the $T_H$ observed for both concentrations are reduced compared to the untreated lipid control. Thus, the DSC thermograms indicated that both polyphemusin I and PV5 induced negative membrane curvature strain and promoted the formation of inverted hexagonal phases by decreasing the phase transition temperature. In addition, the different effects on phase transition peak width indicate that polyphemusin I had a much greater effect on lipid cooperativity, as the phase transition peaks were much broader with polyphemusin I compared to the transition peaks of DiPoPE with or without PV5.

**Discussion**

Due to the excellent antimicrobial activity of polyphemusin I (less than 0.2μM for both Gram negative and Gram positive organisms), but disappointing ability to protect in animal models of infection and sepsis, a series of polyphemusin I analogues were previously designed to improve amphipathic character and/or increase cationic charge (*7*). One analogue, PV5, was found to be quite protective in mice models of bacterial challenge and endotoxemia while retaining effective *in vitro* activity (less than 0.4μM for both Gram negative and Gram positive organisms) (*7*). In our ongoing effort to characterize the antimicrobial mechanism of the polyphemusins, these two peptides were used as representatives of this family. To investigate the structural components involved in their activity, the three-dimensional solution structure of PV5 was determined by $^1$H-NMR, in the absence and presence of DPC micelles, and compared to the previously determined structure of polyphemusin I (*4*). In addition, the interaction of both peptides with lipid membranes was investigated using fluorescence spectroscopy and differential scanning calorimetry.

An ensemble of the lowest energy structures of PV5 in the absence and presence of DPC micelles was determined in this study (Figure 3.2A). The structure of PV5 was that of an anti-parallel β-hairpin. Comparison of the backbone structures of PV5 with the previously determined structure of polyphemusin I (*4*) revealed only small differences between the two peptides (Figure 3.3D). The head and tail regions of PV5 projected further out of the plane formed by the backbone than those of polyphemusin I. The insertion of an arginine at position 12 of PV5 disrupted the four member β-turn region accounting for the change in structure of the head region when compared to polyphemusin I. While there were conformational differences between the tail regions of the representative structures, the large degree of conformational flexibility in this region suggested that these differences likely do not account for differential membrane interactions of these peptides. The structure of PV5 determined in the presence of DPC micelles revealed that the side chains of the molecule undergo a reorganization which resulted in an increased amphipathic conformation (Figure 3.3B). Unfortunately we were unable to study the peptide in the presence of negatively charged SDS micelles as this led to precipitation, presumably due to peptide induced micelle aggregation.

Laederach *et al* have identified a potential hinge region at the centre of the related peptide tachyplesin and have postulated that this allows the peptide to adopt a more surface hydrophobic character when present in a membrane environment (*3*). This hinge-region, proposed as a result of only two weak long-range NOE restraints, was not observed in our study of PV5. It is conceivable that such a hinge could also act to bring the cationic turn and termini regions in closer proximity, to facilitate a larger cationic patch to interact with anionic lipids. If this mechanism of binding were applied, for

instance, to peptide-LPS interactions, where the cationic head and termini of the peptide bind to the anionic phosphate groups present in the LPS, the additional cationic charge imparted by arginine-12 may aid in this function (Figure 3.3A, B and C). This oriented binding and additional cationic charge could also explain why the interaction of PV5 with LPS was less inhibited by the presence of added $Mg^{2+}$ ions than was polyphemusin I (*7*).

Polyphemusin I and PV5 exhibited only minor interactions with neutral membranes composed of PC, PC:Cholesterol, or PC:PE. The partition coefficient of polyphemusin I was two-fold greater than that of PV5 for PC vesicles however, both peptides partitioned relatively poorly into neutral membranes compared to the negative PC:PG vesicles (Table 3.2). The DSC thermograms of PC correlated with the partitioning data and indicated that, even at quite high peptide concentration, pre-transition and main transition peaks were still present (Figure 3.5). Thus, both polyphemusin I and PV5 interacted weakly with the lipid headgroups and acyl chains of neutral membranes although, polyphemusin I displayed a slightly increased membrane interaction as evidenced by the greater reduction in enthalpy of the main gel to liquid crystalline transition compared to PV5.

The addition of biologically significant lipids was also studied to determine their effects on membrane partitioning. Addition of 25 mole percent of the eukaryotic lipid cholesterol to produce PC:Cholesterol vesicles showed little effect on the affinity of both peptides compared to that of POPC alone (Table 3.2). Phosphatidylethanolamine was also used in partition studies due to its relatively high content in prokaryotic cells (>70%) as well as its presence in eukaryotic membranes, albeit to a much lesser extent. In addition, this type II, non-lamellar phase forming lipid was of interest to study when

considering membrane translocation, as *E. coli* mutants deficient in PE synthesis lack the ability to transport proteins across their plasma membrane (*37*). Incorporation of 25 mole percent of PE to produce PC:PE vesicles resulted in similar partition coefficients for both peptides which differed little compared to their partitioning into POPC alone. This indicated the presence of PE alone does not promote the partitioning of either peptide.

Both peptides showed considerably increased affinities for negatively charged membranes composed of PC:PG (Table 3.2), on the order of 10 to 40 fold greater for the negatively charged PC:PG vesicles compared to the neutral PC vesicles. Interestingly however the partition coefficient of PV5 for PC:PG vesicles were almost double that of polyphemusin I. The DSC thermograms for negatively charged membranes were consistent with these partitioning data and indicated that, even at a low peptide concentration, the pre-transition and main transition peaks were greatly reduced in magnitude for both peptides suggesting a large interaction with the negatively charged lipid headgroups and disruption of acyl chain packing (Figure 3.6). The affinity of PV5 appeared to be significantly greater as evidenced by the larger reduction in enthalpy of the main thermal transition peak compared to that induced by polyphemusin I. Since the initial step in peptide-membrane association is thought to be due to electrostatic interaction, the additional arginine in PV5 likely accounts for the observed increase in partitioning into PG containing membranes when compared to polyphemusin I. While the effect of charge modification has not been well studied for the polyphemusins, studies have been conducted on other cationic peptides. Increasing charge of the α-helical peptide magainin II has been shown to increase the permeabilizing ability of negatively charged PG containing vesicles while no relationship was observed for neutral PC

membranes (*38*). This also highlights the limitations in using model membranes to study biological phenomena as the lack of partitioning into neutral PC membranes cannot explain the cytotoxic effects observed with some peptides. Certainly, the various proteins and receptors found in eukaryotic membranes interact with peptides to some extent. Tachyplesin which, due to its similarity to the polyphemusins, would not be expected to partition into zwitterionic membranes, has been demonstrated to act as a secretagogue upon hemocytes (*8*). This finding suggests that the polyphemusins are capable of interacting with eukaryotic cells in some manner that partitioning alone does not explain.

Both polyphemusin I and PV5 promoted negative membrane curvature strain as indicated by a reduction in the hexagonal phase transition temperature of DiPoPE (Figure 3.7). Transient, non-bilayer formation may play a role in the membrane translocation of proteins and peptides and non-bilayer forming lipids are required for protein folding (*39*) and protein transport across membranes (*37*). The promotion of non-bilayer transitions by these peptides may thus explain part of their antimicrobial mechanism. To further assess the importance of negative curvature strain it would be of interest to conduct a study to examine the effects of negative curvature inhibitors such as lysolipids (or other inverted cone shaped lipids) on polyphemusin membrane translocation.

The effects of polyphemusin, on the lamellar to inverted hexagonal phase transition temperature of pure DiPoPE, contrast with those observed for other cationic peptides. Addition of the cationic peptides LL-37 (*40*), magainin 2 (*41*) and an analogue, MSI-78 (*42*) increases the $T_H$ indicating the induction of positive curvature strain as more energy is required to drive the formation of the inverted hexagonal phase (cf. polyphemusins that lowered the $T_H$ and induced negative curvature strain, thus promoting

the formation of the inverted hexagonal phase). The induction of positive membrane curvature strain is consistent with a mechanism involving the torroidal-pore model in which peptide-induced positive membrane curvature would lead to the formation of a torus-like pore, which, upon collapse, may disperse peptide on either side of the lipid bilayer. Due to the induction of negative membrane curvature observed here for polyphemusin I and PV5, it is clear that the polyphemusin family of peptides do not function through this mechanism. This is similar to pardaxin which induces negative curvature strain even at very low concentrations (peptide:lipid mole ratio of 1:50,000) which also does not function through a torroidal mechanism (*35*).

Additional insight into the mechanism of action of the polyphemusins may also be inferred from previous studies focused on lipid flip-flop and dye release. It was shown that at low peptide:lipid ratios (< .005) significant lipid exchange between membrane leaflets is observed (~60%) but very little calcein release occurs (~5%) (*5*). In order to maintain membrane integrity and prevent entrapped contents from leaking out of the vesicles, the peptide must interact with the leaflets sequentially so one will always be intact and impermeable to the dye, or alternatively the disturbance produced must be too small to allow appreciable dye release. Since the degree of flip-flop is so large, the latter explanation seems unlikely. This is because the degree of disturbance necessary for lipid molecules (POPC 760 MW) to switch leaflets should be sufficiently large as to cause appreciable calcein (623 MW) dye release. From these data and the results reported here we can propose a model for the translocation of the polyphemusins (Figure 3.8). It is hypothesized that the peptides translocate the membrane through the formation of a transient, non-bilayer peptide-lipid intermediates. Peptides initially encounter the net

negatively charged membrane bilayer (Step 1) and interact with negatively charged lipid headgroups in the outer leaflet (Step 2). This leads to partial membrane insertion and peptide aggregation within the bilayer causing negative curvature strain (Step 3). Peptide aggregation and induced curvature strain drives the formation of a non-bilayer intermediate (Step 4). It should be noted that the aggregation of peptide at sites already exhibiting some degree of negative curvature such as membrane rippling or invagination would serve to reduce the energy required for such an inverted structure to form. Upon formation of this state, the outer leaflet regains integrity and reforms a permeability barrier. Collapse of this intermediate structure leads to the redistribution of the peptide in both leaflets during which a small amount of dye may be released (Step 5). While the data presented in this paper supports only steps 1 and 2 of this mechanism it serves to further define the aggregate model of membrane translocation previously proposed by our group (*43*) . It should also be noted that the aggregate model is similar in nature to the sinking-raft model proposed by Pokorny *et al* (*44, 45*).

The findings presented here, combined with previous observations that polyphemusin I promotes lipid flip-flop between membrane leaflets, but does not induce significant vesicle leakage (*5*), rule out the torroidal pore (*46*) and carpet mechanisms of action (*47*).

**Table 3.1.** Structural statistics of PV5 determined by $^{1}$H-NMR in $H_2O$:$D_2O$ (9:1) in the presence or absence of 300mM DPC micelles.

| **NOE Restraints** | **$H_2O$:$D_2O$** | | **DPC micelles** | |
|---|---|---|---|---|
| Total | 129 | | 137 | |
| Intra-residue | 67 | | 68 | |
| Inter-residue | 62 | | 69 | |
| **Mean Total Energy (kcal mol$^{-1}$)** | 26.2 ± 0.5 | | 34.3 ± 1.2 | |
| **Mean Pairwise RMSD** | Backbone | Heavy | Backbone | Heavy |
| Turn (8-14) | 0.41 ± 0.10 | 1.43 ± 0.28 | 0.18 ± 0.09 | 1.18 ± 0.18 |
| Sheet (7,8,14,15) | 0.21 ± 0.05 | 0.79 ± 0.09 | 0.23 ± 0.04 | 0.98 ± 0.27 |

**Table 3.2.** Partition coefficients indicating the affinity of polyphemusin I (PM1) and PV5 for liposomes of various lipid compositions.

| **Liposomes** (mol:mol) | **Partition coefficients (x $10^3$ $M^{-1}$)** | |
|---|---|---|
| | **PM1** | **PV5** |
| POPC | 2.7 ± 0.5 | 1.3 ± 0.2 |
| POPC:POPG (3:1) | 31 ± 9 | 53 ± 2 |
| POPC:POPE (3:1) | 2.2 ± 0.3 | 2.0 ± 0.4 |
| POPC:Cholesterol (3:1) | 1.4 ± 0.2 | 1.0 ± 0.1 |

**Figure 3.1.** Primary structures of polyphemusin I (PM1) and its analogue PV5. Disulfide linkages in are shown as solid lines. The spacing in polyphemusin I is done for sequence alignment and does not represent a break in the peptide backbone.

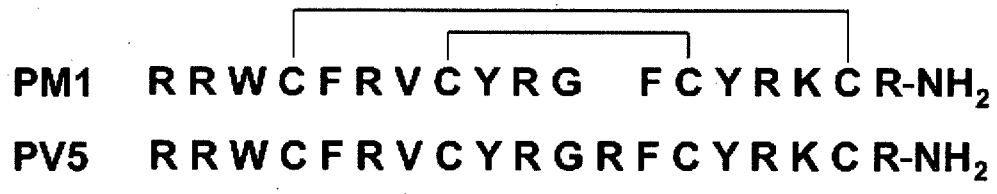

**Figure 3.2.** Three-dimensional solution structure of PV5 in the absence and presence of DPC micelles. **A and C:** the set of structures calculated for PV5. 16 structures are presented for PV5 in aqueous medium (A) and 17 structures are presented for PV5 in DPC micelles (C). The backbone is coloured black and the cysteine side chains are indicated in yellow. Structures are aligned over the β-sheet residues 7, 8, 14 and 15. **B and D:** ribbon diagram of the representative PV5 structures in the absence or presence of DPC micelles respectively. Figures were prepared with MOLMOL (*23*).

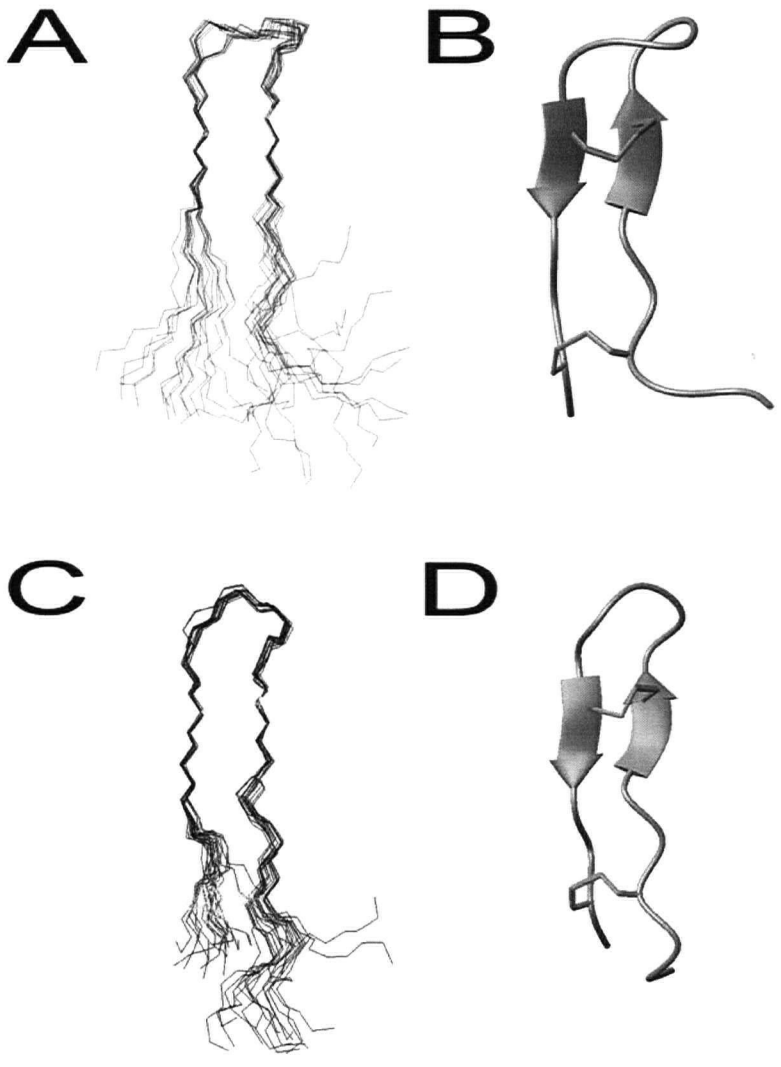

**Figure 3.3.** Contact surfaces and backbone overlay of the representative structures of PV5 and polyphemusin I. **A, B and C:** contact surfaces of the representative structures of PV5, in the absence or presence of DPC micelles, and polyphemusin I respectively, painted with their corresponding electrostatic potentials. The additional arginine (R12) in PV5 is indicated while other residues are labeled for orientation. **D:** backbone overlay of the representative structures of PV5 (black), PV5 in DPC micelles (blue) and polyphemusin I (red). Figures were prepared with MOLMOL (*23*).

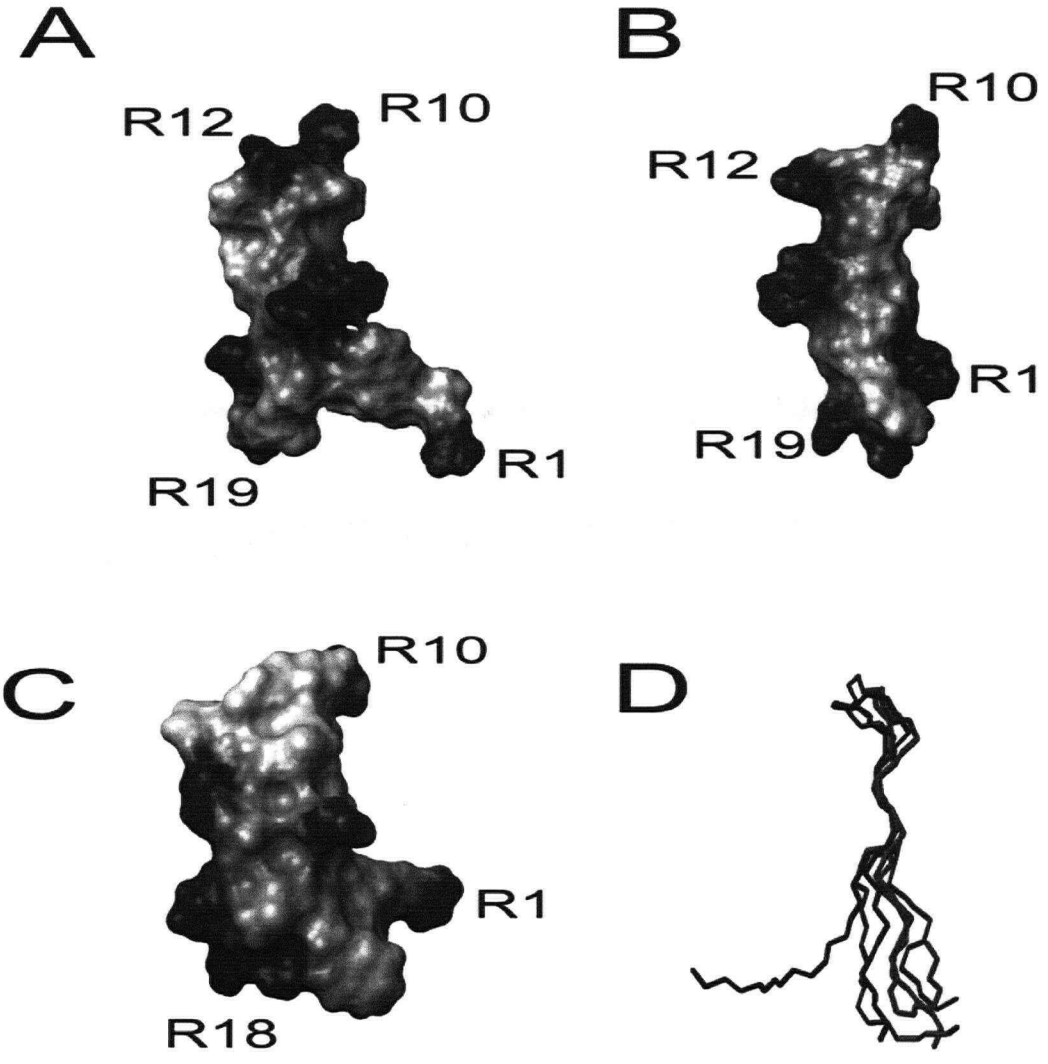

**Figure 4.4.** Fluorescence microscopy of *E. coli* UB1005 treated with PM1-biotin. Bacteria were incubated at 4°C (top panels) or 37°C (bottom panels) without peptide (A, D) and at peptide concentrations of one half MIC (B, E) and 4 times the MIC (C, F) for 30 min. Blue fluorescence staining represents intracellular DAPI-stained DNA while green fluorescence staining represents the Alexa Fluor labeled peptide.

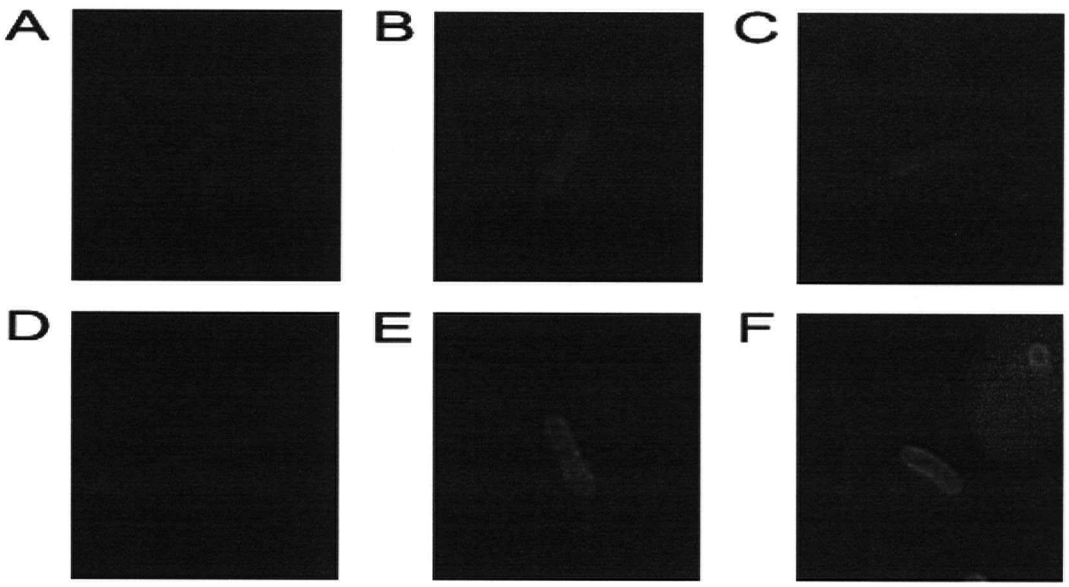

**Figure 3.4.** Peptide partitioning into vesicles. **A, C, E, G:** Fluorescence increase of polyphemusin I (PM1) and PV5 upon titration with vesicles. Samples contained 1μM peptide in 10mM HEPES, 150mM NaCl, pH 7.4. The abscissa indicates the lipid to peptide molar ratio during titration. Excitation and emission wavelengths were 280nm and 335nm respectively. **B, D, F, H:** Binding isotherms of $X_b$* (molar ratio of bound peptide per total lipid) versus $C_f$ (concentration of unbound peptide) determined from the fluorescence curves and the equations indicated in the text. **A** and **B**: POPC; **C** and **D**: POPC:POPG (3:1); **E** and **F**: POPC:Cholesterol (3:1); **G** and **H**: POPC:POPE (3:1). polyphemusin I, filled squares; PV5, unfilled squares. Brackets indicate mole ratios.

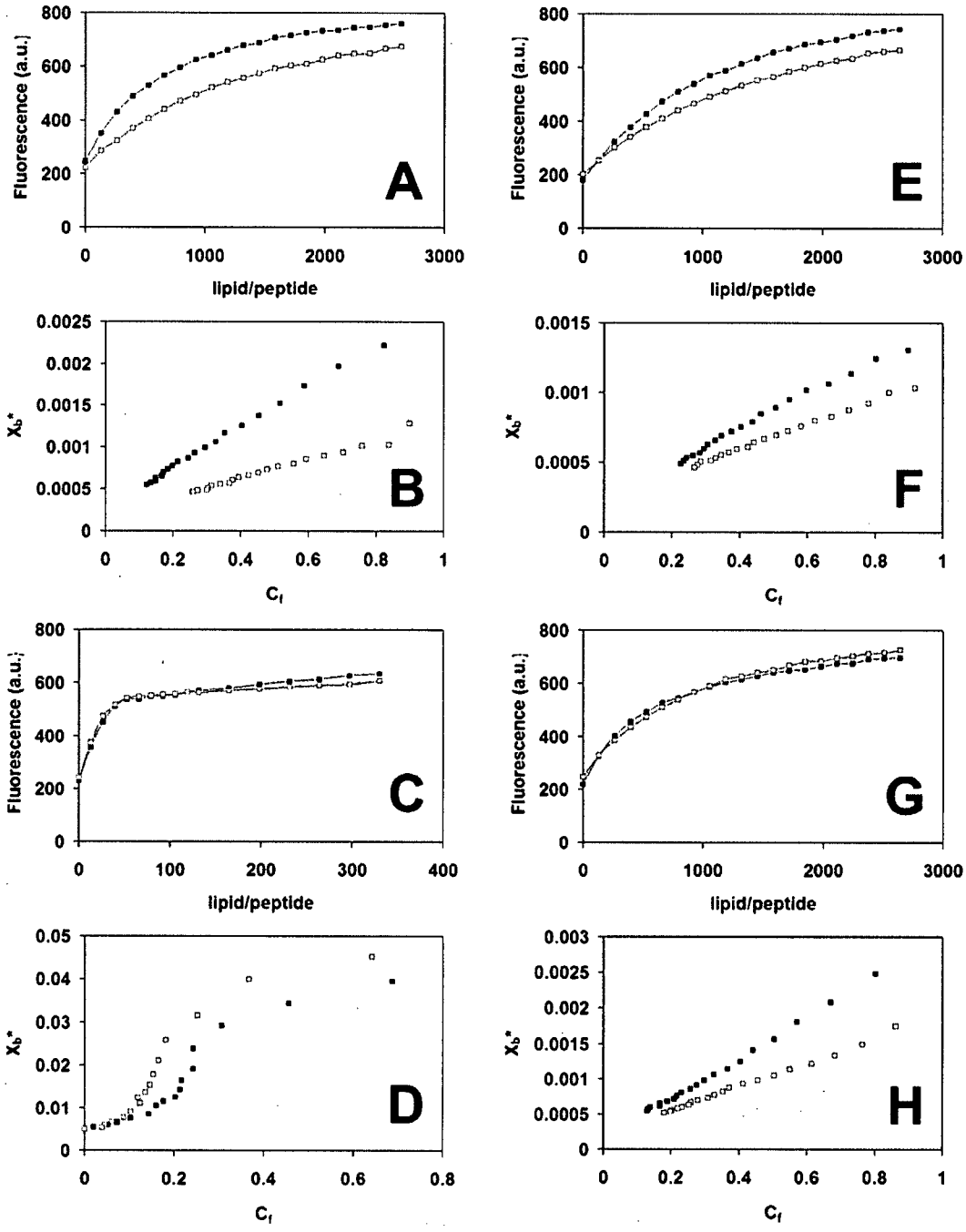
A
Fluorescence (a.u.)
lipid/peptide
B
$X_b$*
$C_f$
C
D
E
F
G
H

**Figure 3.5.** Differential scanning calorimetry of the pre-transition and main gel to liquid crystalline phase transition of DMPC vesicles at the indicated peptide to lipid molar ratios. Lipid was dissolved in chloroform, dried and suspended at a concentration of 1mg/ml.

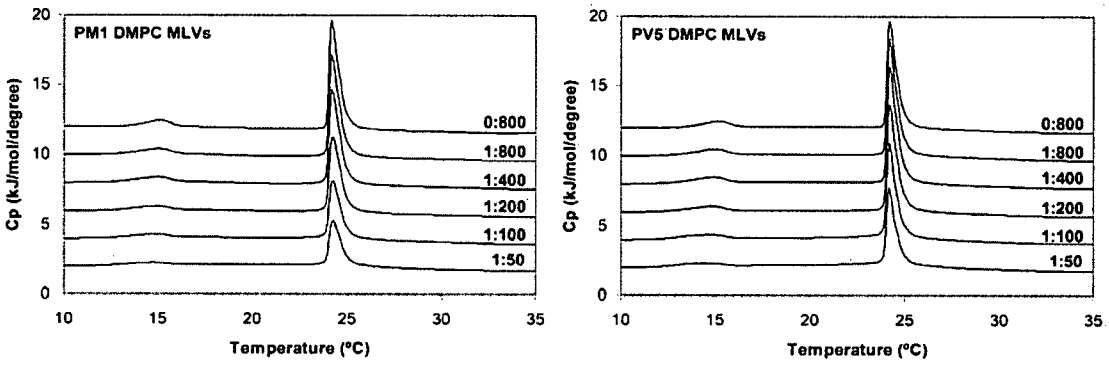

**Figure 3.6.** Differential scanning calorimetry of the pre-transition and main gel to liquid crystalline phase transition of DMPC:DMPG (3:1) vesicles at the indicated peptide to lipid molar ratios. Lipids were dissolved in chloroform at a molar ratio of 3:1, dried and suspended at a concentration of 1mg/ml.

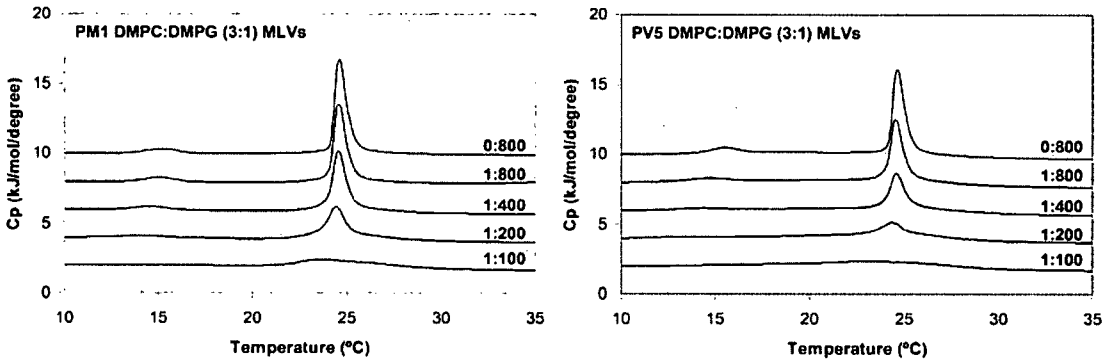

**Figure 3.7.** Differential scanning calorimetry of the lamellar ($L_\alpha$) to inverted hexagonal ($H_{II}$) phase transition of DiPoPE at the indicated peptide to lipid molar ratios. Peptide and lipid were co-dissolved in a chloroform:methanol solution, dried and suspended in 10mM HEPES, 150mM NaCl, pH 7.4 to yield multi-lamellar vesicles at a working concentration of 7.5mg/ml lipid. Peptide to lipid molar ratios are indicated. The vertical line indicates the transition temperature of pure DiPoPE ($T_H$ = 43.8°C) with no added peptide.

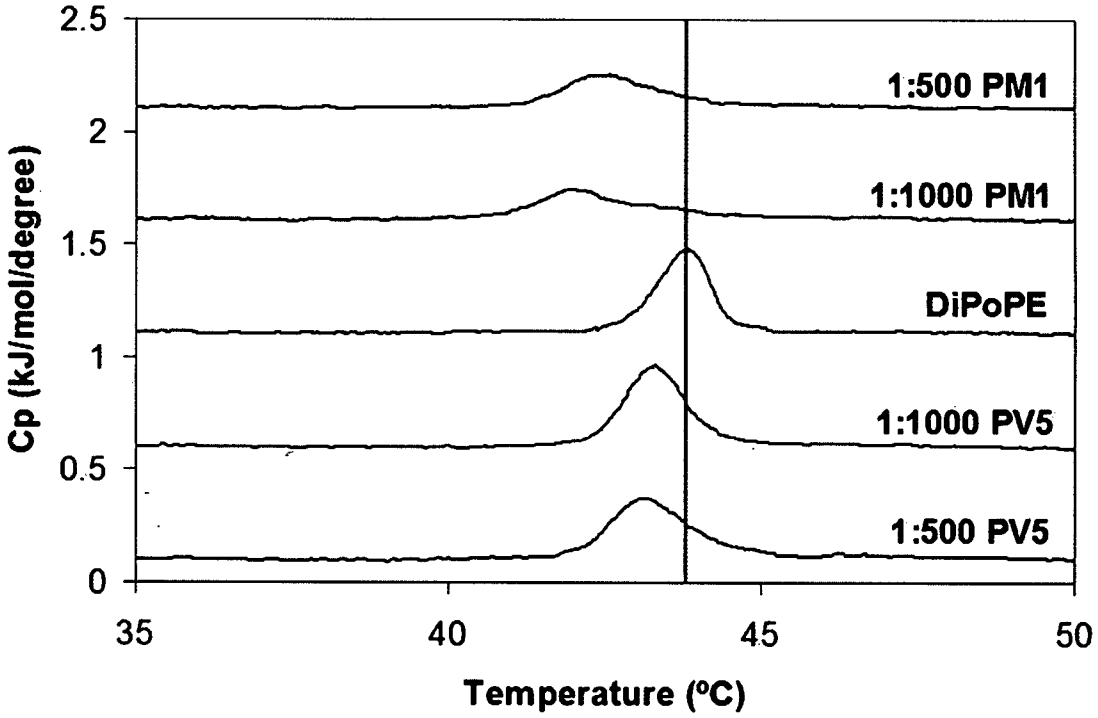

**Figure 3.8.** Mechanism of membrane translocation of the polyphemusins. **1)** Peptides initially encounter the negatively charged lipid bilayer. **2)** Electrostatic interaction of the peptide (hollow) with the negatively charged lipid headgroups (black) and partial membrane insertion. **3)** Aggregation of the bound peptide within the outer leaflet of the bilayer and induction of negative membrane curvature. **4)** Transient non-bilayer formation occurs due to the combination of negative curvature and peptide aggregation. **5)** Collapse of non-bilayer intermediate and corresponding peptide translocation to the membrane inner leaflet. It should be noted that the figure is for clarification purposes and is not intended to infer scale or stoichiometry.

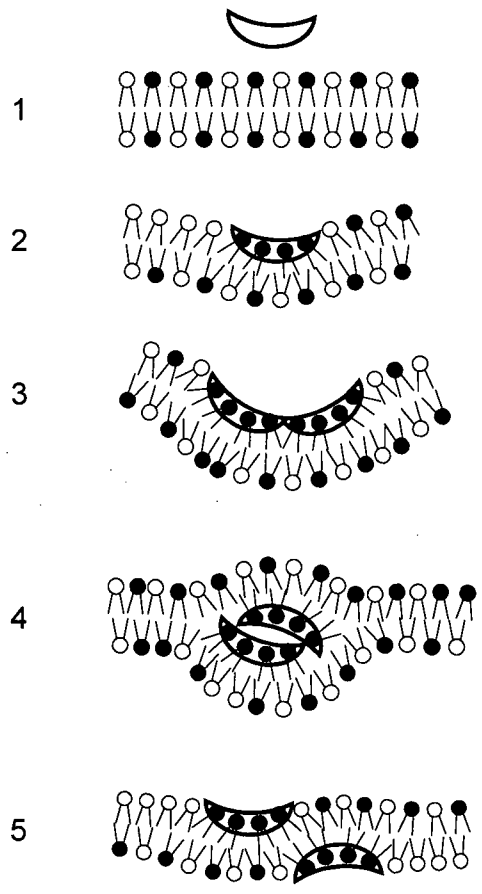

## References


1. Miyata, T., Tokunaga, F., Yoneya, T., Yoshikawa, K., Iwanaga, S., Niwa, M., Takao, T., and Shimonishi, Y. (1989) Antimicrobial peptides, isolated from horseshoe crab hemocytes, tachyplesin II, and polyphemusins I and II: chemical structures and biological activity, *J Biochem (Tokyo) 106*, 663-8.
2. Nakamura, T., Furunaka, H., Miyata, T., Tokunaga, F., Muta, T., Iwanaga, S., Niwa, M., Takao, T., and Shimonishi, Y. (1988) Tachyplesin, a class of antimicrobial peptide from the hemocytes of the horseshoe crab (Tachypleus tridentatus). Isolation and chemical structure, *J Biol Chem 263*, 16709-13.
3. Laederach, A., Andreotti, A. H., and Fulton, D. B. (2002) Solution and micelle-bound structures of tachyplesin I and its active aromatic linear derivatives, *Biochemistry 41*, 12359-68.
4. Powers, J. P. S., Rozek, A., and Hancock, R. E. W. (2004) Structure-activity relationships for the beta-hairpin cationic antimicrobial peptide polyphemusin I, *Biochim Biophys Acta 1698*, 239-50.
5. Zhang, L., Rozek, A., and Hancock, R. E. W. (2001) Interaction of cationic antimicrobial peptides with model membranes, *J Biol Chem 276*, 35714-22.
6. Matsuzaki, K., Yoneyama, S., Fujii, N., Miyajima, K., Yamada, K., Kirino, Y., and Anzai, K. (1997) Membrane permeabilization mechanisms of a cyclic antimicrobial peptide, tachyplesin I, and its linear analog, *Biochemistry 36*, 9799-806.

7. Zhang, L., Scott, M. G., Yan, H., Mayer, L. D., and Hancock, R. E. W. (2000) Interaction of polyphemusin I and structural analogs with bacterial membranes, lipopolysaccharide, and lipid monolayers, *Biochemistry 39*, 14504-14.

8. Ozaki, A., Ariki, S., and Kawabata, S. (2005) An antimicrobial peptide tachyplesin acts as a secondary secretagogue and amplifies lipopolysaccharide-induced hemocyte exocytosis, *Febs J 272*, 3863-71.

9. Tam, J., Wu, C., Liu, W., and Zhang, J. (1991) Disulfide bond formation in peptides by dimethyl sulfoxide. Scope and applications, *J Am Chem Soc 113*, 6657-62.

10. Rance, M., Sorensen, O. W., Bodenhausen, G., Wagner, G., Ernst, R. R., and Wuthrich, K. (1983) Improved spectral resolution in cosy $^{1}H$ NMR spectra of proteins via double quantum filtering, *Biochem Biophys Res Commun 117*, 479-85.

11. Braunschweiler, L., and Ernst, R. R. (1983) Coherence transfer by isotropic mixing: application to proton correlation spectroscopy, *J Magn Res 53*, 521-8.

12. Jeener, J., Meier, B. H., Bachmann, P., and Ernst, R. R. (1979) Investigation of exchange processes by two-dimensional NMR spectroscopy, *J Chem Phys 71*, 4546-53.

13. Piotto, M., Saudek, V., and Sklenar, V. (1992) Gradient-tailored excitation for single-quantum NMR spectroscopy of aqueous solutions, *J Biomol NMR 2*, 661-5.

14. Sklenar, V., Piotto, M., Leppik, R., and Saudek, V. (1993) Gradient-Tailored Water Suppression for $^{1}H$-$^{15}N$ HSQC Experiments Optimized to Retain Full Sensitivity, *J Magn Res A 102*, 241-5.

15. Bax, A., and Davis, D. G. (1985) MLEV-17 based two-dimensional homonuclear magnetization transfer spectroscopy, *J Magn Res 65*, 355-60.

16. Delaglio, F., Grzesiek, S., Vuister, G. W., Zhu, G., Pfeifer, J., and Bax, A. (1995) NMRPipe: a multidimensional spectral processing system based on UNIX pipes, *J Biomol NMR 6*, 277-93.

17. Johnson, B. A., and Blevins, R. A. (1994) NMRView: A computer program for the visualization and analysis of NMR data, *J Biomol NMR 4*, 603-14.

18. Hyberts, S. G., Goldberg, M. S., Havel, T. F., and Wagner, G. (1992) The solution structure of eglin c based on measurements of many NOEs and coupling constants and its comparison with X-ray structures, *Protein Sci 1*, 736-51.

19. Friedrich, C. L., Rozek, A., Patrzykat, A., and Hancock, R. E. W. (2001) Structure and mechanism of action of an indolicidin peptide derivative with improved activity against gram-positive bacteria, *J Biol Chem 276*, 24015-22.

20. Schwieters, C. D., Kuszewski, J. J., Tjandra, N., and Clore, G. M. (2003) The Xplor-NIH NMR Molecular Structure Determination Package, *J Magn Res 160*, 66-74.

21. Morris, A. L., MacArthur, M. W., Hutchinson, E. G., and Thornton, J. M. (1992) Stereochemical quality of protein structure coordinates., *Proteins 12*, 345-64.

22. Laskowski, R. A., MacArthur, M. W., Moss, D. S., and Thornton, J. M. (1993) PROCHECK: a program to check the stereochemical quality of protein structures., *J Appl Cryst 26*, 283-91.

23. Koradi, R., Billeter, M., and Wuthrich, K. (1996) MOLMOL: a program for display and analysis of macromolecular structures, *J Mol Graph 14*, 51-5, 29-32.

24. Rapaport, D., and Shai, Y. (1991) Interaction of fluorescently labeled pardaxin and its analogues with lipid bilayers, *J Biol Chem 266*, 23769-75.

25. Schwarz, G., Stankowski, S., and Rizzo, V. (1986) Thermodynamic analysis of incorporation and aggregation in a membrane: application to the pore-forming peptide alamethicin, *Biochim Biophys Acta 861*, 141-51.

26. Beschiaschvili, G., and Seelig, J. (1990) Melittin binding to mixed phosphatidylglycerol/phosphatidylcholine membranes, *Biochemistry 29*, 52-8.

27. Marsh, D. (1990), CRC Press, Boca Raton, FL.

28. Wuthrich, K. (1986) *NMR of Proteins and Nucleic Acids*, John Wiley & Sons, Toronto.

29. Campbell, I. D., and Dwek, R. A. (1984) *Biological spectroscopy*, The Benjamin/Cummings Publishing Company Inc., Menlo Park.

30. Findlay, E. J., and Barton, P. G. (1978) Phase behavior of synthetic phosphatidylglycerols and binary mixtures with phosphatidylcholines in the presence and absence of calcium ions, *Biochemistry 17*, 2400-5.

31. Prenner, E. J., Lewis, R. N., Kondejewski, L. H., Hodges, R. S., and McElhaney, R. N. (1999) Differential scanning calorimetric study of the effect of the antimicrobial peptide gramicidin S on the thermotropic phase behavior of phosphatidylcholine, phosphatidylethanolamine and phosphatidylglycerol lipid bilayer membranes, *Biochim Biophys Acta 1417*, 211-23.

32. Tournois, H., and de Kruijff, B. (1991) Polymorphic phospholipid phase transitions as tools to understand peptide-lipid interactions, *Chem Phys Lipids 57*, 327-40.

33. van Kan, E. J., Ganchev, D. N., Snel, M. M., Chupin, V., van der Bent, A., and de Kruijff, B. (2003) The peptide antibiotic clavanin A interacts strongly and specifically with lipid bilayers, *Biochemistry 42*, 11366-72.

34. Lohner, K., Staudegger, E., Prenner, E. J., Lewis, R. N., Kriechbaum, M., Degovics, G., and McElhaney, R. N. (1999) Effect of staphylococcal delta-lysin on the thermotropic phase behavior and vesicle morphology of dimyristoylphosphatidylcholine lipid bilayer model membranes. Differential scanning calorimetric, 31P nuclear magnetic resonance and Fourier transform infrared spectroscopic, and X-ray diffraction studies, *Biochemistry 38*, 16514-28.

35. Hallock, K. J., Lee, D. K., Omnaas, J., Mosberg, H. I., and Ramamoorthy, A. (2002) Membrane composition determines pardaxin's mechanism of lipid bilayer disruption, *Biophys J 83*, 1004-13.

36. Davies, S. M., Epand, R. F., Bradshaw, J. P., and Epand, R. M. (1998) Modulation of lipid polymorphism by the feline leukemia virus fusion peptide: implications for the fusion mechanism, *Biochemistry 37*, 5720-9.

37. Rietveld, A. G., Koorengevel, M. C., and de Kruijff, B. (1995) Non-bilayer lipids are required for efficient protein transport across the plasma membrane of Escherichia coli, *Embo J 14*, 5506-13.

38. Dathe, M., Nikolenko, H., Meyer, J., Beyermann, M., and Bienert, M. (2001) Optimization of the antimicrobial activity of magainin peptides by modification of charge, *FEBS Lett 501*, 146-50.

39. Bogdanov, M., Sun, J., Kaback, H. R., and Dowhan, W. (1996) A phospholipid acts as a chaperone in assembly of a membrane transport protein, *J Biol Chem 271*, 11615-8.

40. Henzler Wildman, K. A., Lee, D. K., and Ramamoorthy, A. (2003) Mechanism of lipid bilayer disruption by the human antimicrobial peptide, LL-37, *Biochemistry 42*, 6545-58.

41. Matsuzaki, K., Sugishita, K., Ishibe, N., Ueha, M., Nakata, S., Miyajima, K., and Epand, R. M. (1998) Relationship of membrane curvature to the formation of pores by magainin 2, *Biochemistry 37*, 11856-63.

42. Hallock, K. J., Lee, D. K., and Ramamoorthy, A. (2003) MSI-78, an analogue of the magainin antimicrobial peptides, disrupts lipid bilayer structure via positive curvature strain, *Biophys J 84*, 3052-60.

43. Hancock, R. E. W., and Chapple, D. S. (1999) Peptide antibiotics, *Antimicrob Agents Chemother 43*, 1317-23.

44. Pokorny, A., Birkbeck, T. H., and Almeida, P. F. (2002) Mechanism and kinetics of delta-lysin interaction with phospholipid vesicles, *Biochemistry 41*, 11044-56.

45. Pokorny, A., and Almeida, P. F. (2004) Kinetics of dye efflux and lipid flip-flop induced by delta-lysin in phosphatidylcholine vesicles and the mechanism of graded release by amphipathic, alpha-helical peptides, *Biochemistry 43*, 8846-57.

46. Matsuzaki, K., Mitani, Y., Akada, K. Y., Murase, O., Yoneyama, S., Zasloff, M., and Miyajima, K. (1998) Mechanism of synergism between antimicrobial peptides magainin 2 and PGLa, *Biochemistry 37*, 15144-53.

47. Oren, Z., and Shai, Y. (1998) Mode of action of linear amphipathic alpha-helical antimicrobial peptides, *Biopolymers 47*, 451-63.

## Chapter 1 – The antimicrobial peptide polyphemusin localizes to the cytoplasm of *Escherichia coli* following treatment

### Introduction

Polyphemusin I is a member of a family of antimicrobial peptides isolated from the hemocytes of the American horseshoe crab, *Limulus polyphemus* (*1*). It has a high affinity for LPS (*1*) and excellent antimicrobial activity against Gram negative and Gram positive bacteria, with minimal inhibitory concentrations often less than 1μg/ml, demonstrating rapid killing within 5 min of treatment (*2*).

While the interaction of polyphemusin peptides with model membranes has been well studied (*2-4*), relatively little is known about their mechanism of action in bacteria. Whole cell assays have indicated that polyphemusin I can cause rapid cytoplasmic membrane depolarization of mutant *E.coli*, but this did not correlate with and was not accompanied by cell death (*2*). Conversely, related polyphemusins with similar antimicrobial activity have relatively modest effects on cytoplasmic membrane integrity. Model membrane studies have shown that this peptide interacts preferentially with negatively charged membranes and induces lipid flip-flop between membrane leaflets at concentrations that show little or no disturbance to bilayer integrity (*3*). Polyphemusin I is able to translocate membrane bilayers and gain access to the interior of vesicles (*3, 4*) and, has recently been shown to induce negative membrane curvature strain (Chapter 3), a property that may be involved in the translocation process. Indeed, other peptides, such as buforin II (*5*) and pyrrhocoricin (*6*), have also been shown to translocate across

membranes and have been proposed to act on intracellular targets in eliciting their antimicrobial activity.

To further characterize the antibacterial action of the polyphemusins, it was of significant interest to determine where these peptides localize on or within the bacteria following treatment. While translocation has been inferred from model membrane assays, this finding has yet to be confirmed by whole cell assays. To accomplish this, we synthesized a polyphemusin I analogue with a single C-terminal biotin label. This peptide, PM1-biotin, was then characterized, and compared to the native polyphemusin I, both structurally, by using circular dichroism spectroscopy, and with respect to its antimicrobial activity, using minimal inhibitory concentration and killing kinetics. To determine peptide localization, fluorescence and confocal microscopy were performed after treating a wild type *E. coli* strain with PM1-biotin. The data clearly indicate that polyphemusin translocates into E.coli with only modest cytoplasmic membrane disruption and causes cytoplasmic disorganization.

## Materials and methods

### Strains and reagents

The bacterial *Escherichia coli* (*E. coli*) strain UB1005 ($F^-$, *nal*A37, *met*B1) was used in both the minimal inhibitory concentration (MIC) and killing assays. All strains were grown in Mueller Hinton (MH) or LB broth (Difco Laboratories, Detroit, MI) at 37°C unless otherwise noted. All lipids were purchased from Avanti Polar Lipids Inc. (Alabaster, AL). $N^{\alpha}$-(3-maleimidylpropionyl)biocytin and streptavidin-Alexa Fluor 488 conjugate were purchased from Molecular Probes (Eugene, OR), Vectashield with DAPI

was purchased from Vector Labs. (Burlingame, CA) and glutaraldehyde was purchased from Canemco (Montreal, QC).

**Peptide synthesis**

Both polyphemusin I (PM1, $RRWC^aFRVC^bYRGFC^bYRKC^aR\text{-}NH_2$, where superscript letters define the disulfide connected cysteine residues) and the free C-terminal cysteine polyphemusin (PM1-Cys, $RRWC^aFRVC^bYRGFC^bYRKC^aRC\text{-}NH_2$) were synthesized by the t-BOC method, folded and purified at the Peptide Synthesis Facility, Biomedical Research Centre, University of British Columbia. Briefly, PM1 was oxidized using a Tris-DMSO-2-propanol solution (100mM Tris-HCl, 25% DMSO, 10% 2-propanol, pH 7.5) for 24 hours at room temperature to promote disulfide bond formation. In the case of PM1-Cys, the C-terminal cysteine protecting group (ACM) was then removed and the correctly folded peptides were then purified by reverse-phase chromatography on a Waters HPLC system. Correct disulfide bond formation (between cysteine residues 4-17 and 8-13) of the purified peptides was confirmed by MALDI mass spectrometry through an observed 4 mass unit difference between the reduced and oxidized forms of PM1 and PM1-Cys and further verified by CD spectroscopy (data not shown).

PM1-Cys was labeled with biotin following a method recommended by Molecular Probes. Briefly, PM1-Cys and $N^{\alpha}$-(3-maleimidylpropionyl)biocytin were separately dissolved in 50mM Tris buffer, pH 7.0. The solutions were combined and incubated with shaking at room temperature for 2 hours. Upon completion, excess biocytin was quenched with the addition of 2-mercaptoethanol. PM1-biotin was purified by reverse-

phase chromatography on a Waters HPLC system and confirmed by MALDI mass spectrometry and the expected molecular weight of 3079 (data not shown). For clarity, the sequences and disulfide connectivity of both peptides are indicated in Figure 4.1.

**Circular dichroism (CD) spectroscopy**

CD spectra were recorded on a Jasco model J-715 spectropolarimeter using a quartz cell with a 1 mm path length. Spectra were measured at room temperature between 190 nm and 250 nm at a scan speed of 50nm/min and a total of 10 scans per sample. Spectra were recorded at a peptide concentration of 20μM in 10mM Tris buffer, pH 7.0 with and without 1mM POPC:POPG liposomes (1:1 molar ratio). Liposomes were made by dissolving lipids in chloroform:methanol (2:1 v:v). Solvent was removed under a stream of $N_2$ and the lipid film was held under vacuum for 2 hours. The lipid mixture was resuspended in 10mM Tris buffer, pH 7.0 and unilamellar vesicles were formed by sonicating the solution to clarity. In all cases, the peptide spectra were obtained by subtracting the spectra of the solution components in the absence of peptide.

**Peptide antimicrobial characterization**

Peptide minimal inhibitory concentrations (MICs) against *E. coli* UB1005 were determined using the broth microdilution method in Muller Hinton (MH) medium (*7*). The MIC was taken as the lowest peptide concentration at which no growth was observed after an overnight incubation at 37°C. MIC assays were performed three separate times and the mode values recorded.

Peptide killing curves were performed using *E. coli* UB1005 at peptide concentrations approximately 10 to 20 times the MIC as previously described (*2*). Briefly, *E. coli* was grown to mid-log phase ($OD_{600}$ = 0.3-0.5) and used to inoculate a solution of 5μM peptide in 10mM Tris, 100mM NaCl, pH 7.4 at 37°C. The suspension was incubated at 37°C and aliquots were removed at the indicated time points and plated on LB agar to determine the number of colony forming units (cfus). Killing curves were performed three separate times and a representative trial is shown.

**Fluorescence microscopy**

*E. coli* UB1005 was grown to mid-log phase in LB broth ($OD_{600}$ = 0.3-0.5) and used to inoculate 10mM Tris, 100mM NaCl, pH 7.4 ($5 \times 10^6$ cfu/ml), pre-incubated at 4°C or 37°C with or without 0.25μM or 2μM PM1-biotin. The solutions were incubated with shaking for 30 min at their respective temperatures. Cells were then pelleted, maintaining temperature, and resuspended in 5% glutaraldehyde in PBS with vortexing and incubated at room temperature for 10 min. The cells were washed once with PBS and treated with 0.2% Triton X-100 in PBS for 2 min (a non-Triton treated control was also performed by incubating with PBS alone). The cells were pelletted and suspended in a solution of 20μg/ml streptavidin- Alexa Fluor 488 and incubated with shaking at room temperature for 30 minutes. The cells were washed twice with PBS and the pellets resuspended in Vectashield with DAPI and used to prepare slides for visualization by fluorescence and confocal microscopy.

Fluorescence microscopy was performed on a Zeiss Axioskop fluorescence microscope using a 100X oil immersion lens. Confocal microscopy was performed Bio-

Rad Radiance Plus inverted confocal microscope using a 100X oil-immmersion lens. Confocal stacks were processed with ImageJ (*8*).

## Results

### CD spectroscopy

The effect of the biotin label on the overall structure of polyphemusin I was assayed using CD spectroscopy (Figure 4.2). The CD spectra of native polyphemusin I in both buffer and in lipid environments was indicative of β-sheet structure with maxima at 200nm and minima at 215nm, in agreement with previously published spectra (*2, 4*). The CD spectrum of PM1-biotin in buffer was almost identical to the spectrum of polyphemusin I indicating, in buffer, the biotin label did not cause a change in the overall structure of the peptide. Upon addition of POPC:POPG vesicles to the solution, spectral differences between the peptides became apparent. In both peptide spectra the minima at 215nm were observed to decrease slightly, indicating an increase in β-sheet structure, and the maxima at 235nm were observed to increase indicating an interaction of the single tryptophan residue with the vesicles (*9*). While the main positive ellipticity band at 200nm was observed to increase in the spectrum of polyphemusin I, a decrease was observed in the spectrum of PM1-biotin. Since the higher wavelength, β-sheet ellipticities do not differ between the peptides, the difference in the low wavelength, high sensitivity region of the spectra is likely due to the absorption of light due to the biotin label itself, masking the spectral changes observed in polyphemusin I due to liposome binding.

**Peptide antimicrobial characterization**

To determine the influence of biotinylation on the antimicrobial activity of polyphemusin I, MICs were determined for the biotinylated peptide and compared to those of native polyphemusin I (Table 4.1). The MIC of PM1 against wild type *E. coli* UB1005 was found to be 0.25μM, which is similar to previously published values (*4*), and the MIC of PM1-biotin was two-fold greater at 0.5μM. From this two-fold difference it was concluded that the addition of biotin had a minimal effect on the MIC.

To further characterize the antimicrobial activity of PM1-biotin, killing curves were performed to determine the kinetics of killing. Killing curves obtained for PM1 were similar to those previously published (*2*) where complete killing was observed within 5 min (Figure 4.3). PM1-biotin did not show complete killing at the concentration tested (5μM, or approximately 10 x MIC) however a 3-log order reduction in the number of colony forming units was observed.

**Fluorescence microscopy**

Fluorescence microscopy was performed to determine the effects of polyphemusin on bacterial cells (Figure 4.4). *E. coli* cells treated with PM1-biotin at 37°C appeared as green rods, with fluorescence throughout the cell, indicating the presence of the peptide in the cytoplasm (Figure 4.4E and F). Treatment with 0.25μM PM1-biotin (half MIC) did not appear to affect membrane integrity on a macroscopic level in wild type *E. coli* (Figure 4.4E). Clear, defined membranes were observed and cell lysis was not apparent as the DAPI stained DNA was present inside each cell in a similar condensed state as the untreated samples (Figure 4.4D). Further increasing the

peptide concentration to 2μM (four times the MIC), did not have any increased effect on macroscopic membrane integrity (Figure 4.4F). Interestingly, while the membrane appeared unaffected, the appearance of the DAPI stained DNA was altered, being less condensed than in untreated, control cells (Figures 4.4D and 4F), and was observed predominantly at the edges of the cytoplasm in what appeared to be a membrane "associated" form. As a control, *E. coli* cells were treated with PM1-biotin at 4°C. At this temperature, membrane translocation was prevented due to the rigid state of the lipids in both inner and outer membrane bilayers. Figures 4.4B and C confirmed this choice as a control as intracellular peptide fluorescence was not observed and a clear delineation of the bacterium was observed due to membrane bound peptide. These observations agree with previous studies and supported the view that polyphemusin does not cause pore formation or significant membrane damage (*2, 3*).

To more precisely determine the localization of polyphemusin, confocal microscopy was performed on the same *E. coli* samples treated at one half MIC PM1-biotin as above (Figure 4.5). Control samples incubated with peptide at 4°C (Figure 4.5A) appeared as hollow rods with fluorescence clearly defining the bacterial surface membranes. Intracellular fluorescence was not observed indicating that peptide membrane translocation did not occur. Conversely, *E. coli* treated with peptide at 37°C (Figure 4.5B) appear as solid fluorescent rods indicating the presence of peptide within the cytoplasm.

For these studies, to permit visualization of the peptide, treatment with Triton X-100 was performed after fixation with glutaraldehyde so as to permeabilize the bacteria and allow fluorescent-conjugated streptavidin to access intracellular PM1-biotin. As an

additional control in the confocal experiments, peptide treated *E. coli* samples were left untreated with Triton X-100 (Figures 4.5C and D). By eliminating this treatment, membrane integrity was retained. Thus bacteria appeared as hollow rods, indicating that PM1-biotin did not greatly affect cytoplasmic membrane integrity, and indeed did not permeabilize membranes to fluorescent-conjugated streptavidin, since fluorescence staining was not observed within these cells. These findings confirmed our hypothesis that polyphemusin is capable of translocating membranes and does not cause major membrane damage allowing the entry or leakage of molecules into or out of cells.

**Discussion**

In this study *E. coli* cells treated with polyphemusin I were investigated by using fluorescence microscopy to determine peptide localization. To visualize the peptide, a single biotin was inserted at the C-terminus, permitting secondary detection by the biotin-avidin system. The alternate method of directly labeling the peptide with a fluorophore was decided against due to the relatively poor labeling (as the biotin-avidin system permits signal amplification) and bulky hydrophobic nature of fluorescent labels. As the interaction of antimicrobial peptides with membranes is assumed to play a key role in their mechanism of action, a biotin label was chosen because this was predicted to have the smallest effect on the overall character of the peptide.

Characterization by CD spectroscopy, particularly at low wavelengths, indicated modest structural differences may exist between the native and biotin labeled polyphemusin. In other studies, molecules as large as enzymes that are coupled to small arginine rich peptides are still translocated across membranes (*10*). Molecules of this size

would no doubt alter the structure of such a small peptide, due to their large size alone, yet translocation was still observed. Thus, the significance of the change in elipticity observed here and its implications upon the overall structure and activity of the labeled peptide remain unclear.

The difference in peptide conformation correlated with somewhat altered antimicrobial activity. The minimal inhibitory concentration of PM1-biotin was two-fold greater and, possibly as a consequence, complete killing was not observed after a 30 min incubation at 5μM (10 x MIC) compared to complete killing within 5 min by the native polyphemusin I. While killing was not complete, the 3-log order reduction in the number of viable cells following PM1-biotin treatment indicated that the peptide retained substantial antimicrobial activity.

Upon observation of peptide treated *E. coli* several significant findings became apparent. Examination by fluorescence microscopy revealed, in peptide treated and untreated samples, a clear defined ring of fluorescence surrounding each cell. This observation suggests that the membranes still remain intact. Correspondingly, samples left untreated with Triton-X100 were impermeable to the fluorescent labelled avidin and thus, significant membrane damage or pore formation allowing the entry of this molecule did not occur. This agrees with previous findings that the polyphemusins do not induce large membrane disturbances leading to changes in membrane integrity (*3*).

Perhaps the most significant observation was the presence of intracellular fluorescence indicating the translocation of PM1-biotin through the bacterial inner and outer membranes. In addition, the DAPI stained DNA in cells treated with peptide at four times the MIC appeared markedly different than in untreated and half MIC treated

cells. DNA in the high peptide samples appeared less condensed compared to untreated cells. Indeed, the related horseshoe crab peptide, tachyplesin I, has been shown to bind the minor groove of DNA (*11*) and the less condensed nature observed here may indicate direct PM1-biotin/DNA binding. In addition, the location of the DNA within the cell was altered and appeared at the periphery of each cell almost in a membrane-associated state.

The data presented here, for the first time demonstrate membrane translocation of a polyphemusin I analogue, PM1-biotin, in intact bacterial cells. This finding agrees with previously published translocation studies using model membranes. In addition, the absence of cytoplasmic fluorescence in cells treated with peptide but not permeabilized with Triton X-100 indicated that PM1-biotin did not induce significant membrane damage or pore formation. Combined, these findings support our hypothesis that the polyphemusins are capable of translocating membranes and may act on an intracellular target to elicit their antimicrobial activity.

**Table 4.1.** Antimicrobial activity of PM1 and PM1-biotin versus *E. coli* UB1005.

| Peptide | MIC (μM) |
|---|---|
| PM1 | 0.25 |
| PM1-biotin | 0.5 |

**Figure 4.1.** Primary structures of polyphemusin I (PM1) (top) and biotin labeled analogue, PM1-biotin (bottom). Disulfide linkages, present in both peptides, are indicated in solid lines. The biotin label in PM1-biotin is side chain bound while both peptides possess amidated C-termini.

**Figure 4.2.** CD spectra of polyphemusin I (PM1) and PM1-biotin. Spectra were recorded at 20μM peptide (PM1 squares; PM1-biotin triangles) in 10 mM Tris buffer, pH 7.0 (closed markers) and in 1mM POPC:POPG liposomes (1:1 mole:mole) (open markers).

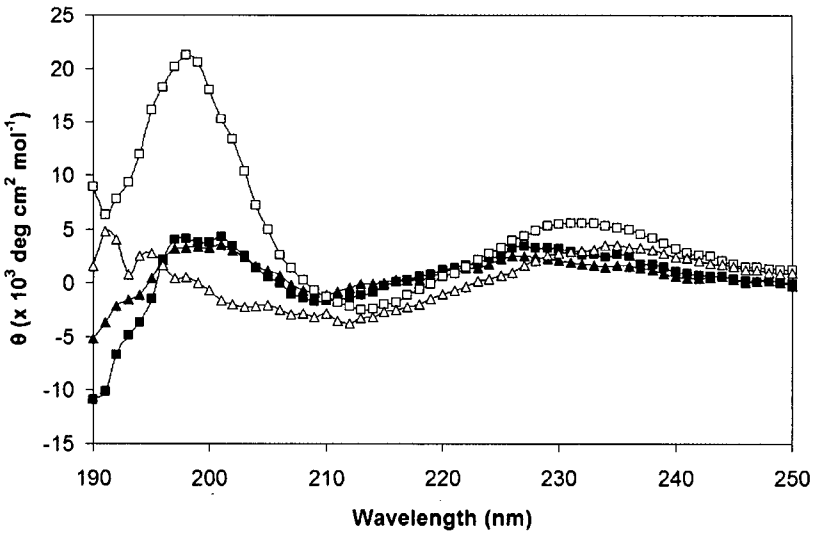

**Figure 4.3.** Killing of *E. coli* UB1005 by polyphemusin I (PM1) and PM1-biotin. Killing curves were performed at 10 times the peptide MIC for PM1 (triangles) and PM1-biotin (circles). A non-peptide treated control (squares) was also performed.

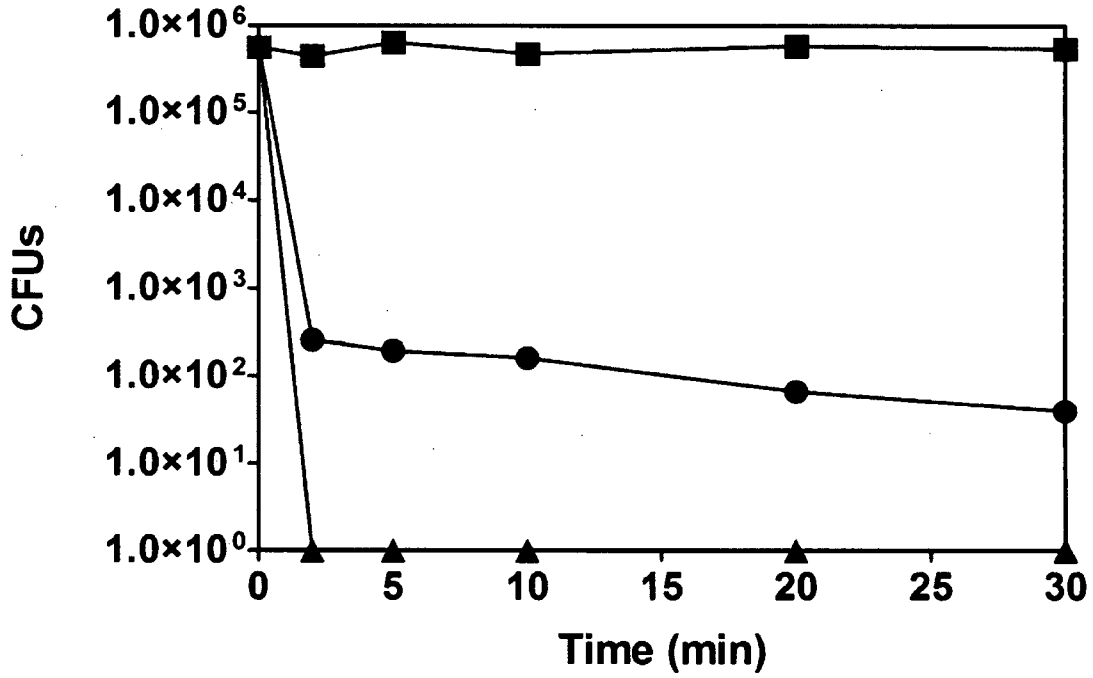

**Figure 4.4.** Fluorescence microscopy of *E. coli* UB1005 treated with PM1-biotin. Bacteria were incubated at 4°C (top panels) or 37°C (bottom panels) without peptide (A, D) and at peptide concentrations of one half MIC (B, E) and 4 times the MIC (C, F) for 30 min. Blue fluorescence staining represents intracellular DAPI-stained DNA while green fluorescence staining represents the Alexa Fluor labeled peptide.

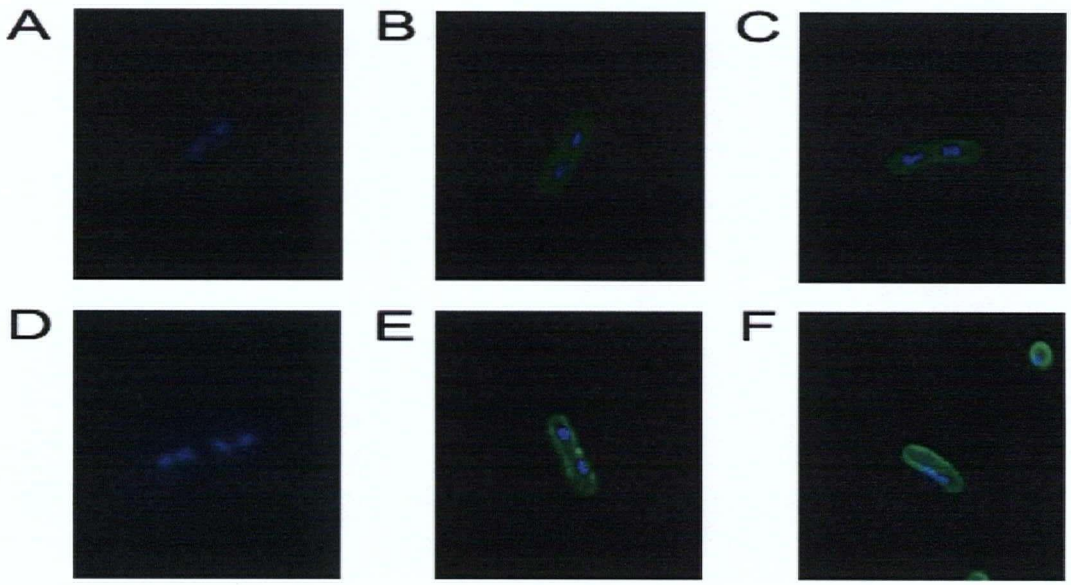

**Figure 4.5.** Confocal microscopy of *E. coli* UB1005 treated with PM1-biotin. Bacteria were incubated with peptide at 4°C (A and C) or 37°C (B and D) at one half MIC for 30 minutes. Prior to fluorescence labeling, cells were treated (A and B) or untreated with 0.2% triton X-100 (C and D).

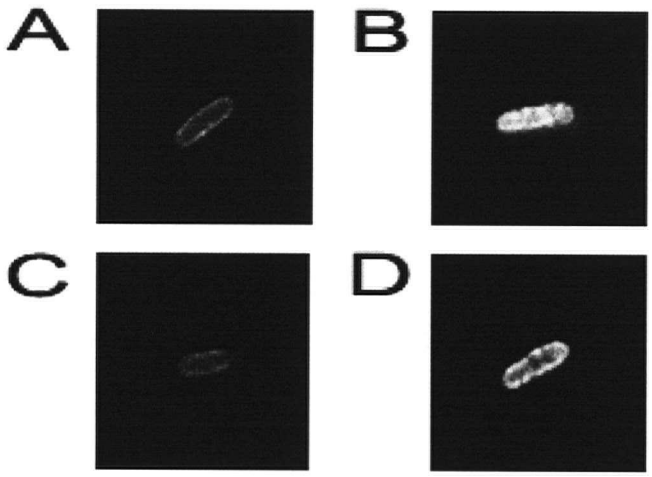

## References


1. Miyata, T., Tokunaga, F., Yoneya, T., Yoshikawa, K., Iwanaga, S., Niwa, M., Takao, T., and Shimonishi, Y. (1989) Antimicrobial peptides, isolated from horseshoe crab hemocytes, tachyplesin II, and polyphemusins I and II: chemical structures and biological activity, *J Biochem (Tokyo) 106*, 663-8.
2. Zhang, L., Scott, M. G., Yan, H., Mayer, L. D., and Hancock, R. E. W. (2000) Interaction of polyphemusin I and structural analogs with bacterial membranes, lipopolysaccharide, and lipid monolayers, *Biochemistry 39*, 14504-14.
3. Zhang, L., Rozek, A., and Hancock, R. E. W. (2001) Interaction of cationic antimicrobial peptides with model membranes, *J Biol Chem 276*, 35714-22.
4. Powers, J. P. S., Rozek, A., and Hancock, R. E. W. (2004) Structure-activity relationships for the beta-hairpin cationic antimicrobial peptide polyphemusin I, *Biochim Biophys Acta 1698*, 239-50.
5. Park, C. B., Kim, H. S., and Kim, S. C. (1998) Mechanism of action of the antimicrobial peptide buforin II: buforin II kills microorganisms by penetrating the cell membrane and inhibiting cellular functions, *Biochem Biophys Res Commun 244*, 253-7.
6. Kragol, G., Hoffmann, R., Chattergoon, M. A., Lovas, S., Cudic, M., Bulet, P., Condie, B. A., Rosengren, K. J., Montaner, L. J., and Otvos, L., Jr. (2002) Identification of crucial residues for the antibacterial activity of the proline-rich peptide, pyrrhocoricin, *Eur J Biochem 269*, 4226-37.

7. Wu, M., and Hancock, R. E. W. (1999) Interaction of the cyclic antimicrobial cationic peptide bactenecin with the outer and cytoplasmic membrane, *J Biol Chem 274*, 29-35.

8. Abramoff, M. D., Magelhaes, P. J., and Ram, S. J. (2004) Image Processing with ImageJ, *Biophotonics International 11*, 36-42.

9. Fasman, G. D. (1996) *Circular dishroism and the conformational analysis of biomolecules*, Plenum Press, New York.

10. Futaki, S., Suzuki, T., Ohashi, W., Yagami, T., Tanaka, S., Ueda, K., and Sugiura, Y. (2001) Arginine-rich peptides. An abundant source of membrane-permeable peptides having potential as carriers for intracellular protein delivery, *J Biol Chem 276*, 5836-40.

11. Yonezawa, A., Kuwahara, J., Fujii, N., and Sugiura, Y. (1992) Binding of tachyplesin I to DNA revealed by footprinting analysis: significant contribution of secondary structure to DNA binding and implication for biological action, *Biochemistry 31*, 2998-3004.

## Chapter 5 – Discussion

Prior to beginning this thesis, it was known that the β-hairpin polyphemusins were extremely active antimicrobial peptides as indicated by their relatively low MICs (less than 0.2μM for both Gram negative and Gram positive organisms) (*1*). It had also been shown that at relevant peptide concentrations (MIC levels), the polyphemusins induced a substantial lipid flip-flop between model membrane leaflets while, at the same time producing relatively low dye release from within liposomes (*2*). Thus, the mechanism of antimicrobial action was believed to involve membrane translocation during which only minor membrane disturbances were caused. In addition, the available three dimensional structures of these peptides were based primarily on computer derived models (*1*) and, more recently, the $^{1}$H-NMR determined structures of the related peptide, tachyplesin (*3*). It was thus of significant interest to determine the solution structure of polyphemusin I by $^{1}$H-NMR as well as to investigate the interaction of the polyphemusins with lipid membranes in an effort to characterize their mechanism of antimicrobial activity.

### Peptide linearization

The linearization of disulfide bond containing peptides has been studied for a variety of reasons. In the case of the polyphemusins, knowledge of the structural components required for the activity of these peptides may provide some insight into the mechanism of action itself. Secondly, due to its low MIC values, polyphemusin I is of interest as a potential therapeutic. The increased cost of manufacturing a peptide that requires post-synthesis folding and re-purification is prohibitive for the production of such a therapeutic agent. Thus, if a linear polyphemusin analogue, possessing similar

properties and activity could be produced, its therapeutic potential would be greatly improved.

Previous studies, focused on linear analogues of the related peptide tachyplesin, have been performed with mixed findings. Matsuzaki *et al* accomplished tachyplesin linearization by leaving bulky protecting groups (ACM) on the cysteine thiols (*4*). Structural characterization by CD spectroscopy revealed that both the native and linear peptide adopted a β-sheet conformation in the presence of anionic liposomes however the linear analogue caused a greater degree of membrane disruption. Further experimentation found that linearization impaired the ability of the peptide to translocate membranes and increased the membrane disruption ability (*5*). Thus, linearization effectively transformed the mechanism of tachyplesin action from non-membrane acting to a membrane acting peptide.

In another study, Rao achieved tachyplesin linearization through amino acid substitution using a variety of aliphatic (A, L, I, V, M), aromatic (F, Y) and acidic (D) residues in place of the four native cysteines (*6*). Characterization by $^{1}$H-NMR confirmed that tachyplesin linearized using tyrosine substitution adopted a beta sheet structure in solution due to aromatic ring stacking (*3*). The addition of DPC micelles disturbed the aromatic interactions thus disrupting the native structure and activity of the linearized peptide (*3*), again suggesting the requirement of disulfides for maximum antimicrobial activity.

I chose to investigate the effect of linearization on the activity of polyphemusin I. In my study, serine was chosen as a cysteine substitute as both residues possess lone pair electrons and similar polarities. In addition, the ACM protecting group is quite

hydrophobic which would change the hydrophobic character of the linear peptide. Thus, by using serine as a substitute, the overall character of the peptide was expected to be retained except for the ability to form disulfide bonds. Characterization of the resulting PM1-S and comparison with native polyphemusin I revealed deficiencies in the antimicrobial activity and membrane depolarization ability of the linear peptide. In addition the peptide was devoid of the membrane translocating ability of polyphemusin I. Further characterization indicated that PM1-S did not adopt a β-hairpin conformation in solution or in a lipid environment. It was concluded that, similar to the studies of Matsuzaki *et al* (*4*), that disulfide bonding was required to stabilize the β-hairpin conformation of polyphemusin I and this conformation imparted the ability to translocate membranes.

While its *in vitro* membrane translocating ability was ablated, PM1-S possessed respectable antimicrobial activity, at least when compared to other peptides in the literature (*7-9*). It is our belief that this peptide is indeed antimicrobial and simply possesses a different mechanism of action than polyphemusin I. Our hypothesis is that PM1-S functions through an, as yet, undefined mechanism of action similar to the peptides in the extended structural class such as indolicidin (*10*).

**Peptide translocation**

At the onset of this thesis project there was one main theory for the antimicrobial mechanism of action of cationic, antimicrobial peptides. This theory involved the disruption of the phospholipid bilayers through the formation of peptide pores or channels (*11*). Channel formation was believed to lead to the disruption of the

permeability barrier of the membrane causing depolarization and leakage of cytoplasmic contents and, ultimately, cell lysis. At the same time, a lesser held but emerging belief was that some peptides acted upon cytoplasmic targets and possessed the ability to translocate membranes. One mechanism of membrane translocation, termed self-promoted uptake, involved the initial interaction of cationic peptides with the anionic LPS located in Gram negative bacteria outer membrane (*12*). This lead to displacement of divalent cations and a corresponding destabilization of the permeability barrier of the membrane. The result is the formation of informal peptide aggregates within the bilayer which, upon collapse, lead to peptide translocation. After translocation across the outer membrane, the peptide could now associate with the negatively charged lipids in the inner membrane where the peptide is proposed to go through one of several possible aggregative, membrane-spanning intermediates that will spontaneously resolve with some peptide molecules finding their way to the internal leaflet of the cytoplasmic membrane. This aggregate mechanism would also serve as the mechanism of translocation in Gram positive bacteria that lack outer membranes.

**Polyphemusin membrane interaction**

The first step in defining the aggregate model of peptide action involved characterizing peptide-membrane interactions. The evidence that cationic peptides may possess targets other than membranes led to a more detailed investigation of polyphemusin I with model membrane systems. Using a membrane translocation assay, Zhang *et al*, demonstrated that polyphemusin I was able to access the interior of liposomes (*2*). In the same study, the authors also showed that polyphemusin produced a

large degree of lipid flip-flop between membrane leaflets while producing a small degree of membrane damage as evidenced by calcein dye release. This led to the hypothesis that the polyphemusins may function through an aggregate model (*12*) and act upon a cytoplasmic target.

The findings presented here, for the first time investigated the effects of the polyphemusins on lipid phase transitions as observed by differential scanning calorimetry in addition to membrane partitioning. In the process of membrane interaction, peptides initially encounter organisms with varying cell membrane compositions. These membranes may be either anionic or neutral in charge and this serves as an important determinant of peptide activity. An encounter between a polyphemusin and a neutral membrane will yield a limited interaction due to the relatively low affinity and poor partitioning of the peptide into this environment. When polyphemusin encounters a negatively charged membrane, the electrostatic interactions and hydrophobic components of the peptide combine to result in a high partitioning into this environment and membrane binding and partial peptide insertion occurs. This differential selection of neutral versus anionic membranes agrees with previously published membrane data and explains the large difference between the minimal inhibitory concentration against bacteria and the minimal hemolytic concentration against red blood cells (*1*).

Once membrane bound, peptides possessing the native polyphemusin β-hairpin conformation induced negative curvature strain and, possibly through a conformational change and/or peptide aggregation, transient, non-bilayer formation occurred. Upon collapse of this intermediate complex, which has not been directly observed due to its presumably short lifetime, the membrane is restored to its lamellar form. It is worth

noting however that the observance of transient channels of short duration and variable magnitude in planar bilayer studies is entirely consistent with the formation of such an intermediate (*13*). The collapse of the intermediate structure would be the driving force behind membrane translocation and is proposed to lead to the redistribution of peptide into both membrane leaflets due to the initial concentration gradient. Pokorny *et al* have proposed a similar model, termed the sinking-raft model, to explain the mechanism of δ-lysin interaction with membranes (*14, 15*).

Once the peptide has translocated into the cytoplasm, multiple events may occur. The peptide may simply re-associate with the inner-leaflet of the membrane or it may interact with anionic cytoplasmic components. Previously, confocal microscopy studies of *E. coli* treated with the helical peptide, buforin II, indicated that the peptide translocated across membranes and accumulated in the cytoplasm without causing significant membrane damage (*16*). We have demonstrated here, that polyphemusin I also gains access to the bacterial cytoplasm, at which point the interaction of the cationic peptide with various anionic macromolecules is possible. Thus further study is required to clarify these final steps in the mechanism of action of the polyphemusins.

**Antimicrobial targets of the polyphemusins**

At the beginning of this thesis relatively little was known regarding the mechanism of action of the polyphemusins. Initial studies followed the long-held dogma in the peptide field that focused on membrane disruption and cell lysis as the lethal event. Studies involving other peptides however, suggest that simple membrane disruption may not explain the effects of all cationic peptides. While membrane translocation has been

demonstrated, definitive cytoplasmic targets remain few. It was demonstrated by Patrzykat *et al* that sub-lethal concentrations of a synthetic peptide, built on a hybrid of fish pleurocidin and frog dermaseptin, inhibited the synthesis of DNA, RNA and protein in *E. coli*, although the exact cause of this inhibition is unknown (*17*). Perhaps the most complete study involved the proline-rich insect peptide, pyrrhocoricin, which was shown to translocate *E. coli* membranes and bind the cytoplasmic heat shock protein DnaK (*18, 19*).

The findings presented here demonstrate, for the first time, that polyphemusin I is capable of translocating both the outer and inner membranes of *E. coli* and accumulates in the cytoplasm. Interestingly, the related peptide tachyplesin I, has previously been shown to bind the minor groove of DNA in *in vitro* studies (*20*). This finding, combined with membrane translocation in whole cells, becomes more relevant to the antimicrobial mechanism of action of these peptides. Indeed in my studies, the DNA in polyphemusin I treated *E. coli* appeared less condensed than in untreated cells. Although the significance of this finding is not clear, one may speculate this is due to the interaction of polyphemusin I and DNA within the cytoplasm, and further experimentation is warranted.

**Future directions**

While it has been shown that polyphemusin I is capable of translocating membranes and gaining access to the cytoplasm, many questions remain as to the exact killing mechanism of this family of peptides. There have been relatively few demonstrated cellular targets of cationic, antimicrobial peptides and thus the question

remains as to whether a single intracellular target exists for polyphemusin I or if the mechanism of killing is simply a combination of multiple events. It has been proposed that these and other antimicrobial peptides may act by binding to DNA, RNA or cellular proteins to elicit their activity. Indeed this probably occurs; however, it should be cautioned that, considering any of these a specific target may be in error as all of these cellular molecules contain multiple anionic components and thus binding may be of a non-specific nature.

In an effort to further clarify the mechanism of the polyphemusins, a variety of experiments may be suggested. To continue to define peptide localization, it is of interest to obtain higher resolution images of the bacteria following treatment. An excellent method would be to use electron energy loss spectroscopy (EELS) coupled with transmission electron microscopy to provide a better picture of peptide treated bacteria. In this method, sectioned bacteria that have been treated with biotin-labeled peptide are labeled with streptavidin-gold and enhanced with silver for visualization through EM where the gold and silver bound peptides appear as clearly defined dots on the micrograph. This high resolution image of the peptide-treated bacteria may provide enough detail to determine peptide co-localization with cytoplasmic macromolecules such as DNA or ribosomes without the need for additional counterstains. In addition, this method is also easily adapted for time or concentration dependant studies.

An additional method to search for a specific bacterial target is the use of an affinity column where immobilized peptide is used to capture molecules from individually separated bacterial fractions. While this method is certainly more complicated, it may define whether or not a specific target exists. It would be expected

that many anionic components will bind the immobilized peptide however these may be eliminated to determine the degree of specificity by increasing the stringency of the elution buffer by increasing salt concentration.

**References**


1. Zhang, L., Scott, M. G., Yan, H., Mayer, L. D., and Hancock, R. E. W. (2000) Interaction of polyphemusin I and structural analogs with bacterial membranes, lipopolysaccharide, and lipid monolayers, *Biochemistry 39*, 14504-14.
2. Zhang, L., Rozek, A., and Hancock, R. E. W. (2001) Interaction of cationic antimicrobial peptides with model membranes, *J Biol Chem 276*, 35714-22.
3. Laederach, A., Andreotti, A. H., and Fulton, D. B. (2002) Solution and micelle-bound structures of tachyplesin I and its active aromatic linear derivatives, *Biochemistry 41*, 12359-68.
4. Matsuzaki, K., Nakayama, M., Fukui, M., Otaka, A., Funakoshi, S., Fujii, N., Bessho, K., and Miyajima, K. (1993) Role of disulfide linkages in tachyplesin-lipid interactions, *Biochemistry 32*, 11704-10.
5. Matsuzaki, K., Yoneyama, S., Fujii, N., Miyajima, K., Yamada, K., Kirino, Y., and Anzai, K. (1997) Membrane permeabilization mechanisms of a cyclic antimicrobial peptide, tachyplesin I, and its linear analog, *Biochemistry 36*, 9799-806.
6. Rao, A. G. (1999) Conformation and antimicrobial activity of linear derivatives of tachyplesin lacking disulfide bonds, *Arch Biochem Biophys 361*, 127-34.
7. Falla, T. J., and Hancock, R. E. (1997) Improved activity of a synthetic indolicidin analog, *Antimicrob Agents Chemother 41*, 771-5.
8. Turner, J., Cho, Y., Dinh, N. N., Waring, A. J., and Lehrer, R. I. (1998) Activities of LL-37, a cathelin-associated antimicrobial peptide of human neutrophils, *Antimicrob Agents Chemother 42*, 2206-14.

9. Friedrich, C. L., Moyles, D., Beveridge, T. J., and Hancock, R. E. (2000) Antibacterial action of structurally diverse cationic peptides on gram-positive bacteria, *Antimicrob Agents Chemother 44*, 2086-92.

10. Falla, T. J., Karunaratne, D. N., and Hancock, R. E. (1996) Mode of action of the antimicrobial peptide indolicidin, *J Biol Chem 271*, 19298-303.

11. Huang, H. W. (2000) Action of antimicrobial peptides: two-state model, *Biochemistry 39*, 8347-52.

12. Hancock, R. E. W., and Chapple, D. S. (1999) Peptide antibiotics, *Antimicrob Agents Chemother 43*, 1317-23.

13. Wu, M., Maier, E., Benz, R., and Hancock, R. E. W. (1999) Mechanism of interaction of different classes of cationic antimicrobial peptides with planar bilayers and with the cytoplasmic membrane of Escherichia coli, *Biochemistry 38*, 7235-42.

14. Pokorny, A., Birkbeck, T. H., and Almeida, P. F. (2002) Mechanism and kinetics of delta-lysin interaction with phospholipid vesicles, *Biochemistry 41*, 11044-56.

15. Pokorny, A., and Almeida, P. F. (2004) Kinetics of dye efflux and lipid flip-flop induced by delta-lysin in phosphatidylcholine vesicles and the mechanism of graded release by amphipathic, alpha-helical peptides, *Biochemistry 43*, 8846-57.

16. Park, C. B., Yi, K. S., Matsuzaki, K., Kim, M. S., and Kim, S. C. (2000) Structure-activity analysis of buforin II, a histone H2A-derived antimicrobial peptide: the proline hinge is responsible for the cell- penetrating ability of buforin II, *Proc Natl Acad Sci U S A 97*, 8245-50.

17. Patrzykat, A., Friedrich, C. L., Zhang, L., Mendoza, V., and Hancock, R. E. W. (2002) Sublethal concentrations of pleurocidin-derived antimicrobial peptides inhibit macromolecular synthesis in Escherichia coli, *Antimicrob Agents Chemother 46*, 605-14.

18. Kragol, G., Hoffmann, R., Chattergoon, M. A., Lovas, S., Cudic, M., Bulet, P., Condie, B. A., Rosengren, K. J., Montaner, L. J., and Otvos, L., Jr. (2002) Identification of crucial residues for the antibacterial activity of the proline-rich peptide, pyrrhocoricin, *Eur J Biochem 269*, 4226-37.

19. Kragol, G., Lovas, S., Varadi, G., Condie, B. A., Hoffmann, R., and Otvos, L., Jr. (2001) The antibacterial peptide pyrrhocoricin inhibits the ATPase actions of DnaK and prevents chaperone-assisted protein folding, *Biochemistry 40*, 3016-26.

20. Yonezawa, A., Kuwahara, J., Fujii, N., and Sugiura, Y. (1992) Binding of tachyplesin I to DNA revealed by footprinting analysis: significant contribution of secondary structure to DNA binding and implication for biological action, *Biochemistry 31*, 2998-3004.

## Appendix 1 – Proton chemical shifts of polyphemusin I

Proton chemical shifts of polyphemusin I (PM1) in $H_2O$:$D_2O$ (9:1) at pH 4.0 and 27°C.

| Residue # | Residue Name | Chemical Shift (ppm) | | | |
|---|---|---|---|---|---|
| | | NH | Hα | Hβ | Others |
| 1 | Arg | | 4.06 | 1.89 | Hγ 1.53; Hδ 3.08; NHε 6.94 |
| 2 | Arg | 8.74 | 4.73 | 1.77 | Hγ 1.60, 1.66; Hδ 3.17; NHε 7.16 |
| 3 | Trp | 8.85 | 4.92 | 3.29, 3.37 | Hδ1 7.28; Hε1 10.14; Hζ2 7.69; Hζ3 7.18; Hη 7.13; Hε3 7.46 |
| 4 | Cys | 8.35 | 5.57 | 2.58, 3.03 | -- |
| 5 | Phe | 8.82 | 4.84 | 3.02, 3.08 | Hδ 6.931; Hε 7.12 |
| 6 | Arg | 8.62 | 4.85 | 1.64, 1.76 | Hγ 1.42, 1.47; NHε 7.20 |
| 7 | Val | 8.86 | 4.33 | 0.82, 0.89 | -- |
| 8 | Cys | 8.60 | 5.66 | 2.76, 3.02 | -- |
| 9 | Tyr | 9.25 | 4.80 | 3.14 | Hδ 7.30; Hε 6.91 |
| 10 | Arg | 9.28 | 3.76 | 1.67, 1.99 | Hγ 0.94, 1.27; Hδ 3.10; NHε 7.07 |
| 11 | Gly | 8.59 | 3.58, 4.15 | -- | -- |
| 12 | Phe | 7.99 | 4.91 | 3.15, 3.24 | Hδ 7.36; Hε 7.88 |
| 13 | Cys | 8.41 | 5.80 | 2.55, 2.94 | -- |
| 14 | Tyr | 9.05 | 4.75 | 2.99 | Hδ 6.97; Hε 6.76 |
| 15 | Arg | 8.58 | 4.76 | 1.68 | Hγ 1.37, 1.48; Hδ 3.116; NHε 7.20 |
| 16 | Lys | 8.80 | 4.57 | 1.30, 1.44 | Hγ 1.34; Hδ 1.77; Hε 3.03; NHε 7.67 |
| 17 | Cys | 8.68 | 5.52 | 2.81, 2.99 | -- |
| 18 | Arg | 8.95 | 4.58 | 1.83, 2.00 | Hγ 1.78; Hδ 3.25; NHε 7.24; $NH_2$ 7.88 |

## Appendix 2 – Proton chemical shifts of PV5

Proton chemical shifts of PV5 in $H_2O$:$D_2O$ (9:1) at pH 3.80 and 25°C.

| Residue | Chemical Shift (ppm) | | | |
|---|---|---|---|---|
| | NH | Hα | Hβ | Others |
| Arg-1 | | 4.004 | 1.828 | Hγ 1.447; Hδ 3.019; NHε 6.883 |
| Arg-2 | 8.688 | 4.642 | 1.704 | Hγ 1.541, 1.593; Hδ 3.112; NHε 7.112 |
| Trp-3 | 8.787 | 4.852 | 3.217, 3.297 | Hδ1 7.214; Hε1 10.092; Hζ2 7.405; Hη 7.132 |
| Cys-4 | 8.324 | 5.464 | 2.550, 2.958 | |
| Phe-5 | 8.752 | 4.763 | 2.946, 3.017 | Hδ 6.876; Hε 7.078; Hζ 7.620 |
| Arg-6 | 8.572 | 4.722 | | Hδ 3.075 |
| Val-7 | 8.812 | 4.159 | 1.368 | Hγ 0.740, 0.765 |
| Cys-8 | 8.532 | 5.088 | 2.759, 2.923 | |
| Tyr-9 | 8.915 | 4.760 | 2.971, 3.073 | Hδ 7.177; Hε 6.824 |
| Arg-10 | 8.930 | 3.898 | 1.733, 1.887 | Hγ 1.264, 1.382; Hδ 3.104; NHε 7.088 |
| Gly-11 | 8.500 | 3.596, 4.118 | | |
| Arg-12 | 7.941 | 4.474 | 1.605 | Hγ 1.388; Hδ 3.052; NHε 7.049 |
| Phe-13 | 8.042 | 4.702 | 3.218 | Hδ 7.289; Hε 7.341 |
| Cys-14 | 8.442 | 5.534 | 2.581, 3.029 | |
| Tyr-15 | 9.085 | 4.829 | 2.971, 3.052 | Hδ 7.017; Hε 6.679 |
| Arg-16 | 8.557 | 4.708 | | |
| Lys-17 | 8.712 | 4.489 | 1.299, 1.402 | |
| Cys-18 | 8.630 | 5.406 | 2.783, 2.936 | |
| Arg-19 | 8.871 | 4.509 | 1.771, 1.933 | Hγ 1.730; Hδ 3.194; NHε 7.189 |
| $NH_2$ | 7.304, 7.827 | | | |

Proton chemical shifts of PV5 in 300mM DPC, $H_2O$:$D_2O$ (9:1) at pH 3.95 and 40°C.

| Residue | Chemical Shift (ppm) | | | |
|---|---|---|---|---|
| | **NH** | **Hα** | **Hβ** | **Others** |
| Arg-1 | | 3.969 | 1.779 | Hγ 1.391, 1.470; Hδ 2.953 |
| Arg-2 | 8.562 | 4.526 | 1.669 | Hγ 1.491, 1.559; Hδ 3.072; NHε 7.148 |
| Trp-3 | 8.615 | 4.710 | 3.189 | Hδ1 7.214; Hε1 10.431; Hζ2 7.378 |
| Cys-4 | 8.218 | 5.353 | 2.596, 2.932 | |
| Phe-5 | 8.562 | 4.790 | 2.948 | Hδ 7.052; Hε 7.097 |
| Arg-6 | 8.312 | 5.072 | 1.681 | Hδ 1.370, 1.495; Hδ 3.019; NHε 7.200 |
| Val-7 | 8.658 | 4.454 | 1.939 | Hγ 0.971 |
| Cys-8 | 8.578 | 5.448 | 2.579, 3.008 | |
| Tyr-9 | 8.872 | 4.778 | 2.865 | Hδ 7.045; Hε 6.768 |
| Arg-10 | 9.094 | 3.712 | 1.451, 1.860 | Hγ 0.867, 1.099; Hδ 2.955; NHε 7.174 |
| Gly-11 | 8.276 | 3.541, 4.009 | | |
| Arg-12 | 7.941 | 4.382 | 1.509 | Hγ 1.277, 1.208; Hδ 2.987; NHε 7.247 |
| Phe-13 | 7.624 | 4.811 | 3.175, 3.250 | |
| Cys-14 | 8.394 | 5.594 | 2.578, 2.964 | |
| Tyr-15 | 9.065 | 4.691 | 2.801, 2.890 | Hδ 6.953; Hε 6.672 |
| Arg-16 | 7.943 | 4.947 | 1.573, 1.442 | Hγ 1.280, 1.365; Hδ 2.997 |
| Lys-17 | 8.203 | 4.406 | 1.486 | |
| Cys-18 | 8.558 | 5.434 | 2.787, 2.934 | |
| Arg-19 | 8.725 | 4.394 | 1.630 | Hγ 1.865; Hδ 3.152; NHε 6.881, 7.601 |
| $NH_2$ | 7.152, 7.911 | | | |

## Appendix 3 - Publications arising from graduate work

### *Peer-reviewed publications*

- **Powers, J.P.S.**, Martin, M.M., Goosney, D.L., and Hancock, R.E.W. 2006. The antimicrobial peptide polyphemusin localizes to the cytoplasm of *Escherichia coli* following treatment. *Antimicrobial Agents and Chemotherapy*. In press.
- **Powers, J.P.S.**, Tan, A., Ramamoorthy, A., and Hancock, R.E.W. 2005. Solution structure and interaction of the antimicrobial polyphemusins with lipid membranes. *Biochemistry* **44**:15504-13.
- **Powers, J.P.S.**, Rozek, A., and Hancock, R.E.W. 2004. Structure-activity relationships for the β-hairpin cationic antimicrobial peptide polyphemusin I. *Biochimica et Biophysica Acta* **1698**:239-50.
- Lee, D.L., **Powers, J.P.S.**, Pflegerl, K., Vasil, M.L., Hancock, R.E.W., and Hodges, R.S. 2004. Effects of single D-amino acid substitutions on disruption of beta-sheet structure and hydrophobicity in cyclic 14-residue antimicrobial peptide analogs related to gramicidin S. *Journal of Peptide Research* **63**:69-84.
- **Powers, J.P.S.**, and Hancock, R.E.W. 2003. The relationship between peptide structure and antibacterial activity. *Peptides* **24**:1681-91.
- Rozek, A., **Powers, J.P.S.**, Friedrich, C.L., and Hancock, R.E.W. 2003. Structure-based design of an indolicidin peptide analog with increased protease stability. *Biochemistry* **42**:14130-8.

### *Patents and Copyrights*

- Effectors of innate immunity. R.E.W. Hancock, B. Finlay, M. Scott, D. Bowdish, C. Rosenberger and **J.P.S. Powers**. US PTO serial no. 10/308,905, filed Dec. 2, 2002. PCT serial no. PCT/CA02/01830, filed Dec. 2, 2002.
- Effectors of innate immunity. R.E.W. Hancock, B. Finlay, M. Scott, D. Bowdish, C. Rosenberger and **J.P.S. Powers**. US PTO CIP (of 10/308,905) serial no. 10/661,471, filed Sept. 12, 2003. PCT serial no. PCT/CA2004/001602, filed Sept. 10, 2004. Malaysia serial no. PI20043699, filed Sept. 11, 2004. Taiwan serial no. 093127497, filed Sept. 11, 2004.

### *Non-refereed publications*

- **Powers, J.P.S.**, Bowdish, D.M.E., and Hancock, R.E.W. 2002. On the nature of cationic peptides. *Pharmachem* **July/August**: 40-44.

### *Abstracts*

- Zhang, L., Parente, J., Harris, S.M., **Powers, J.P.S.**, Yano, J., Fidel, P., Nair, M. and Falla, T.J. Novel Hexapeptides with Potent Antimicrobial Activity and Low Toxicity. Gordon Research Conference on Antimicrobial Peptides. March 6-11,2005. Ventura, CA.

- **Powers, J.P.S.**, Tan, A., Ramamoorthy, A., and Hancock, R.E.W. Interaction of the cationic antimicrobial peptides polyphemusin I and PV5 with model membrane systems: A spectroscopic and calorimetric analysis. Canadian Bacterial Diseases Network AGM. February 13-16, 2005. Banff, AB.
- Mookherjee, N., Brown,K., Falsafi, R., Bryan, J., Hokamp, K., Roche, F.M., Doria, S., Bowdish, D., **Powers, J.P.S.**, Pistolic, J., Lee, S.J., Fan, S., Chan, M., Brinkman, F.S.L., and Hancock, R.E.W. Transcriptional profiling of human monocytic cell responses to host defence peptide LL-37: role of LL-37 in modulation of inflammation. The Keystone Symposia; Innate Immunity to Pathogens. January 8-13, 2005. Steamboat Springs, CO.
- Mookherjee, N., Wilson, H., Aich, P., Brown, K., Falsafi1, R., Popowych, Y., Bakare, A., Hokamp, K., Roche, R., Doria, S., Pistolic, J., Chan, M., **Powers, J.P.S.**, Griebel, P., Brinkman, F., Babiuk, L., and Hancock, R.E.W. Comparative Genomic Analysis of Transcriptional Responses from Human and Bovine Monocytic Cells to Cationic Peptides. Genome Canada National Genomics and Proteomics Symposium. November 24 - 25, 2004. Vancouver, BC.
- **Powers, J.P.S.**, Rozek, A., Zhang, L., and Hancock, R.E.W. Structure-activity relationships of the antimicrobial peptide polyphemusin I. University of Alberta / University of Calgary Conference on Infectious Diseases. April 21-24, 2002. Banff, AB.